

ADAPTIVE POWER CONTROL
FOR SINGLE AND MULTIUSER OPPORTUNISTIC SYSTEMS

A Dissertation
by
SUNG SIK NAM

Submitted to the Office of Graduate Studies of
Texas A&M University
in partial fulfillment of the requirements for the degree of
DOCTOR OF PHILOSOPHY

May 2009

Major Subject: Electrical Engineering

ADAPTIVE POWER CONTROL
FOR SINGLE AND MULTIUSER OPPORTUNISTIC SYSTEMS

A Dissertation
by
SUNG SIK NAM

Submitted to the Office of Graduate Studies of
Texas A&M University
in partial fulfillment of the requirements for the degree of
DOCTOR OF PHILOSOPHY

Approved by:

Co-Chairs of Committee,	Mohamed-Slim Alouini Costas N. Georghiades
Committee Members,	Khalid A. Qaraqe Krzysztof Michalski Won-Jong Kim
Head of Department,	Costas N. Georghiades

May 2009

Major Subject: Electrical Engineering

ABSTRACT

Adaptive Power Control

for Single and Multiuser Opportunistic Systems. (May 2009)

Sung Sik Nam, B.S., Hanyang University;

M.S., Hanyang University;

M.S., University of Southern California

Co-Chairs of Advisory Committee: Dr. Mohamed-Slim Alouini
Dr. Costas N. Georghiades

In this dissertation, adaptive power control for single and multiuser opportunistic systems is investigated. First, a new adaptive power-controlled diversity combining scheme for single user systems is proposed, upon which is extended to the multiusers case. In the multiuser case, we first propose two new threshold based parallel multiuser scheduling schemes without power control. The first scheme is named on-off based scheduling (OOBS) scheme and the second scheme is named switched based scheduling (SBS) scheme. We then propose and study the performance of threshold-based power allocation algorithms for the SBS scheme. Finally, we introduce a unified analytical framework to determine the joint statistics of partial sums of ordered RVs with i.i.d. and then the impact of interference on the performance of parallel multiuser scheduling is investigated based on our unified analytical framework.

DEDICATION

*To my wife, Jung Sun Lee
my sons, Isaiah Byung Jun and Joshua Woo Jun,
my parents, and my sister's family.*

I could not have completed my study without their love, encouragement, and
patience.

*“Be joyful always, pray continually, and give thanks in all circumstances, for this is
God's will for you in Christ Jesus.”*

ACKNOWLEDGMENTS

O God of love, make us more thankful for all the boundless mercies of our daily life. Giving thanks and knowledge always for all things in the name of Christ our Lord.

There are a number of people I would like to acknowledge for giving me the great opportunity to be a graduate student; one of the most rewarding periods of my life. First, I would like to thank my advisor, Prof. Mohamed-Slim Alouini, for his continual support and invaluable advice over the years. Prof. Mohamed-Slim Alouini has always been the best reference and his continual encouragement allowed me to work quite independently. His broad expertise, right and detailed comments at the necessary time have been a source of inspiration to my research and academic interest, and broadened my depth of knowledge of my field.

I am also grateful to Professor Costas N. Georghiades for being my co-chair, and Prof. Khalid A. Qaraqe, Prof. Krzysztof Michalski, and Prof. Won-Jong Kim for sharing their important time serving on my orals and reading committee. They have been a great resource and advisors.

I would also like to thank Prof. Hong-Chuan Yang for his excellent advice and discussions on topics of common interest. Prof. Hong-Chuan Yang always shared his time to answer my questions and feedbacks. I have learned from the very best in the mathematical analysis.

I am also deeply indebted to current and past colleagues and alumni friends at Texas A&M University, University of Minnesota, and University of Southern California (USC). I will sorely miss their kindness, help, the great times and enjoyable experiences with them. In addition, I would like to thank the staff at Texas A&M

University for their kindness and effort.

I particularly want to thank to my family. Without their love, support and sacrifice, my accomplishment would never have been possible. My father and mother have always supported my every endeavor without any doubt. In particular, their integrity, sincerity, and faith to God, have been always the perfect example of life and motivation for me. I would also like to express my thanks to my sister, brother-in-law, and their son, for their belief, love, and support. Finally, I would also like to acknowledge the most important contributions made by my wife Jung Sun Lee, my sons Isaiah Byung Jun and Joshua Woo Jun for their love, patience, and sacrifice. They brought me so much love to my life. In reality, this dissertation is partly theirs, too.

NOMENCLATURE

AFL	Average Number of Feedback Load
ASE	Average Spectral Efficiency
AT-GSC	Absolute Threshold Generalized Selection Combining
AWGN	Additive White Gaussian Noise
BER	Bit Error Rate
BPSK	Binary Phase Shift Keying
BS	Base Station
CDF	Cumulative Distribution Function
CDMA	Code Division Multiple Access
CSI	Channel State Information
EDF	Exceedance Distribution Function
EGC	Equal Gain Combining
GSC	Generalized Selection Combining
GSEC	Generalized Switch and-Examine Combining
HF	High Frequency
i.i.d.	Independent and Identically Distributed
ISI	Inter Sysmbol Interference
MEC GSC	Minimum Estimation and Combining Generalized Selection Combining
MGF	Moment Generating Function
MRC	Maximal Ratio Combining
MS GSC	Minimum Selection Generalized Selection Combining
MU	Mobile Unit
MUI	Multi User Interference

M-QAM	M-Quadrature Amplitude Modulation
OOBS	On-Off Based Scheduling
OT GSC	Output Threshold Generalized Selection Combining
PDF	Probability Density Function
RV	Random Variable
SBS	Switched Based Scheduling
SC	Selection Combining
SEC	Switch-and-Examine Combining
SINR	Signal-to-Interference plus Noise Ratio
SNR	Signal-to-Noise Ratio
SSC	Switch-and-Stay Combining
TDMA	Time Division Multiple Access
UPC-DC	Up-link Power Controlled Diversity Combining

TABLE OF CONTENTS

	Page
ABSTRACT	iii
DEDICATION	iv
ACKNOWLEDGMENTS	v
NOMENCLATURE	vii
TABLE OF CONTENTS	ix
LIST OF FIGURES	xiv
CHAPTER	
I INTRODUCTION	1
II BACKGROUND	4
A. Fading Channels and Mitigation Methods	4
1. Fading Channels	4
2. Mitigation Methods	8
B. Block Fading Channel	8
C. Diversity Techniques	10
D. Adaptive Modulation	13
III DIVERSITY COMBINING WITH UP-LINK POWER CONTROL	15
A. Introduction	15
B. Models and Mode of Operation	16
1. System Model	16
2. Channel Model	17
3. Mode of Operation of UPC-DC	17
C. Performance Analysis	19
1. Statistics of the Combined SNR	19

CHAPTER	Page
2. Continuous Adaptation without Amplifier Gain Sat- uration	20
3. Continuous Adaptation with Amplifier Gain Saturation	21
4. Discrete Adaptation without Amplifier Gain Saturation	22
5. Discrete Adaptation with Amplifier Gain Saturation .	23
D. Numerical Examples	25
E. Conclusion	29
 IV	
THRESHOLD-BASED PARALLEL MULTIUSER SCHEDULING	30
A. Introduction	30
B. Models and Mode of Operation	32
1. System Model	32
2. Channel Model	33
3. Mode of Operation	33
a. OOBS Scheme	33
b. SBS Scheme	34
4. Discussion	37
C. Performance Analysis	38
1. OOBS Scheme	39
a. Statistics of the Output SNR of a Scheduled User with the OOBS Scheme	39
b. AFL	39
c. ASE	40
d. $\overline{\text{BER}}$	42
2. SBS Scheme	43
a. Statistics of the Output SNR of a Scheduled User with the SBS Scheme	43
b. AFL	49
c. ASE	50
d. $\overline{\text{BER}}$	51
D. Numerical Examples	51
E. Conclusion	57
 V	
PERFORMANCE EVALUATION OF THRESHOLD-BASED POWER ALLOCATION ALGORITHMS FOR DOWN-LINK SWITCHED-BASED PARALLEL SCHEDULING	59
A. Introduction	59
B. System and Channel Models	61

CHAPTER	Page
1. System Model	61
2. Channel Model	62
C. Power Allocation Algorithms	62
1. Algorithm 1	62
2. Algorithm 2	65
3. Algorithm 3	66
D. Simulation Results	67
E. Performance Analysis	72
1. Average Number of Effective Acceptable Users	73
2. Statistics of Output SNR	75
3. Average Spectral Efficiency	78
4. Average BER	79
F. Conclusion	79
VI A MGF-BASED UNIFIED FRAMEWORK TO DETERMINE THE JOINT STATISTICS OF PARTIAL SUMS OF OR- DERED RANDOM VARIABLES	81
A. Introduction	81
B. The Main Idea	82
1. Common Functions	87
2. Simplifying Relationship	87
C. Sample Cases When All K Ordered RVs Are Considered	88
1. Joint PDF of $\gamma_{m:K}$ and $\sum_{\substack{n=1 \\ n \neq m}}^K \gamma_{n:K}$	89
2. Joint PDF of $\sum_{n=1}^m \gamma_{n:K}$ and $\sum_{n=m+1}^K \gamma_{n:K}$	90
D. Sample Cases When Only K_s Ordered RVs Are Considered	91
1. PDF of $\sum_{n=1}^{K_s} \gamma_{n:K}$	91
2. Joint PDF of $\gamma_{m:K}$ and $\sum_{\substack{n=1 \\ n \neq m}}^{K_s} \gamma_{n:K}$	92
3. Joint PDF of $\sum_{n=1}^m \gamma_{n:K}$ and $\sum_{n=m+1}^{K_s} \gamma_{n:K}$	97
E. Closed-form Expressions for Exponential RV Case	98
F. Applications	101
1. Example i)	101
2. Example ii)	102

CHAPTER	Page	
VII	IMPACT OF INTERFERENCE ON THE PERFORMANCE OF SELECTION BASED PARALLEL MULTIUSER SCHEDULING	104
	A. Introduction	104
	B. System and Channel Models	106
	C. Statistics of the SINRs of the Scheduled Users	108
	1. Joint PDF $\gamma_{m:K}$ and $\sum_{\substack{n=1 \\ n \neq m}}^{K_s} \gamma_{n:K}$	108
	2. I.I.D Rayleigh Fading Special Case	111
	D. Performance Analysis	114
	1. Total Average Sum Rate Capacity	114
	a. Analysis	114
	b. Numerical Examples	115
	2. Average Spectral Efficiency	119
	a. Analysis	119
	b. Numerical Examples	119
	E. Conclusion	123
VIII	CONCLUSION AND FUTURE WORK	125
	A. Summary of Conclusions	125
	B. Future Research Directions	128
	REFERENCES	130
	APPENDIX A	139
	APPENDIX B	140
	APPENDIX C	141
	APPENDIX D	143
	APPENDIX E	144
	APPENDIX F	145
	APPENDIX G	147
	APPENDIX H	150

CHAPTER	Page
APPENDIX I	151
APPENDIX J	154
APPENDIX K	156
APPENDIX L	157
APPENDIX M	159
APPENDIX N	161
APPENDIX O	162
VITA	168

LIST OF FIGURES

FIGURE	Page
1	Basic mitigation methods. 9
2	Block fading channel model. 17
3	Average BER of BPSK with (i) continuous UPC-DC and no amplifier gain saturation, (ii) continuous UPC-DC and amplifier gain saturation, and (iii) MRC and no power control ($L_c = L = 6$, $\gamma_T = 5$ dB, and $G_{\max} = 3$ dB). 26
4	Average additional dB gain of the transmitter amplifier using continuous UPC-DC with and without saturation ($L_c = L = 6$, $\gamma_T = 5$ dB, and $G_{\max} = 3$ dB). 26
5	Average BER of BPSK with (i) continuous UPC-DC and no amplifier gain saturation and (ii) discrete UPC-DC and no amplifier gain saturation ($L_c = L = 6$ and $\gamma_T = 5$ dB). 27
6	Average additional dB gain of the transmitter amplifier with (i) continuous UPC-DC and no amplifier gain saturation and (ii) discrete UPC-DC and no amplifier gain saturation ($L_c = L = 6$ and $\gamma_T = 5$ dB). 27
7	Average BER of BPSK with (i) continuous UPC-DC and amplifier gain saturation and (ii) discrete UPC-DC and amplifier gain saturation ($L_c = L = 6$, $\gamma_T = 5$ dB, and $G_{\max} = 4$ dB). 28
8	Average additional dB gain of the transmitter amplifier with (i) continuous UPC-DC and amplifier gain saturation and (ii) discrete UPC-DC and amplifier gain saturation ($L_c = L = 6$, $\gamma_T = 5$ dB, and $G_{\max} = 4$ dB). 28
9	Mode of operation of the OOBs parallel scheduling scheme. 35
10	Mode of operation of the SBS parallel scheduling scheme. 36

FIGURE	Page
11	PDF comparison between the analytical and the simulation results of the SBS scheme for $K = 5$, $K_s = 3$, $\gamma_T = 10$ dB , $\bar{\gamma} = 10$ dB, and i.i.d. Rayleigh fading condition. 48
12	Average BER of adaptive coded M-QAM modulation with the (i) OOBS scheme, (ii) SBS scheme, and (iii) GSC based scheduling scheme for $K = 5$, $K_s = 3$, and i.i.d. Rayleigh fading conditions. . . . 54
13	Average feedback loads for the (i) OOBS scheme, (ii) SBS scheme, and (iii) GSC based scheduling scheme ($K = 5$ and $K_s = 3$). 56
14	Average spectral efficiencies of adaptive coded M-QAM modulation for the (i) OOBS scheme, (ii) SBS scheme, and (iii) GSC based scheduling scheme over i.i.d. Rayleigh fading conditions with $K = 5$ and $K_s = 3$ 58
15	Flowchart of the power allocation process for algorithm 1. 64
16	Flowchart of the power allocation process for algorithm 3. 68
17	Average number of effective acceptable users with SBS over i.i.d. Rayleigh fading conditions with $K = 20$, $K_s = 15$, and $\gamma_T = \gamma_{TP} = 7.1$ dB. 69
18	ASE with SBS over i.i.d. Rayleigh fading conditions with $K = 20$, $K_s = 15$, and $\gamma_T = \gamma_{TP} = 7.1$ dB. 71
19	Average BER with SBS over i.i.d. Rayleigh fading conditions with $K = 20$, $K_s = 15$, and $\gamma_T = \gamma_{TP} = 7.1$ dB. 72
20	Examples for 3-dimensional joint PDF with non-splitted groups. . . . 85
21	Examples for 3-dimensional joint PDF with splitted groups. 85
22	Flow Chart. 86
23	Joint MGF of $\gamma_{m:K}$ and $\sum_{\substack{n=1 \\ n \neq m}}^{K_s} \gamma_{n:K}$ 94
24	Total average sum rate capacity as a function of the average SNR for selection based parallel multiuser scheduling over i.i.d. Rayleigh fading channels with $K = 20$ and various values of K_s and α 116

FIGURE	Page
25	Total average sum rate capacity of scheduled users as a function of the number of scheduled users for selection based parallel multiuser scheduling over i.i.d. Rayleigh fading channels with $K = 20$ and various values of α 117
26	Average spectral efficiency of scheduled users as a function of the average SNR for selection based parallel multiuser scheduling over i.i.d. Rayleigh fading channels with $K = 20$ and various values of K_s and α . . . 120
27	Average spectral efficiency of scheduled users as a function of the number of scheduled users for selection based parallel multiuser scheduling over i.i.d. Rayleigh fading channels with $K = 20$ and various values of α 121

CHAPTER I

INTRODUCTION

Wireless communications are subject to a complex and harsh radio propagation environment which leads to frequent fading dips in the received signal. In addition, there exist constraints such that a limited radio spectrum and a limited power and size for hand-held terminals. These difficult conditions make reliable communication very hard, and, as a result, various effective fading mitigation techniques are required to improve the performance of these systems. For instance, power control and diversity combining are typically used in existing and emerging wireless communication systems to mitigate the problem of signal power fading. In this dissertation, we look into adaptive power control for single and multiuser opportunistic systems. First, we propose a new adaptive power-controlled diversity combining scheme for single user system. After that, we extend it to the multiusers case. In the multiuser case, we first propose a threshold based parallel multiuser scheduling schemes without power control. The first scheme is named on-off based scheduling (OOBS) scheme and the second scheme is named switched based scheduling (SBS) scheme. We then propose threshold-based power allocation algorithms for the SBS scheme. Finally, we introduce a unified analytical framework to determine the joint statistics of partial sums of ordered random variables (RVs) with independent identical distributions (i.i.d) and then we investigate the impact of interference on the performance of parallel multiuser scheduling based on our unified analytical framework to determine the joint statistics of partial sums of ordered RVs with i.i.d. In conventional parallel multiuser scheduling schemes, every scheduled user is interfering with every other scheduled

user. This is a factor which limits the capacity and performance of multiuser systems and the level of interference becomes substantial as the number of scheduled users increases. Based on the above motivation, we investigate the trade-off between the throughput and the number of scheduled users.

For the new adaptive power-controlled diversity combining scheme, the system reduces the average transmitted power of the mobile units while meeting a certain minimum required quality of service. The key idea is i) to collect and combine all the available diversity paths at the base station and then ii) to request the mobile unit to increase or decrease its transmitted power just to track the required target signal-to-noise ratio (SNR). Four power control variants accounting for practical implementation constraints including discrete power levels and transmitter gain saturation are proposed and studied.

In the second part of our work, we propose i) an OOBS scheme and ii) an SBS scheme. The objective is to reduce the complexity of implementation without a considerable performance loss in comparison with conventional selection based scheduling. While the OOBS scheme schedules all the users with an SNR above a fixed preselected SNR threshold, the SBS scheme schedules only the K_s users with an acceptable SNR if there are enough acceptable users. Otherwise, the scheduler selects the best K_s users. We analyze statistical characteristics and performances of these proposed schemes.

In the third part of our work, we propose and study threshold-based power allocation algorithms for our proposed down-link SBS scheme. In our proposed algorithms, the system re-allocates the extracted excess SNR from some acceptable users to unacceptable users among the scheduled users. After the power allocation process, the unacceptable users can reach acceptable SNRs and as such the number of effective acceptable users with an acceptable SNR threshold among the scheduled users is

increased without any additional down-link transmit power.

In the fourth part of our work, we introduce a unified analytical framework to determine the joint statistics of partial sums of ordered RVs with i.i.d. With the proposed approach, we can systematically derive the joint statistics of any partial sums of ordered statistics, in terms of the moment generating function (MGF) and probability density function (PDF), not only when all the K ordered RVs are considered but also when only the K_s ($K_s < K$) best RVs are considered among K RVs. In addition, we derive the closed form expressions for the exponential special case. These results can apply to the performance analysis of various wireless communication systems over i.i.d. Rayleigh fading conditions.

Finally, we investigate the impact of interference on the performance of selection based parallel multiuser scheduling based on our unified analytical framework to determine the joint statistics of partial sums of ordered RVs with i.i.d. In particular, we derive the total average sum rate capacity and the average spectral efficiency (ASE). The major difficulty in the total average sum rate capacity and the ASE analysis resides in the determination of the statistics of the signal-to-interference plus noise ratio (SINR) of the scheduled user. Fortunately, we can derive the accurate statistical characterization of the SINR of the scheduled user in terms of the MGF and PDF. With these accurate statistical analysis, we derive the total average sum rate capacity and the average spectral efficiency based on the SINR.

CHAPTER II

BACKGROUND

The primary goal of this chapter is to introduce models, terminology and notations which will be used through the dissertation. Therefore, we briefly review the principal characteristics and models of fading channels, the basic mitigation techniques (i.e. diversity techniques and adaptive modulation) for combating the effects of channel fading.

A. Fading Channels and Mitigation Methods

1. Fading Channels

There are three basic mechanisms that impact signal propagation in a mobile communication system. They are reflection, diffraction, and scattering [1–4]:

- Reflection occurs when a propagating electromagnetic wave impinges on a smooth surface with very large dimensions compared to the RF signal wavelength (λ).
- Diffraction occurs when the radio path between the transmitter and receiver is obstructed by a dense body with large dimensions compared to λ , causing secondary waves to be formed behind the obstructing body. Diffraction is a phenomenon that accounts for RF energy traveling from transmitter to receiver without a line-of-sight path between the two. It is often termed shadowing because the diffracted field can reach the receiver even when shadowed by an impenetrable obstruction.
- Scattering occurs when a radio wave impinges on either a large rough surface or any surface whose dimensions are on the order of λ or less, causing the reflected

energy to spread out (scatter) in all directions. In an urban environment, typical signal obstructions that yield scattering are lampposts, street signs, and foliage.

In a wireless mobile communication system, a signal can travel from transmitter to receiver over multiple reflective paths; this phenomenon is referred to as multipath propagation [1–3, 5, 6]. The effect can cause fluctuations in the received signal’s amplitude, phase, and angle of arrival, giving rise to the terminology multipath fading. Another name, scintillation, which originated in radio astronomy, is used to describe the multipath fading caused by physical changes in the propagating medium, such as variations in the density of ions in the ionospheric layers that reflect high-frequency (HF) radio signals. Both names, fading and scintillation, refer to a signals random fluctuations or fading due to multipath propagation. The main difference is that scintillation involves mechanisms (e.g., ions) that are much smaller than a wavelength. The end-to-end modeling and design of systems that mitigate the effects of fading are usually more challenging than those whose sole source of performance degradation is additive white gaussian noise (AWGN).

The most common way of classification of fading can be represented by two types of fading effects that characterize mobile communications: large-scale and small-scale fading [1–3, 5, 6].

- Large-Scale fading (Shadowing) : Large-scale fading represents the average signal power attenuation or path loss due to motion over large areas. This phenomenon is affected by prominent terrain contours (hills, forests, billboards, clumps of buildings, etc.) between the transmitter and receiver. The receiver is often represented as being “shadowed” by such prominences. The statistics of large-scale fading provide a way of computing an estimate of path loss as a function of distance. This is described in terms of a mean-path loss (n-th power

law) and a log-normally distributed variation about the mean. Small-scale fading refers to the dramatic changes in signal amplitude and phase that can be experienced as a result of small changes (as small as a half-wavelength) in the spatial separation between a receiver and transmitter.

- Small-Scale fading (Multi-path fading) : Small-scale fading manifests itself in two mechanisms, namely, time-spreading of the signal (or signal dispersion) and time-variant behavior of the channel. For mobile radio applications, the channel is time-variant because motion between the transmitter and receiver results in propagation path changes. The rate of change of these propagation conditions accounts for the fading rapidity (rate of change of the fading impairments). Small-scale fading is also called Rayleigh fading because if the multiple reflective paths are large in number and there is no line-of-sight signal component, the envelope of the received signal is statistically described by a Rayleigh PDF. When there is a dominant non-fading signal component present, such as a line-of-sight propagation path, the smallscale fading envelope is described by a Rician PDF [4, 6, 7].

For signal dispersion, we categorize the degradation types of small-scale fading as frequency-selective or frequency-nonselective (flat) and for the time-variant manifestation, we categorize the fading degradation types as fast-fading or slow-fading [1–3, 5, 6] as the following:

The terminology “fast fading” is used to describe channels in which the channel coherence time is less than the time duration of a transmission symbol. Fast fading describes a condition where the time duration in which the channel behaves in a correlated manner is short compared to the time duration of a symbol. Therefore, it can be expected that the fading character of the channel will change several times while a

symbol is propagating, leading to distortion of the baseband pulse shape. Analogous to the distortion previously described as channel induced inter symbol interference (ISI), here distortion takes place because the received signal's components are not all highly correlated throughout time. Hence, fast fading can cause the baseband pulse to be distorted, resulting in a loss of SNR that often yields an irreducible error rate. Such distorted pulses cause synchronization problems (failure of phase-locked-loop receivers), in addition to difficulties in adequately defining a matched filter.

A channel is generally referred to as introducing slow fading if the channel coherence time is greater than the time duration of a transmission symbol. Here, the time duration that the channel behaves in a correlated manner is long compared to the time duration of a transmission symbol. Thus, one can expect the channel state to virtually remain unchanged during the time in which a symbol is transmitted. The propagating symbols will likely not suffer from the pulse distortion described above. The primary degradation in a slow-fading channel, as with flat fading, is loss in SNR.

A channel is referred to as frequency-selective if the bandwidth of the transmission symbol is greater than the coherence bandwidth of the channel. Frequency-selective fading distortion occurs whenever a signal's spectral components are not all affected equally by the channel. Some of the signal's spectral components, falling outside the coherence bandwidth, will be affected differently (independently) compared to those components contained within the coherence bandwidth.

Frequency-nonselective or flat fading degradation occurs whenever the bandwidth of the transmission symbol is less than the coherence bandwidth of the channel. Hence, all of the signal's spectral components will be affected by the channel in a similar manner (e.g., fading or no fading). Flat-fading does not introduce channel-induced ISI distortion, but performance degradation can still be expected due to loss in SNR whenever the signal is fading.

Note that large-scale fading is more relevant to issues such as cell-site planning while small-scale fading is more relevant to the design of reliable and efficient communication systems. In this dissertation, we focus on small-scale fading caused mainly by multiple paths.

2. Mitigation Methods

If the channel introduces signal distortion as a result of fading, the system performance can exhibit an irreducible error rate; when larger than the desired error rate, no amount of E_b/N_0 will help achieve the desired level of performance. In such cases, the general approach for improving performance is to use some form of mitigation to remove or reduce the distortion. The mitigation method depends on whether the distortion is caused by frequency-selective or fast fading.

In Fig. 2 from [8], several mitigation techniques for combating the effects of both signal distortion and loss in SNR are listed. The mitigation approach to be used should follow two basic steps: first, provide distortion mitigation; next, provide diversity.

B. Block Fading Channel

Through this dissertation, we adopt a block fading channel model. The block-fading channel was introduced in [9–11] in order to model slowly varying fading. The block fading channel is a simplified, generic model for a slow, frequency selective or non-selective fading channel subject to average input energy and decoding delay constraints, where the received signal is accompanied by AWGN. It is assumed throughout that the fading process occurs in blocks during which K symbols are transmitted. In other words, the fading level is a sequence of random variables (RV) which are in-

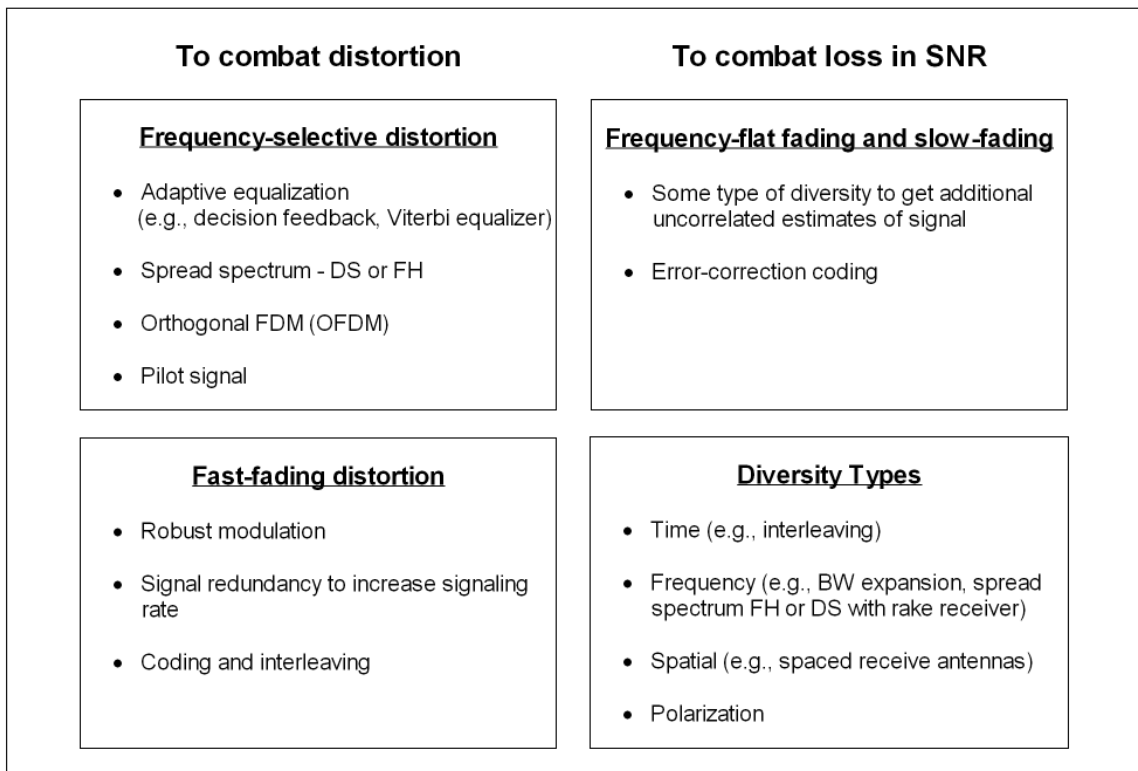


Fig. 1. Basic mitigation methods.

dependent identically distributed (i.i.d.) from block to block, with any of the popular fading models such as Rayleigh, Rice, or Nakagami-m. More specifically, the data burst is divided into K blocks of duration T and each block is transmitted through a faded multipath channel which is assumed constant through the whole block but may vary from one block to the other. In this model, the data burst is assumed to experience roughly the same fading as that occurring in the preceding guard period. On the other hand, the fading conditions during different guard period and data burst pairs are assumed to be independent. In addition, we assume that the fading on each diversity path follows any of the popular fading models such as Rayleigh, Rice, or Nakagami-m.

C. Diversity Techniques

Many of the current and emerging wireless communication systems use diversity techniques [6, 7] to combat the effects of multipath fading. Indeed, diversity combining, in which two or more copies of the same information bearing signal are skillfully combined in order to increase the overall SNR, still offers one of the greatest potentials for radio link performance improvement to many of the current and future wireless technologies.

Diversity combining consists of i) receiving redundantly the same information bearing signal over 2 or more fading channels and then ii) combining these multiple replicas at the receiver in order to increase the overall received SNR.

The intuition behind diversity combining is to take advantage of the low probability of concurrence of deep fades in all the diversity branches to lower the probability of error and outage.

Multiple replicas can be obtained by extracting the signals via different radio

paths as the following:

- Space: Multiple receiver antennas (antenna or site diversity).
- Frequency: Multiple frequency channels which are separated by at least the coherence bandwidth of the channel (frequency hopping or multicarrier systems).
- Time: Multiple time slots which are separated by at least the coherence time of the channel (coded systems).
- Multipath: Resolving multipath components at different delays (direct-sequence spread-spectrum systems with RAKE reception).

Diversity schemes can be classified according to the type of combining employed at the receiver. At this point, we should distinguish the classical “pure” combining schemes from the more recently proposed “hybrid” techniques. There are four principal types of combining techniques [2, 3, 5–7, 12] that depend essentially on the i) complexity restrictions put on the communication system and ii) amount of channel state information (CSI) available at the receiver as the following:

- Maximal-ratio combining (MRC):
 - Optimal scheme but requires knowledge of all channel parameters (i.e., fading amplitude and phase of every diversity path).
 - Used with coherent modulations.
- Equal gain combining (EGC)
 - Coherent version limited in practice to constant envelope modulations.
 - Noncoherent version optimum in the maximum-likelihood sense for i.i.d. Rayleigh channels.

- Selection combining (SC)
 - Uses the diversity path/branch with the best quality.
 - Requires simultaneous and continuous monitoring of all diversity branches.
- Switched (or scanning diversity)
 - Two variants: Switch-and-stay combining (SSC) and switch-and-examine combining (SEC).
 - Least complex diversity scheme.

Because of additional complexity constraints or because of the potential of a higher diversity gain with more sophisticated diversity schemes, newly proposed hybrid techniques have been receiving a great deal of attention in view of their promising offer to meet the specifications of emerging wideband communication systems. These schemes can be categorized into two groups: i) Generalized selection combining (GSC) [13–19] and generalized switch and-examine combining (GSEC) [20–22] and ii) Two-dimensional diversity schemes. Additionally, recently newly proposed hybrid diversity techniques have been a great deal of attention in view of their promising offer to meet the specifications of emerging wideband communications system. As a power-saving implementation of GSC, minimum selection GSC (MS-GSC) [23–26], minimum estimation and combining GSC (MEC-GSC) [27], and output-threshold GSC (OT-GSC) [28, 29] were recently proposed. With MS GSC, after examining and ranking all available paths, the receiver tries to raise the combined SNR above a certain threshold by combining in an MRC fashion the least number of the best diversity paths and as such, MS-GSC can save considerable amount of processing power by keeping less MRC branch active on average in comparison to the conventional GSC scheme. Further estimation savings can be done by using MEC-GSC. On an other

hand, OT-GSC successively estimates available diversity paths and applies MRC or GSC to them in order to make the combined SNR exceed a certain SNR threshold.

D. Adaptive Modulation

Adaptive modulation schemes [30–39] are currently receiving a great deal of attention as very promising techniques to achieve high spectral efficiency.

The basic concept of adaptive transmission is real link budget through adaptive variation of the transmitted power level, symbol transmission rate, constellation size, coding rate, scheme, or any combination of these parameters. Thus, without wasting power or sacrificing BER, these schemes provide a higher average link spectral efficiency by taking advantage of the time-varying nature of wireless channels, transmitting at high speeds under favorable channel conditions and responding to channel degradation through a smooth reduction of their data throughput. Furthermore since outage probability of such schemes can be quite high especially for channels with low average SNR, buffering of the input data may be required, and adaptive systems are therefore best suited to applications without stringent delay constraints.

Wireless transmission schemes have traditionally been designed for the worst-case scenario by focusing on enabling the system to perform acceptably even in deep fading conditions. With such a design principle, spectral efficiency is sacrificed for link reliability. A design principle focusing more on spectral efficiency is rate-adaptive transmission, where the basic concept is to exploit and track the time varying characteristics of the wireless channel to transmit with as high information rate as possible when the channel quality is good, and to lower the information rate (and trade it for link reliability) when the channel quality is reduced. With such a transmission scheme, a feedback channel is required, on which the receiver reports channel state

information (CSI) to the transmitter. Based on the reported CSI, the transmitter can make a decision on which rate to employ for the next transmission period. In particular, the transmitter may choose to select symbols from the biggest constellation meeting a predefined BER requirement, to ensure that the spectral efficiency is maximized for an acceptable (target) BER.

For example, let the regions be defined by the thresholds $\gamma_1 < \gamma_2 < \dots < \gamma_{N+1}$. When the instantaneous SNR γ falls within the fading region $\gamma_n \leq \gamma < \gamma_{n+1}$, the associated CSI, i.e. the fading region index n , is sent back to the transmitter. The transmitter then adapts its transmission rate and coding scheme by transmitting with a code realizing a spectral efficiency of R_n (measured in [bits/s/Hz]). The spectral efficiencies of the applied codes are organized such that $R_1 < R_2 < \dots < R_N$. This enables the system to transmit with high spectral efficiency when the instantaneous SNR is high, and to reduce the spectral efficiency as the SNR decreases. The target BER is not achieved when $\gamma < \gamma_1$, so no information is transmitted when γ falls into the leftmost interval $0 \leq \gamma < \gamma_1$ (outage). During this situation, the information must be buffered at the transmitter.

CHAPTER III

DIVERSITY COMBINING WITH UP-LINK POWER CONTROL*

A. Introduction

As mentioned in the previous chapter, wireless communication systems are subject to a harsh propagation environment which leads to frequent fading dips in the received signal. These tough conditions make reliable communication very hard, and, as a result, various fading countermeasure techniques are needed to improve the performance of these systems. For instance, power control and diversity combining are typically used in existing and emerging wireless communication systems to mitigate the problem of signal power fading. In this chapter, inspired by the mode of operation of power control algorithms in the 3GPP standard [40], we propose and study an up-link power controlled diversity combining (UPC-DC) scheme. As its name indicates, UPC-DC combines the features of classical diversity combining with some up-link power control from the mobile unit (MU) to the base station (BS). UPC-DC capitalizes first on diversity combining by collecting and combining all the available diversity paths at the BS. Subsequently and based on the resulting combined signal-to-noise ratio (SNR), the BS requests via a feedback path the MU to increase or decrease its transmitted power just to track a particular required target SNR. In this chapter, we study the performance of the proposed scheme and show how this scheme reduces the average bit-error-rate (BER) with, of course, an attendant (and quantifiable) small increase in transmitted power only in the low average SNR range.

*Reprinted with permission from “Diversity Combining with Up-Link Power Control” by S. S. Nam, 2008, *Wiley Journal on Wireless Communications and Mobile Computing*, vol. 8, no. 9, pp. 1091 - 1101, Copyright [2008] by John Wiley & Sons.

The remainder of the chapter is organized as follows. Section B presents the system and channel models then gives the details behind the mode of operation of various variants of UPC-DC. While section C provides some analytical results, section D illustrates these results via some selected figures. Finally, section E offers some concluding remarks.

B. Models and Mode of Operation

1. System Model

We consider a generic diversity system with L available diversity paths. This includes for example, RAKE receivers which are used in wideband CDMA systems to combine the available resolvable multipaths. For hardware complexity considerations, we assume that up to L_c branches can be combined at the receiver side (i.e., the number of fingers of the RAKE receiver is limited to L_c). We also assume that the proposed UPC-DC scheme has a reliable feedback path between the receiver and the transmitter and is implemented in a discrete-time fashion. More specifically, and as shown in Fig. 2, short guard periods are periodically inserted into the transmitted signal. During these guard periods, the receiver performs a series of operation, including (i) path estimation, (ii) combined SNR comparison with respect to the predetermined SNR threshold, and (iii) request to the MU power amplifier to increase or decrease its gain by a specific amount. Once all the available diversity paths are selected and once the appropriate transmitted power is reached, the combiner (at the receiver end) and the power amplifier (at the transmitter) are configured accordingly and this transmitter and receiver settings are used throughout the subsequent data burst.

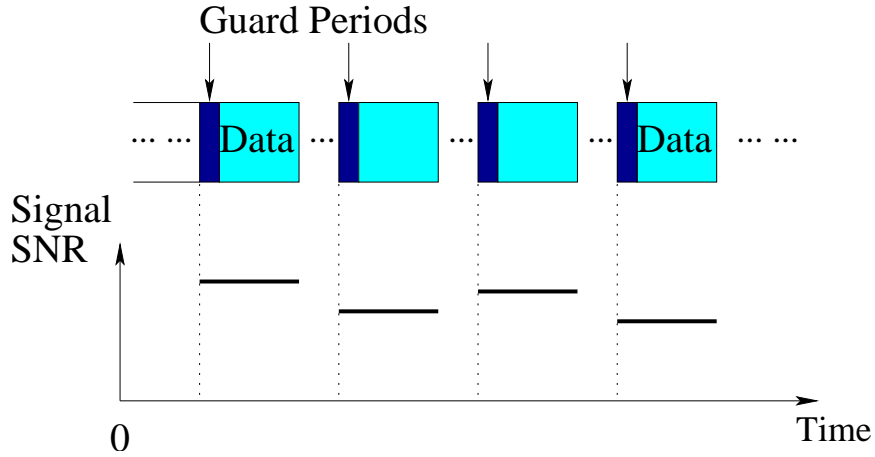


Fig. 2. Block fading channel model.

2. Channel Model

We denote by γ_l ($l = 1, 2, \dots, L$), the received SNR of the l th diversity path (under nominal transmitted power from the MU ¹) and, as illustrated in Fig. 2, we adopt a block flat fading channel model. More specifically, assuming slowly-varying fading conditions, the different diversity paths experience roughly the same fading conditions (or equivalently the same SNR) during the data burst and its preceding guard period. In addition, the fading conditions are assumed to (i) be independent across the diversity paths and between different guard period and data burst pairs, and (ii) follow anyone of the popular fading models such as Rayleigh, Rice, or Nakagami- m .

3. Mode of Operation of UPC-DC

If the number L of available paths in the BS is below the number L_c of paths that can be combined, the BS combines all the available paths as per the rules of maximal-

¹The MU nominal transmitted power is assumed to correspond to an initial level of output power that is adjusted/set to minimize the average outer cell interference in a particular deployment.

ratio combining (MRC) [6]. On the other hand, if the number L of available diversity paths exceeds the number L_c of paths that can be combined, the BS uses generalized selection combining (GSC) (see for example [41–44]). With GSC, the L_c (among the L available) diversity branches with the best quality (quantified for example in terms of fading amplitude or equivalently instantaneous SNR)) are selected and combined in an MRC fashion. At the beginning of the guard period, the MU power amplifier gain G (with respect to the nominal transmitted power) is initially set to 0 dB and based on this setting the combining process described above is performed. If the combiner fails to meet the γ_T requirement during the combining process phase, the receiver activates the power control mechanism and requests the transmitter to increase its gain in order to meet the target SNR requirement. If on the other hand, the required output SNR γ_T is reached during this initial phase, then the receiver activates also the power control mechanism but requests in this case the transmitter to decrease its gain such that the output combined SNR just matches the target SNR requirement. We consider in our study, four power adaptation variants:

1. **Continuous Adaptation without Amplifier Gain Saturation** In this first ideal case, we assume that the gain of the MU amplifier G can be adjusted in a continuous fashion and is not limited by any maximal value.
2. **Continuous Adaptation with Amplifier Gain Saturation** In this case, we still assume that the gain of the transmitter amplifier can be adjusted continuously but saturates to a certain maximal value G_{\max} . In the case, that a gain beyond G_{\max} is needed to meet the required target SNR, we assume that the MU units deactivates the power control mechanism and transmits with the nominal power level. This is done to save some valuable battery lifetime but comes of course at the expense of the violation of the target SNR requirement

in very adverse channel fading conditions.

3. **Discrete Adaptation without Amplifier Gain Saturation** Similar to the power control algorithms that are implemented in the 3 GPP standard, we assume in this case that the MU amplifier gain can only take discrete values. This gain can be adjusted using a binary feedback and a power control step size G_δ .
4. **Discrete Adaptation with Amplifier Gain Saturation** In this most practical case, we assume that the gain takes discrete values and saturates to a fixed maximal value G_{\max} . We again assume that the MU transmits with nominal power level if a gain beyond G_{\max} is needed to meet the required target SNR.

C. Performance Analysis

1. Statistics of the Combined SNR

Regardless of the type of adaptation used, the probability density function (PDF), $p_{\gamma_c}(\cdot)$, of the combined SNR at the end of the diversity combining stage is given by

$$p_{\gamma_c}(\gamma) = (1 - P_L(L_c))p_{\gamma_{\text{mrc}}}(\gamma) + P_L(L_c)p_{\gamma_{\text{gsc}}}(\gamma), \quad (3.1)$$

where $P_L(l) = P[L \leq l]$ is the cumulative distribution function (CDF) of the number of available diversity paths in the area of deployment, which can be for example modeled by a Poisson distribution [45, 46], $p_{\gamma_{\text{mrc}}}(\cdot)$ is the PDF at the output of an L -branch MRC diversity combiner which is known in closed-form for many fading scenarios of interest [6], and $p_{\gamma_{\text{gsc}}}(\cdot)$ is the PDF at the output of a GSC receiver combining the L_c strongest branches among the L available ones which is also known in closed-form for many fading scenarios of interest [6].

With the PDF of the combined SNR available, we can find the average BER and the additional average dB gain G^2 that is required by the uplink power control for the four power adaptation variants under consideration. In the following we provide the final analytical formulas as well as some selected numerical results illustrating the performance of our proposed UPC-DC. Detailed derivations of the formulas are given in Appendices.

2. Continuous Adaptation without Amplifier Gain Saturation

In this case, the average BER is constant and equal to $\text{BER}(\gamma_T)$, where $\text{BER}(\gamma)$ is the BER of the modulation when used over an additive white Gaussian noise (AWGN) channel with SNR γ . The corresponding additional average dB gain can be shown to be given by

$$G_{\text{dB}} = \gamma_{T_{\text{dB}}} - 10 \int_0^\infty \log_{10}(\gamma) p_{\gamma_c}(\gamma) d\gamma. \quad (3.2)$$

For independent identically distributed (i.i.d.) Rayleigh fading conditions and $L_c \geq L$ (i.e. the receiver combines the L available diversity paths in an MRC fashion), the combined SNR is given by [7, Eq.(6.23)] as

$$p_{\gamma_c}(\gamma) = \frac{1}{(L-1)! \bar{\gamma}^L} \gamma^{L-1} e^{-\frac{\gamma}{\bar{\gamma}}}, \quad (3.3)$$

where $\bar{\gamma}$ is the average SNR per symbol.

Inserting (3.3) in (3.2), it can be shown with the help of [47, Eq. (4.352.1)] and [47, Eq. (8.365.4)] that

$$G_{\text{dB}} = \gamma_{T_{\text{dB}}} - \frac{10}{\ln 10} \left(-C + \sum_{l=1}^{L-1} \frac{1}{l} + \ln \bar{\gamma} \right), \quad (3.4)$$

²The additional average dB gain G_{dB} is defined as the average of the additional dB gain and is therefore given by $G_{\text{dB}} = E[\gamma_{T_{\text{dB}}} - \gamma_{c_{\text{dB}}}]$

where $C = 0.577215664$ is the Euler constant.

3. Continuous Adaptation with Amplifier Gain Saturation

In this case, the average BER can be shown to be given by

$$\begin{aligned} \text{BER} &= \int_0^{\gamma_T/G_{\max}} \text{BER}(\gamma) p_{\gamma_c}(\gamma) d\gamma + \\ &+ \text{BER}(\gamma_T)(1 - P_{\gamma_c}(\gamma_T/G_{\max})), \end{aligned} \quad (3.5)$$

where $P_{\gamma_c}(\cdot)$ is the CDF of the combined SNR at the end of the combining phase and which is known to be given by [7, Eq.(6.25)] as

$$\begin{aligned} P_{\gamma_c}(\gamma) &= \int_0^{\gamma} p_{\gamma_c}(x) dx \\ &= 1 - \frac{\Gamma\left(L, \frac{\gamma}{\bar{\gamma}}\right)}{(L-1)!}, \end{aligned} \quad (3.6)$$

where $\Gamma(\cdot, \cdot)$ is the incomplete gamma function defined for positive integer n in [47, Eq. (8.352.2)] as

$$\Gamma(n, x) = (n-1)! e^{-x} \sum_{m=0}^{n-1} \frac{x^m}{m!}, \quad (3.7)$$

and for general real α as [47, Eq. (8.350.2)]

$$\Gamma(\alpha, x) = \int_x^{+\infty} t^{\alpha-1} e^{-t} dt. \quad (3.8)$$

For binary phase shift keying (BPSK), the BER(γ) over AWGN is known to be given by the following

$$\text{BER}(\gamma) = 0.5 \operatorname{erfc}(\sqrt{\gamma}), \quad (3.9)$$

where $\operatorname{erfc}(\cdot)$ is the complementary error function defined in [47, Eq. (8.350.2)] as

$$\operatorname{erfc}(x) = \frac{2}{\sqrt{\pi}} \int_x^{+\infty} e^{-t^2} dt. \quad (3.10)$$

Inserting (3.3), (3.6), and (3.9) in (3.5), (3.5) can be re-written in closed-form by using [47, Eq. (2.321.2)] followed by integration by part yielding

$$\begin{aligned} \text{BER} = & 0.5 \left[-\operatorname{erfc}(\sqrt{\gamma}) \frac{\Gamma\left(L, \frac{\gamma}{\bar{\gamma}}\right)}{(L-1)!} \right]_0^{\frac{\gamma_T}{G_{\max}}} \\ & + 0.5 \sum_{l=0}^{L-1} \frac{1}{\sqrt{\pi} l!} \left(\frac{1}{\bar{\gamma}}\right)^l \mu^{-(l+\frac{1}{2})} \left[\Gamma\left(l + \frac{1}{2}, \mu\gamma\right) \right]_0^{\frac{\gamma_T}{G_{\max}}} \\ & + 0.5 \operatorname{erfc}(\sqrt{\gamma_T}) \frac{\Gamma\left(L, \frac{\gamma_T}{\bar{\gamma} G_{\max}}\right)}{(L-1)!}, \end{aligned} \quad (3.11)$$

where $\mu = 1 + \frac{1}{\bar{\gamma}}$.

The corresponding additional average dB gain can be shown to be given by

$$\begin{aligned} G_{\text{dB}} = & \gamma_{T_{\text{dB}}} (1 - P_{\gamma_c}(\gamma_T/G_{\max})) \\ & - 10 \int_{\frac{\gamma_T}{G_{\max}}}^{+\infty} \log_{10}(\gamma) p_{\gamma_c}(\gamma) d\gamma. \end{aligned} \quad (3.12)$$

For i.i.d. Rayleigh fading conditions and $L_c \geq L$, we show in Appendix B that (3.12) can be written in the desired closed form as

$$\begin{aligned} G_{\text{dB}} = & \frac{\gamma_{T_{\text{dB}}}}{(L-1)!} \Gamma\left(L, \frac{\gamma_T}{\bar{\gamma} G_{\max}}\right) \\ & - \frac{10}{\ln 10} \frac{1}{(L-1)!} \left(\frac{\gamma_T}{\bar{\gamma} G_{\max}}\right)^L \ln\left(\frac{\gamma_T}{G_{\max}}\right) \Gamma\left(L, \frac{\gamma_T}{\bar{\gamma} G_{\max}}\right) \\ & - \frac{10}{\ln 10} \sum_{l=0}^{L-1} \frac{\Gamma\left(l, \frac{\gamma_T}{\bar{\gamma} G_{\max}}\right)}{l!}. \end{aligned} \quad (3.13)$$

4. Discrete Adaptation without Amplifier Gain Saturation

In this case, the average BER can be shown to be given by

$$\text{BER} = \sum_{k=-\infty}^{+\infty} \int_{10^{\frac{\gamma T_{\text{dB}} - k G_{\text{dB}}}{10}}}^{10^{\frac{\gamma T_{\text{dB}} - (k-1) G_{\text{dB}}}{10}}} \text{BER} \left(10^{\frac{k G_{\text{dB}}}{10}} \gamma \right) p_{\gamma_c}(\gamma) d\gamma. \quad (3.14)$$

For i.i.d. Rayleigh fading conditions and $L_c \geq L$, we show in Appendix C that

$$\begin{aligned} \text{BER} = & \sum_{k=-\infty}^{+\infty} 0.5 \left[-\text{erfc}(\sqrt{a(k)}\gamma) \frac{\Gamma\left(L, \frac{\gamma}{\bar{\gamma}}\right)}{(L-1)!} \right. \\ & \left. + \sum_{l=0}^{L-1} \sqrt{\frac{a(k)l}{\pi}} \left(\frac{1}{\bar{\gamma}}\right)^l \beta^{-(l+\frac{1}{2})} \Gamma\left(l+\frac{1}{2}, \beta\gamma\right) \right] \int_{10^{\frac{\gamma T_{\text{dB}} - k G_{\text{dB}}}{10}}}^{10^{\frac{\gamma T_{\text{dB}} - (k-1) G_{\text{dB}}}{10}}} d\gamma, \end{aligned} \quad (3.15)$$

where $a(k) = 10^{\frac{k G_{\text{dB}}}{10}}$ and $\beta = a(k) + \frac{1}{\bar{\gamma}}$.

The corresponding additional average dB gain can be easily shown to be given by

$$G_{\text{dB}} = \sum_{k=-\infty}^{+\infty} P_{\gamma_c} \left(10^{\frac{\gamma T_{\text{dB}} - (k-1) G_{\text{dB}}}{10}} \right) G_{\text{dB}}. \quad (3.16)$$

For i.i.d. Rayleigh fading conditions and $L_c \geq L$, we get after using (3.6) the desired closed form result as

$$G_{\text{dB}} = \sum_{k=-\infty}^{+\infty} \left(1 - \frac{\Gamma\left(L, \frac{10^{\frac{\gamma T_{\text{dB}} - (k-1) G_{\text{dB}}}{10}}}{\bar{\gamma}}\right)}{(L-1)!} \right) G_{\text{dB}}. \quad (3.17)$$

5. Discrete Adaptation with Amplifier Gain Saturation

In this case, the average BER can be shown to be given by

$$\begin{aligned} \text{BER} = & \sum_{k=-\infty}^{+K_M} \int_{10^{\frac{\gamma T_{\text{dB}} - k G_{\text{dB}}}{10}}}^{10^{\frac{\gamma T_{\text{dB}} - (k-1) G_{\text{dB}}}{10}}} \text{BER} \left(10^{\frac{k G_{\text{dB}}}{10}} \gamma \right) p_{\gamma_c}(\gamma) d\gamma \\ & + \int_0^{\gamma_T / G_{\text{max}}} \text{BER}(\gamma) p_{\gamma_c}(\gamma) d\gamma, \end{aligned} \quad (3.18)$$

where $K_M = G_{\max\text{dB}}/G_{\delta\text{dB}}$. For i.i.d. Rayleigh fading conditions and $L_c \geq L$, we can get the desired closed form by applying (3.11) and (3.15) to (3.18) yielding

$$\begin{aligned}
\text{BER} = & \sum_{k=-\infty}^{K_M} 0.5 \left[-\text{erfc}(\sqrt{a(k)\gamma}) \frac{\Gamma\left(L, \frac{\gamma}{\bar{\gamma}}\right)}{(L-1)!} \right. \\
& + \sum_{l=0}^{L-1} \sqrt{\frac{a(k)1}{\pi}} \frac{1}{l!} \left(\frac{1}{\bar{\gamma}}\right)^l \beta^{-(l+\frac{1}{2})} \Gamma\left(l+\frac{1}{2}, \beta\gamma\right) \left. \right]_{10^{\frac{\gamma T_{\text{dB}} - (k-1)G_{\delta\text{dB}}}{10}}}^{10^{\frac{\gamma T_{\text{dB}} - kG_{\delta\text{dB}}}{10}}} \\
& + 0.5 \left[-\text{erfc}(\sqrt{\gamma}) \frac{\Gamma\left(L, \frac{\gamma}{\bar{\gamma}}\right)}{(L-1)!} \right]_0^{\frac{\gamma T}{G_{\max}}} \\
& + 0.5 \sum_{l=0}^{L-1} \frac{1}{\sqrt{\pi}} \frac{1}{l!} \left(\frac{1}{\bar{\gamma}}\right)^l \mu^{-(l+\frac{1}{2})} \left[\Gamma\left(l+\frac{1}{2}, \mu\gamma\right) \right]_0^{\frac{\gamma T}{G_{\max}}}.
\end{aligned} \tag{3.19}$$

where

$$\begin{aligned}
\mu &= 1 + \frac{1}{\bar{\gamma}} \\
\beta &= a(k) + \frac{1}{\bar{\gamma}} \\
a(k) &= 10^{\frac{kG_{\delta\text{dB}}}{10}} \\
K_M &= \frac{G_{\max\text{dB}}}{G_{\delta\text{dB}}}.
\end{aligned}$$

The corresponding additional average dB gain can be easily shown to be given by

$$G_{\text{dB}} = \sum_{k=-\infty}^{K_M+1} f(k) P_{\gamma_c} \left(10^{\frac{\gamma T_{\text{dB}} - (k-1)G_{\delta\text{dB}}}{10}} \right) G_{\delta\text{dB}}, \tag{3.20}$$

where

$$f(k) = \begin{cases} 1 & k = -\infty, \dots, K_M \\ -K_M & k = K_M + 1. \end{cases} \tag{3.21}$$

For i.i.d. Rayleigh fading conditions and $L_c \geq L$, inserting (3.6) in (3.20), it can be shown that

$$G_{\text{dB}} = \sum_{k=-\infty}^{K_M+1} f(k) \left(1 - \frac{\Gamma \left(L, \frac{10^{\frac{\gamma_{T_{\text{dB}}} - (k-1) G_{\text{dB}}}{10}}}{\bar{\gamma}} \right)}{(L-1)!} \right) G_{\delta_{\text{dB}}}. \quad (3.22)$$

D. Numerical Examples

Fig. 3 compares the BER of BPSK when used with MRC and no power control and when used in conjunction with continuous UPC-DC with and without amplifier gain saturation. Clearly UPC makes the system just meet the target BER over the whole SNR range while systems without PC either fails to meet this target BER in the low average SNR region or exceeds it in the high average SNR region. In addition, when UPC is used the saturation of the transmitter amplifier leads to a violation of the target BER requirement in the low average SNR region. However, we can see from Fig. 4 that this peak power constraint at the transmitter side leads to a considerable decrease in the required additional average transmitter gain in this same low average SNR region.

While Figs. 5 and 6 compare continuous and discrete power adaptation (with different step sizes) without amplifier gain saturation, Figs. 7 and 8 do the same comparison when there exists a peak power constraint at the transmitter side. One can see from these figures, that as long as $G_{\text{max}_{\text{dB}}}$ is an integer multiple of $G_{\delta_{\text{dB}}}$ discrete power control requires a slightly higher average gain but offers correspondingly a decrease in the average BER over the whole average SNR range. However if the value of $G_{\text{max}_{\text{dB}}}$ is not an integer multiple of $G_{\delta_{\text{dB}}}$, this behavior is reversed in the low average SNR range.

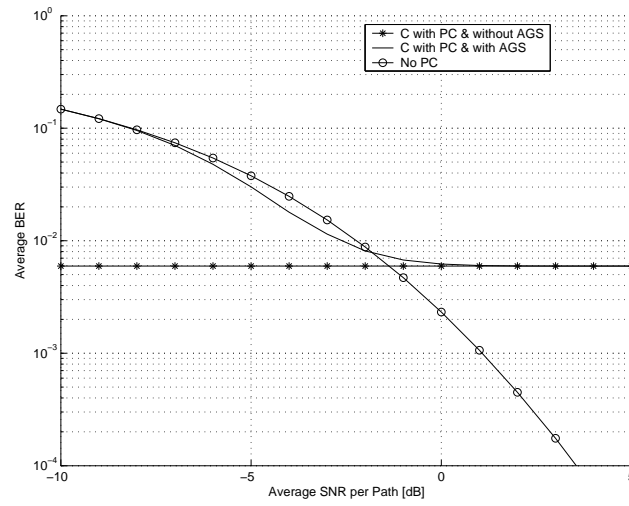


Fig. 3. Average BER of BPSK with (i) continuous UPC-DC and no amplifier gain saturation, (ii) continuous UPC-DC and amplifier gain saturation, and (iii) MRC and no power control ($L_c = L = 6$, $\gamma_T = 5$ dB, and $G_{\max} = 3$ dB).

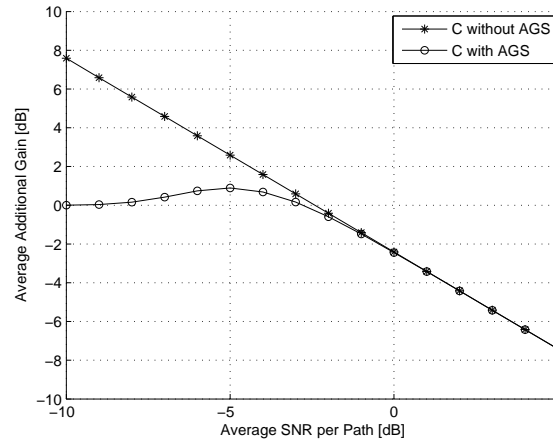


Fig. 4. Average additional dB gain of the transmitter amplifier using continuous UPC-DC with and without saturation ($L_c = L = 6$, $\gamma_T = 5$ dB, and $G_{\max} = 3$ dB).

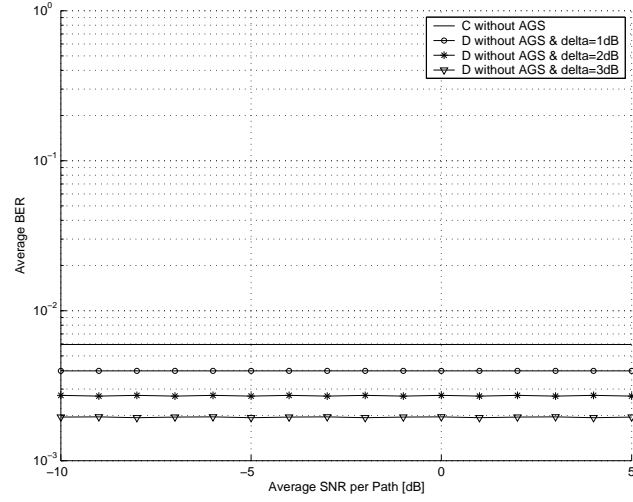


Fig. 5. Average BER of BPSK with (i) continuous UPC-DC and no amplifier gain saturation and (ii) discrete UPC-DC and no amplifier gain saturation ($L_c = L = 6$ and $\gamma_T = 5$ dB).

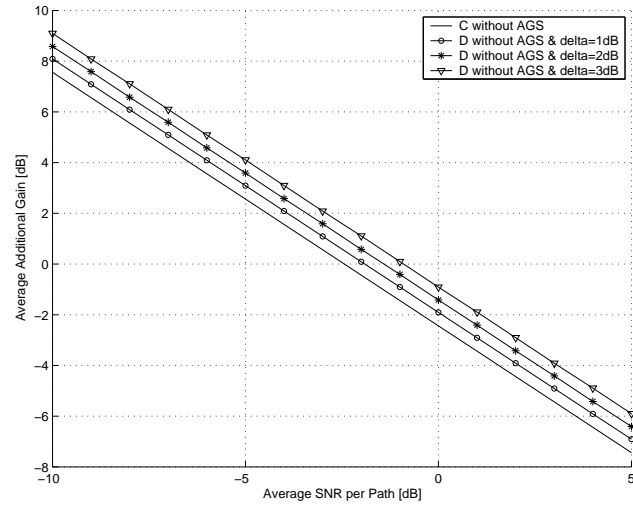


Fig. 6. Average additional dB gain of the transmitter amplifier with (i) continuous UPC-DC and no amplifier gain saturation and (ii) discrete UPC-DC and no amplifier gain saturation ($L_c = L = 6$ and $\gamma_T = 5$ dB).

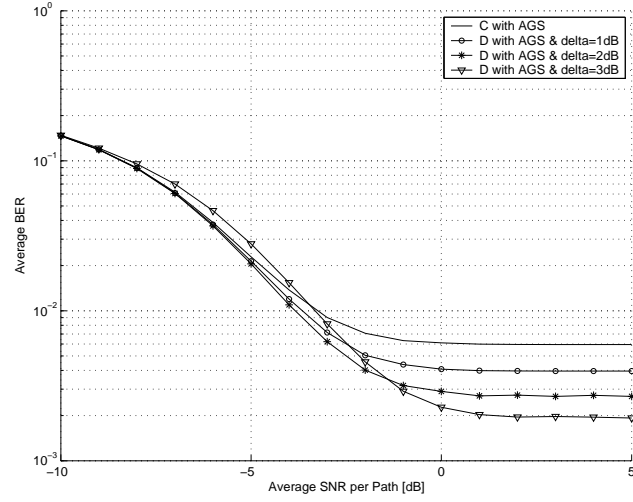


Fig. 7. Average BER of BPSK with (i) continuous UPC-DC and amplifier gain saturation and (ii) discrete UPC-DC and amplifier gain saturation ($L_c = L = 6$, $\gamma_T = 5$ dB, and $G_{\max} = 4$ dB).

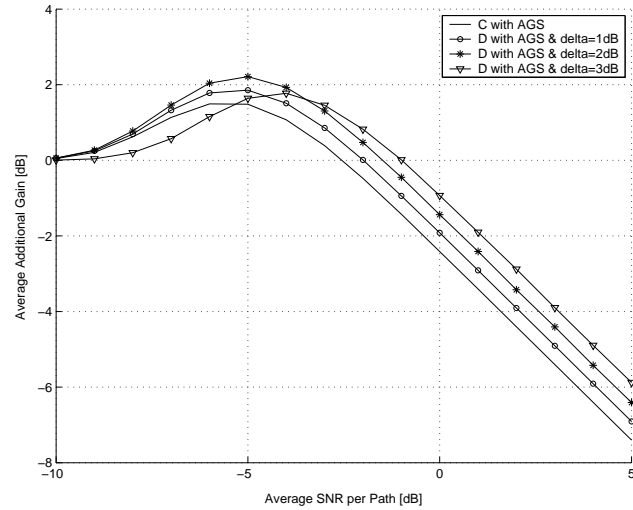


Fig. 8. Average additional dB gain of the transmitter amplifier with (i) continuous UPC-DC and amplifier gain saturation and (ii) discrete UPC-DC and amplifier gain saturation ($L_c = L = 6$, $\gamma_T = 5$ dB, and $G_{\max} = 4$ dB).

E. Conclusion

In this chapter, we proposed a new adaptive up-link diversity combining scheme. The key idea is to take advantage of all the diversity offered by the channel and then request the transmitter (i) to increase its power level during very adverse channel conditions in order to reach the target SNR and (ii) to decrease its power level during favorable channel conditions just to keep the SNR level at the target required SNR. Four power control variants accounting for practical implementation constraints including discrete power levels and transmitter gain saturation were proposed and studied. For each power control variant, we obtained a closed form solution for the average BER and the required additional average dB gain. Based on some selected results, we showed that our proposed scheme makes the system meet the target BER over the whole SNR range but the amplifier saturation leads to a violation of the target BER requirement in the low average SNR range. However, these results also show that our proposed scheme offer considerable savings in the transmitted power levels over a wide SNR range even when the practical implementation constraints such as amplifier saturation and/or discrete power adaptation are taken into account.

CHAPTER IV

THRESHOLD-BASED PARALLEL MULTIUSER SCHEDULING*

A. Introduction

Traditional multiuser scheduling schemes [48,49] rely on time division multiple access (TDMA) type of systems to schedule the user with the best channel quality to either upload or download data. With this type of system, the average spectral efficiency (ASE) can be maximized because the selected channel supports the highest possible rate. However, this high spectral efficiency comes at the expense of a high feedback load since the scheduler needs to probe all active users before it can identify the most qualified one.

To simplify the selection process and reduce the feedback load, a multiuser switched diversity scheme based on the switched diversity scheme was proposed in [50]. By using a signal to noise ratio (SNR) threshold a multiuser switched diversity was shown to reduce significantly the feedback load [50,51]. With this scheme, the BS probes the users in a sequential manner, not looking for the best one but just for an acceptable user. In addition, to the reduction in feedback load, this scheme was shown to experience minimal ASE loss and an increase in fairness by randomizing the probing sequence from one scheduling round to the next.

The TDMA-based scheduling schemes mentioned above schedule only one user at a given time. In order to improve the frequency of access of such kinds of systems, a multiuser simultaneous scheduling scheme based on generalized selection combining

*Reprinted with permission from “Threshold-Based Parallel Multiuser Scheduling” by S. S. Nam, 2008, *IEEE Trans Wireless Commun.*, Accepted, Copyright [2008] by IEEE.

(GSC) was proposed in [52]. In this scheme, the scheduler selects in each time-slot the K_s users with the largest SNRs among the K active users ($K_s \leq K$). Similar to the selection based TDMA scheme described above, the scheme in [52] needs to probe then rank all the active K users.

In this chapter, we propose two new parallel multiuser scheduling schemes that rely on a SNR threshold to reduce the complexity of implementation and increase the user frequency of access without experiencing a considerable ASE loss in comparison with the GSC based scheduling scheme presented in [52]. The first scheme termed on-off based scheduling (OOBS) scheme is based on the absolute threshold generalized selection combining (AT-GSC) scheme [53] and the on-off type of schemes introduced in [51, 54]. With this scheme, the scheduler selects in each time-slot all the users with a SNR above a preselected threshold SNR. The second scheme termed switched based scheduling (SBS) scheme is based on the switched diversity concept [50, 55]. Along the spirit of multiuser switched diversity transmission described in [50], the scheduler selects K_s users with acceptable SNRs instead of the ones with the best K_s SNRs. When the acceptable K_a users are less than K_s , the scheduler selects also the best unacceptable ($K_s - K_a$) users.

The remainder of the chapter is organized as follows. Section B presents the system and channel models as well as the mode of operation of the OOBS and SBS schemes. While section C provides some analytical results of our two proposed schemes, section D illustrates these results via some selected figures. Finally, section E offers some concluding remarks.

B. Models and Mode of Operation

In this section, we present the system, channel model and the mode of operation of our proposed schemes. More specifically, after introducing the system and channel model, we explain the mode of operation of our proposed multiuser scheduling schemes.

1. System Model

In our system model, we consider a code division multiple access (CDMA) system instead of a TDMA system because the BS needs to simultaneously schedule K_s ($K_s = 0, 1, 2, \dots, K$) users among K users per time-slot (for uplink or downlink). We assume that multiuser signals are orthogonal and there are no inter-cell interference and no co-interference among the users. We also assume that the proposed OOBs and SBS schemes have a reliable feedback path between the receiver and transmitter and that they are implemented in a discrete-time fashion with a time-slot composed of a guard time period followed by a data transmitting time period. During the guard time period, the BS makes the necessary actions to schedule the K_s users that will be granted channel access in the following transmission time. Finally, it is assumed that the channel estimation is perfect at the receiver and that the feedback to the transmitter is performed without error upon request.

For scheduled users, a rate-adaptive N multidimensional trellis coded M -quadrature amplitude modulation (M-QAM) modulation for additive white Gaussian noise (AWGN) channels is employed to ensure a high system ASE [34]. In [34, 50], the constellation size M_n is restricted 2^{n+1} ($n = 0, 1, 2, \dots, N$) for $N=8$ different codes based on QAM signal. In this case, rate adaptation is performed by dividing the SNR range into $N+1$ fading regions which are defined by the SNR thresholds, denoted by $0 < \gamma_{T_1} < \gamma_{T_2} < \dots < \gamma_{T_N} < \gamma_{T_{N+1}} = \infty$. When the estimated SNR of scheduled user is in the n th region

(*i.e.*, $\gamma_{T_n} \leq \gamma < \gamma_{T_{n+1}}$), the constellation size M_n (*i.e.*, $M_n = 4, 8, 16, 32, 64, 128, 256, 512$) with spectral efficiency R_n (*i.e.*, $R_n = 1.5, 2.5, 3.5, 4.5, 5.5, 6.5, 7.5, 8.5$) [bits/s/Hz] is transmitted. The lower SNR boundary γ_{T_n} of each fading region is set to the lowest SNR required to achieve the predefined target BER_0 .

2. Channel Model

We denote by γ_i ($i = 1, 2, \dots, K$), the received SNR of the i th user and we adopt a block flat fading channel model. More specifically, assuming slowly-varying fading conditions, the different paths from users experience roughly the same fading conditions during the data burst and its preceding guard time period. In addition, the fading conditions are assumed to be independent across the paths from users and between guard time period and data burst pairs.

3. Mode of Operation

a. OOBS Scheme

The OOBS scheme is inspired from the AT-GSC scheme [53] and the on-off type of schemes discussed in [51, 54]. The difference between the OOBS scheme and the AT-GSC scheme is that there is no combining process in the OOBS scheme. The flow chart in Fig. 9 illustrates the mode of operation of the OOBS scheme. With the OOBS scheme, at the beginning of the guard time period, the BS sends a pilot signal to all K users at a time. Once the pilot signal is received by all users, during the guard time period, these users estimate the SNR γ_i and compare it to a preselected threshold SNR, denoted by γ_T which is known ahead of time by all users. The users feed back their channel state information to the BS only if their SNRs are above the preselected threshold SNR γ_T . Only these acceptable users are then scheduled by the

BS for the subsequent transmission time. If all users do not have an acceptable SNR, the BS simply waits a period of the order of a channel coherence time before starting a new round of scheduling.

Note that with the GSC based scheduling scheme, the BS needs always full K feedbacks from all K users for SNRs comparison before ranking and determination of the K_s scheduled users. From the mode of operation of the OOBS scheme, it is clear that the number of feedbacks is random and this scheme needs to perform at most K feedbacks during the guard time period. Therefore, the OOBS scheme requires, on average, fewer feedbacks than the GSC based scheduling scheme.

b. SBS Scheme

The SBS scheme is inspired from the switched diversity based schemes [50, 55]. With the SBS scheme, the BS schedules a predetermined total number, denoted by K_s , of acceptable users and if necessary, the best unacceptable users in a GSC fashion. Fig. 10 shows the mode of operation of the SBS scheme. More specifically, in each guard time period, the BS sends a pilot signal sequentially to each user in order to request a channel state information from each user in a sequential manner. After receiving the pilot signal from the BS, each user estimates its SNR γ_i and compares it to the preselected SNR threshold. After that, each user sends back its channel state information to the BS. If the SNR γ_i is acceptable, this user is considered for scheduling by the BS. This process repeats until either the BS finds all K_s acceptable users or fails to find all K_s users (i.e. finds only $K_a < K_s$ acceptable users) after estimating and comparing all K users. In the former case, the BS does not need to probe all K users and just stops the process after finding the K_s acceptable users. In the latter case, the BS ranks the $K - K_a$ unacceptable users and schedules the best $K_s - K_a$ unacceptable users along the already acceptable K_a users.

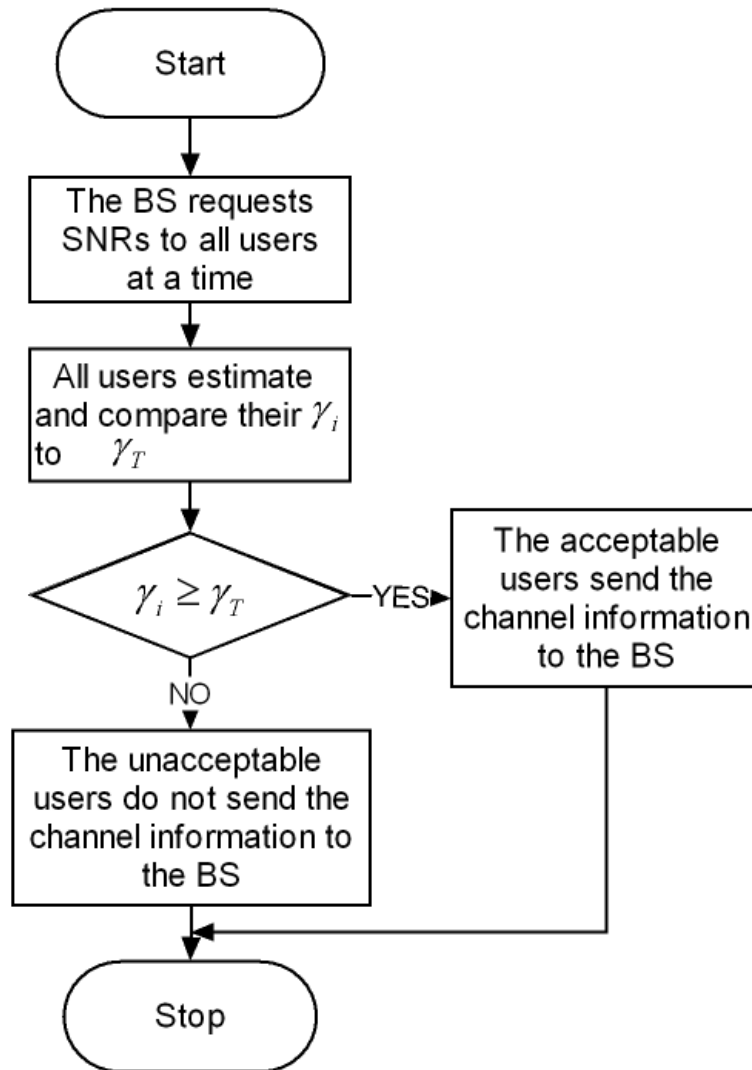


Fig. 9. Mode of operation of the OOBs parallel scheduling scheme.

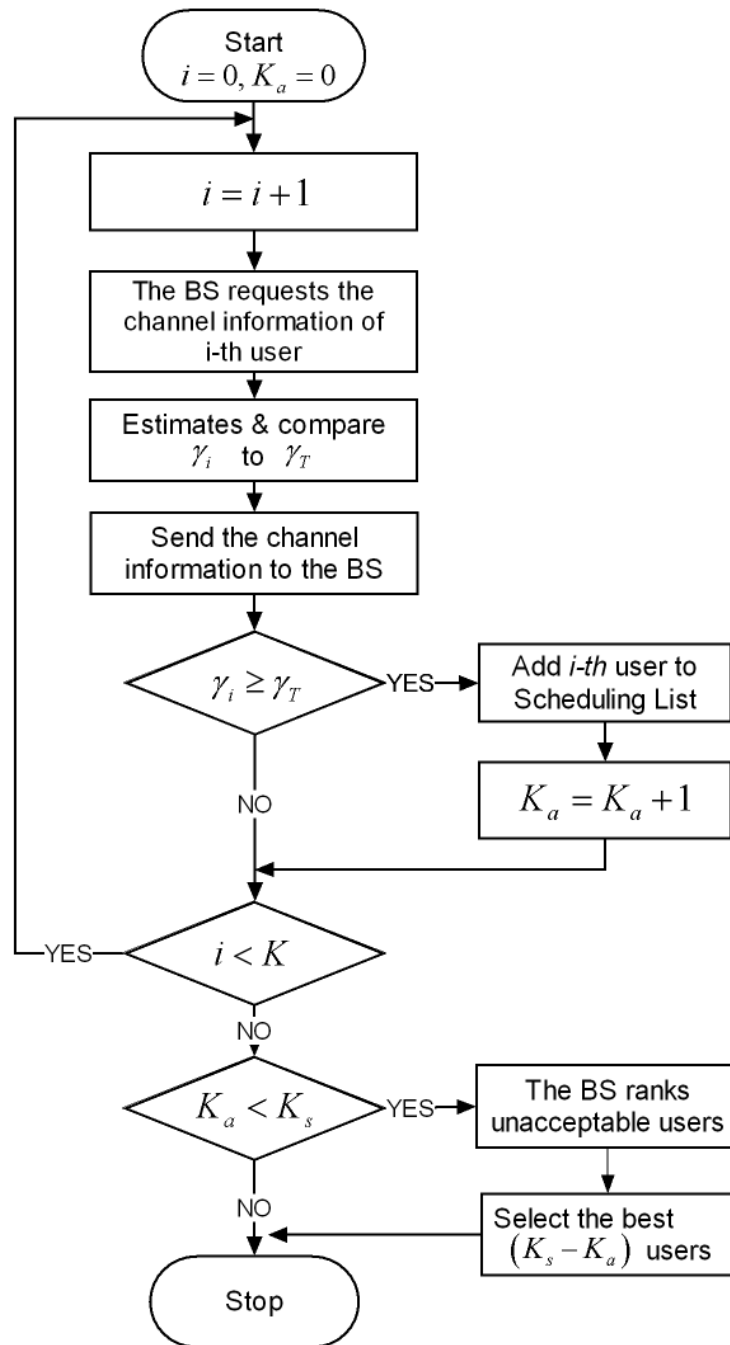


Fig. 10. Mode of operation of the SBS parallel scheduling scheme.

Compared to the GSC based scheduling scheme, the user with the best SNR can be excluded with this scheme. Therefore, for low γ_T (in comparison with average SNR), the outage performance of the GSC based scheduling scheme is expected to be better than that of the SBS scheme because the probability that the best user can not be selected increases as γ_T decreases. On the other hand, the SBS scheme approaches the outage performance of the GSC based scheduling scheme as γ_T increases. However, the SBS scheme needs less than K feedbacks whereas the GSC based scheduling scheme needs always full K feedbacks during the guard time period.

4. Discussion

In this subsection, we discuss practical implementation issues related to the feedback rate which is the required data rate to transmit the channel state information. In the GSC based scheduling scheme [52], the feedback rate is important since all users have to send a full channel state information to the BS that is needed for SNRs ranking. However with the OOBS scheme, the feedback rate can be reduced significantly without any performance loss since the users need to send to the BS only an information indicating their SNR region instead of sending the full channel state information. With the SBS scheme, the BS only needs the information indicating the SNR region if there are enough acceptable users. If the BS fails to find K_s acceptable users, the BS needs more information since it needs to rank the $K - K_a$ unacceptable users and pick the best $K_s - K_a$ among them. However, the feedback rate with the SBS scheme can be further reduced with a minimal performance loss. For instance, the acceptable users may need to send only the minimum channel state information by indicating their SNR region and the unacceptable users may need only to send one bit of information for indicating whether the user is acceptable or not. If the BS fails to find K_s acceptable users, the unacceptable users need to send more informa-

tion. Another example is that all users send an SNR region information along with the minimum information for indicating whether the user is acceptable or not. In this case, if the BS fails to find all K_s users, the BS will schedule the unacceptable $K_s - K_a$ users located in the higher SNR region. If there are more unacceptable users than the BS needs to schedule in the same SNR region, the BS randomly schedules a user as many as the BS needs because the users located in the same SNR region offer the same spectral efficiency. If the SNR threshold for scheduling is less than the minimum SNR region threshold γ_{T_1} , then (i) the BS also randomly schedules the needed users or (ii) we can divide the SNR range (below γ_{T_1}) into subregions to rank $K - K_a$ unacceptable users and schedule the best $K_s - K_a$ among them.

C. Performance Analysis

In this section, we analyze the performance of the OOBS and SBS schemes in terms of average bit error rate (BER), ASE, and average number of feedback load (AFL), which is average number of users need to transmit a feedback information to the BS, over i.i.d. Rayleigh fading conditions. Based on the i.i.d. Rayleigh fading assumption, the received SNR γ_i will share a common probability density function (PDF), given by

$$p_\gamma(\gamma) = \frac{1}{\bar{\gamma}} \exp\left(-\frac{\gamma}{\bar{\gamma}}\right), \quad (4.1)$$

where $\bar{\gamma}$ is the common average SNR for all users. The corresponding cumulative distribution function (CDF) is given by

$$P_\gamma(\gamma) = 1 - \exp\left(-\frac{\gamma}{\bar{\gamma}}\right). \quad (4.2)$$

To obtain these performance measures, we need at first to characterize the statistics of the output SNR γ_s of a scheduled user. Before we derive these performance measures, we need to define several common parameters for the OOBS and SBS schemes. For

later reference, K denotes the total number of users, K_s denotes the total number of scheduled users for the SBS scheme, K_a denotes the total number of acceptable users, and γ_T denotes the preselected SNR threshold.

1. OOBS Scheme

a. Statistics of the Output SNR of a Scheduled User with the OOBS Scheme

Based on the mode of operation of the OOBS scheme described above, the scheduled user has a conditional PDF of a truncated (above γ_T) random variable (RV) γ_i . With the help of [21, Eq. (5)], it can be shown that over the i.i.d. Rayleigh fading channel, the PDF of the output SNR of a scheduled user is given by

$$p_{\gamma_{OOBS}}(\gamma) = \begin{cases} \frac{p_\gamma(\gamma)}{1-P_\gamma(\gamma_T)} & \gamma \geq \gamma_T \\ 0 & \text{otherwise} \end{cases}. \quad (4.3)$$

For the i.i.d. Rayleigh fading condition, we can re-write (4.3) as

$$p_{\gamma_{OOBS}}(\gamma) = \begin{cases} \frac{1}{\gamma} \exp\left(-\frac{\gamma_T - \gamma}{\gamma}\right) & \gamma \geq \gamma_T \\ 0 & \text{otherwise} \end{cases}. \quad (4.4)$$

With the PDF of the output SNR of the scheduled user of the OOBS scheme at hand, we can now find the average BER, ASE, and AFL. In the following we provide some analytical formulas as well as some selected results illustrating the performance of our proposed OOBS scheme.

b. AFL

In this section, we calculate the AFL required by the OOBS scheme during the guard period. This study allows a thorough comparison between the OOBS scheme and the GSC based scheduling scheme. Recall that the scheduler asks for feedbacks from the users that are above an SNR threshold value γ_T . In this case the number of

feedback is the same as the number of acceptable user. The number of acceptable users K_a being above the threshold value is random and takes values from 0 to K and each user among the total K users can be either scheduled or not. Therefore, the number of acceptable users follows a binomial distribution. Since the diversity paths are assumed to be i.i.d. faded, we can easily write

$$\begin{aligned} P_{K_a}(k) &= \Pr[K_a = k], \\ &= \binom{K}{k} [1 - P_\gamma(\gamma_T)]^k [P_\gamma(\gamma_T)]^{K-k}, \quad k = 0, \dots, K. \end{aligned} \quad (4.5)$$

We can then write the AFL of the OOBS scheme during the guard period as

$$\begin{aligned} \text{AFL} &= E[K_a] \\ &= \sum_{k=0}^K k P_{K_a}(k) \\ &= \sum_{k=0}^K k \binom{K}{k} [1 - P_\gamma(\gamma_T)]^k [P_\gamma(\gamma_T)]^{K-k} \\ &= K [1 - P_\gamma(\gamma_T)]. \end{aligned} \quad (4.6)$$

For the i.i.d. Rayleigh fading condition, replacing $P_\gamma(\gamma)$ with $\left(1 - \exp\left(-\frac{\gamma}{\bar{\gamma}}\right)\right)$ the following AFL is obtained:

$$\begin{aligned} \text{AFL} &= \sum_{k=0}^K k \binom{K}{k} \left[\exp\left(-\frac{\gamma_T}{\bar{\gamma}}\right)\right]^k \left[1 - \exp\left(-\frac{\gamma_T}{\bar{\gamma}}\right)\right]^{K-k} \\ &= K \exp\left(-\frac{\gamma_T}{\bar{\gamma}}\right). \end{aligned} \quad (4.7)$$

c. ASE

The ASE of a scheduled user is obtained as the sum of the all spectral efficiencies $\{R_n\}_{n=1}^N$ of the individual codes, weighted by the probability P_n that the SNR of a

scheduled user is assigned to the n th region:

$$\text{ASE} = \sum_{n=1}^N R_n P_n, \quad (4.8)$$

where the probability P_n can be obtained by integrating $p_{\gamma_{\text{OBS}}}(\gamma)$ from γ_{T_n} to $\gamma_{T_{n+1}}$ as the following:

$$\begin{aligned} P_n &= \int_{\gamma_{T_n}}^{\gamma_{T_{n+1}}} p_{\gamma_{\text{OBS}}}(\gamma) d\gamma \\ &= \frac{1}{1 - P_\gamma(\gamma_T)} [P_\gamma(\gamma_{T_{n+1}}) - P_\gamma(\gamma_{T_n})]. \end{aligned} \quad (4.9)$$

In this case, to obtain the ASE of scheduled users for each time-slot, we need to multiply the average number of scheduled users by the above equation. Since the number of scheduled users is the same as the number of feedbacks, the average number of scheduled users of the OOB scheme is also $K [1 - P_\gamma(\gamma_T)]$. Finally, the ASE of the scheduled users for each time-slot becomes

$$\text{ASE}_{\text{time-slot}} = [K (1 - P_\gamma(\gamma_T))] \sum_{n=1}^N R_n \int_{\gamma_{T_n}}^{\gamma_{T_{n+1}}} p_{\gamma_{\text{OBS}}}(\gamma) d\gamma. \quad (4.10)$$

Inserting (4.3) into (5.16), we can write

$$\text{ASE}_{\text{time-slot}} = K \sum_{n=1}^N R_n \int_{\gamma_{T_n}}^{\gamma_{T_{n+1}}} p_\gamma(\gamma) U(\gamma - \gamma_T) d\gamma. \quad (4.11)$$

For the i.i.d. Rayleigh fading assumption, inserting (4.4) into (4.11) and after integration, we can write

$$\text{ASE}_{\text{time-slot}} = K \sum_{n=1}^N R_n P_{\gamma_n}, \quad (4.12)$$

where

$$P_{\gamma_n} = \begin{cases} \exp\left(-\frac{\max(\gamma_T, \gamma_{T_n})}{\bar{\gamma}}\right) - \exp\left(-\frac{\gamma_{T_{n+1}}}{\bar{\gamma}}\right) & \text{if } \gamma_{T_{n+1}} \geq \gamma_T \\ 0 & \text{if } \gamma_{T_{n+1}} < \gamma_T \end{cases}. \quad (4.13)$$

If the SNR threshold $\gamma_T = \gamma_{T_q}$ where $q \in \{1, 2, 3, \dots, N\}$, then $\{R_n\}_{n=1}^{q-1} = 0$ and (4.12) simplifies to

$$\text{ASE}_{\text{time-slot}, \gamma_{T_q}} = K \left[\sum_{n=q}^{N-1} R_n \left\{ \exp\left(-\frac{\gamma_{T_n}}{\bar{\gamma}}\right) - \exp\left(-\frac{\gamma_{T_{n+1}}}{\bar{\gamma}}\right) \right\} + R_N \exp\left(-\frac{\gamma_{T_N}}{\bar{\gamma}}\right) \right]. \quad (4.14)$$

d. $\overline{\text{BER}}$

The average BER for over all codes and SNRs of the scheduled users is given as the average number of bits in error divided by the average number of bits transmitted [32, 34]

$$\overline{\text{BER}} = \frac{\sum_{n=1}^N R_n \overline{\text{BER}}_n}{\sum_{n=1}^N R_n P_n}, \quad (4.15)$$

where $\overline{\text{BER}}_n$ denotes the average BER when code n is used

$$\begin{aligned} \overline{\text{BER}}_n &= \int_{\gamma_{T_n}}^{\gamma_{T_{n+1}}} \text{BER}_n p_{r_{OBS}}(\gamma) d\gamma \\ &= \int_{\gamma_{T_n}}^{\gamma_{T_{n+1}}} a_n \exp\left(-\frac{b_n \gamma}{M_n}\right) p_{r_{OBS}}(\gamma) d\gamma, \end{aligned} \quad (4.16)$$

where a_n and b_n are code-dependent constants which were found by least square fitting to simulated data on AWGN channels [34, Table I].

For the i.i.d. Rayleigh fading assumption, inserting (4.4) into (5.18) then performing the integration, we can write the $\overline{\text{BER}}_n$ in closed form as

$$\overline{\text{BER}}_n = \begin{cases} \left(\frac{a_n M_n}{M_n + b_n \bar{\gamma}} \right) \exp\left(\frac{\gamma_T}{\bar{\gamma}}\right) \left[\exp\left(-\frac{M_n + b_n \bar{\gamma}}{M_n \bar{\gamma}} \max(\gamma_T, \gamma_{T_n})\right) - \exp\left(-\frac{M_n + b_n \bar{\gamma}}{M_n \bar{\gamma}} \gamma_{T_{n+1}}\right) \right] & \text{if } \gamma_{T_{n+1}} \geq \gamma_T \\ 0 & \text{if } \gamma_{T_{n+1}} < \gamma_T \end{cases}, \quad (4.17)$$

and the P_n can be re-written as

$$P_n = \begin{cases} \exp\left(\frac{\gamma_T}{\bar{\gamma}}\right) \left[\exp\left(-\frac{\max(\gamma_T, \gamma_{T_n})}{\bar{\gamma}}\right) - \exp\left(-\frac{\gamma_{T_{n+1}}}{\bar{\gamma}}\right) \right] & \text{if } \gamma_{T_{n+1}} \geq \gamma_T \\ 0 & \text{if } \gamma_{T_{n+1}} < \gamma_T \end{cases}. \quad (4.18)$$

Substituting (4.17) and (4.18) in (4.15) gives a closed form expression for the average BER of the scheduled users with the OOBs scheme.

If the SNR threshold $\gamma_T = \gamma_{T_q}$ where $q \in \{1, 2, 3, \dots, N\}$, then $\{R_n\}_{n=1}^{q-1} = 0$ and we have

$$\begin{aligned} & \sum_{n=q}^N R_n \overline{\text{BER}}_n \\ &= \sum_{n=q}^{N-1} R_n \left(\frac{a_n M_n}{M_n + b_n \bar{\gamma}} \right) \exp\left(\frac{\gamma_{T_q}}{\bar{\gamma}}\right) \left\{ \exp\left(-\frac{M_n + b_n \bar{\gamma}}{M_n \bar{\gamma}} \gamma_{T_n}\right) - \exp\left(-\frac{M_n + b_n \bar{\gamma}}{M_n \bar{\gamma}} \gamma_{T_{n+1}}\right) \right\} \\ &+ R_N \left(\frac{a_N M_N}{M_N + b_N \bar{\gamma}} \right) \exp\left(\frac{\gamma_{T_q}}{\bar{\gamma}}\right) \exp\left(-\frac{M_N + b_N \bar{\gamma}}{M_N \bar{\gamma}} \gamma_{T_N}\right), \end{aligned} \quad (4.19)$$

and

$$\begin{aligned} & \sum_{n=q}^N R_n P_n \\ &= \sum_{n=q}^{N-1} R_n \exp\left(\frac{\gamma_{T_q}}{\bar{\gamma}}\right) \left\{ \exp\left(-\frac{\gamma_{T_n}}{\bar{\gamma}}\right) - \exp\left(-\frac{\gamma_{T_{n+1}}}{\bar{\gamma}}\right) \right\} + R_N \exp\left(\frac{\gamma_{T_q} - \gamma_{T_N}}{\bar{\gamma}}\right). \end{aligned} \quad (4.20)$$

Substituting (4.19) and (4.20) in (4.15) yields the average BER expression for the scheduled users for $\gamma_T = \gamma_{T_q}$.

2. SBS Scheme

a. Statistics of the Output SNR of a Scheduled User with the SBS Scheme

Based on the mode of operation of the SBS scheme, we need to condition on the number of acceptable users above the threshold in order to derive the statistics of the output SNR of a scheduled user. More specifically, we need to condition on the number of acceptable users (K_a) being greater or equal to K_s and K_a being smaller than K_s . From these conditions, we can write the PDF of the output SNR of a

scheduled user as

$$p_{\gamma_{SBS}}(\gamma) = \Pr[K_a < K_s] p_{\gamma_{s_1}}(\gamma) + \Pr[K_a \geq K_s] p_{\gamma_{s_2}}(\gamma), \quad (4.21)$$

where $p_{\gamma_{s_1}}(\gamma)$ is the PDF of a scheduled user in case of $K_a \geq K_s$ and $p_{\gamma_{s_2}}(\gamma)$ is the PDF of a scheduled user in case of $K_a < K_s$. Note that $K_a \geq K_s$ holds if and only if the K_s th selected user is above threshold. Also $K_a < K_s$ holds if and only if the K_s best users is below threshold.

In case of $K_a \geq K_s$, the statistics of a scheduled user is just a truncated PDF of a standard fading channel since all K_s users have acceptable SNRs [21, Eq. (5)]

$$p_{\gamma_{s_2}}(\gamma) = \frac{p_{\gamma}(\gamma)}{1 - P_{\gamma}(\gamma_T)} U(\gamma - \gamma_T), \quad (4.22)$$

where $U(x)$ is the unit step function.

When $K_a < K_s$, the PDF of a scheduled user is the PDF of any one of the K_s best users given the fact that the K_s th best user is below threshold. The first $(K_s - 1)$ largest users have the PDF of the i th largest SNR $\gamma_{(i)}$ given the fact that $\gamma_{(K_s)} < \gamma_T$. This PDF can be obtained from the joint PDF of $\gamma_{(i)}$ and $\gamma_{(K_s)}$ and then we need to integrate it with respect to γ_{K_s} from 0 to $\min(\gamma_T, x)$ because there is condition that (i) $\gamma_{(i)} < \gamma_{(i+1)}$ if $\gamma_{(i+1)} < \gamma_T$ and (ii) $\gamma_{(i)} < \gamma_T$ if $\gamma_{(i+1)} \geq \gamma_T$. As a result, the PDF can be written as

$$p_{\gamma_{(i)}|\gamma_{(K_s)}}(x) = \frac{\int_0^{\min(\gamma_T, x)} p_{\gamma_{(i)}, \gamma_{(K_s)}}(x, y) dy}{\int_0^{\gamma_T} p_{\gamma_{(K_s)}}(\gamma) d\gamma}, \quad (4.23)$$

where $p_{\gamma_{(j)}}(\gamma)$ is the PDF of the j th largest SNR and $p_{\gamma_{(i)}, \gamma_{(K_s)}}(x, y)$ is the joint PDF of $\gamma_{(i)}$ and $\gamma_{(K_s)}$ given by

$$\begin{aligned}
p_{\gamma_{(i)}, \gamma_{(K_s)}}(x, y) &= \frac{K!}{(K - K_s)!(K_s - i - 1)!(i - 1)!} \\
&\times [P_\gamma(y)]^{K - K_s} [P_\gamma(x) - P_\gamma(y)]^{K_s - i - 1} \\
&\times [1 - P_\gamma(x)]^{i - 1} p_\gamma(x) p_\gamma(y), \\
&x > y \text{ and } 1 \leq i < K_s \leq K
\end{aligned} \tag{4.24}$$

$$p_{\gamma_{(j)}}(\gamma) = \binom{K}{j} j \cdot p_\gamma(\gamma) [1 - P_\gamma(\gamma)]^{j-1} [P_\gamma(\gamma)]^{K-j}, \tag{4.25}$$

where the K_s th scheduled user has the PDF of a truncated version of the PDF of the K_s th largest SNR and this PDF is valid for $0 < x < \gamma_T$

$$\frac{p_{\gamma_{(K_s)}}(\gamma)}{P_{\gamma_{(K_s)}}(\gamma_T)} (1 - U(\gamma - \gamma_T)). \tag{4.26}$$

Therefore, the PDF of a scheduled user for $K_a < K_s$ is the average of the summation of the PDF of the i th largest path SNR $\gamma_{(i)}$ given the fact that $\gamma_{(K_s)} < \gamma_T$ for from the first to the $(K_s - 1)$ th largest user and the PDF of the truncated version of K_s th largest SNR is

$$p_{\gamma_{s_1}}(\gamma) = \frac{1}{K_s} \left(\sum_{i=1}^{K_s-1} p_{\gamma_{(i)}|\gamma_{(K_s)}}(\gamma) + \frac{p_{\gamma_{(K_s)}}(\gamma)}{P_{\gamma_{(K_s)}}(\gamma_T)} (1 - U(\gamma - \gamma_T)) \right). \tag{4.27}$$

Finally, by applying the total probability theorem, we can write the PDF of the output SNR of a scheduled user for the i.i.d. Rayleigh fading case as

$$\begin{aligned}
p_{\gamma_{SBS}}(\gamma) &= \Pr[K_a < K_s] \frac{1}{K_s} \left(\sum_{i=1}^{K_s-1} p_{\gamma_{(i)}|\gamma_{(K_s)}}(\gamma) + \frac{p_{\gamma_{(K_s)}}(\gamma)}{P_{\gamma_{(K_s)}}(\gamma_T)} (1 - U(\gamma - \gamma_T)) \right) \\
&+ \Pr[K_a \geq K_s] \frac{p_\gamma(\gamma)}{1 - P_\gamma(\gamma_T)} U(\gamma - \gamma_T),
\end{aligned} \tag{4.28}$$

where

$$\Pr [K_a \geq K_s] = \sum_{K_a=K_s}^K \binom{K}{K_a} [1 - P_\gamma(\gamma_T)]^{K_a} [P_\gamma(\gamma_T)]^{K-K_a}, \quad (4.29)$$

$$\Pr [K_a < K_s] = \sum_{K_a=0}^{K_s-1} \binom{K}{K_a} [1 - P_\gamma(\gamma_T)]^{K_a} [P_\gamma(\gamma_T)]^{K-K_a}, \quad (4.30)$$

$$p_{\gamma_{(i)}|\gamma_{(K_s)}}(x) = \frac{\int_0^{\min(\gamma_T, x)} p_{\gamma_{(i)}, \gamma_{(K_s)}}(x, y) dy}{P_{\gamma_{(K_s)}}(\gamma_T)}, \quad (4.31)$$

$$\begin{aligned} p_{\gamma_{(i)}, \gamma_{(K_s)}}(x, y) &= \frac{K!}{(K - K_s)!(K_s - i - 1)!(i - 1)!} \\ &\quad \times [P_\gamma(y)]^{K-K_s} [P_\gamma(x) - P_\gamma(y)]^{K_s-i-1} \\ &\quad \times [1 - P_\gamma(x)]^{i-1} p_\gamma(x) p_\gamma(y), \end{aligned} \quad (4.32)$$

$x > y$ and $1 \leq i < K_s \leq K$, and

$$p_{\gamma_{(j)}}(\gamma) = \binom{K}{j} j \cdot p_\gamma(\gamma) [1 - P_\gamma(\gamma)]^{j-1} [P_\gamma(\gamma)]^{K-j}. \quad (4.33)$$

For the i.i.d. Rayleigh fading conditions, after some manipulations and with the help of [47, Eq. (3.194.1)], we can re-write (4.28) in closed form as

$$\begin{aligned}
p_{\gamma_{SBS}}(\gamma) &= \sum_{K_a=0}^{K_s-1} \frac{K!}{(K-K_a)!K_a!} \left[\exp\left(-\frac{\gamma T}{\bar{\gamma}}\right) \right]^{K_a} \left[1 - \exp\left(-\frac{\gamma T}{\bar{\gamma}}\right) \right]^{K-K_a} \\
&\times \frac{1}{K_s} \left[\sum_{i=1}^{K_s-1} \left\{ \frac{1}{\bar{\gamma}} \frac{(K_s-1)!}{(K_s-i-1)!(i-1)!} \right. \right. \\
&\times \frac{\left[\exp\left(-\frac{\gamma}{\bar{\gamma}}\right) \right]^i \left[1 - \exp\left(-\frac{\gamma}{\bar{\gamma}}\right) \right]^{K_s-i-1} \left[1 - \exp\left(-\frac{\min(\gamma T, \gamma)}{\bar{\gamma}}\right) \right]^{K-K_s+1}}{\left[1 - \exp\left(-\frac{\gamma T}{\bar{\gamma}}\right) \right]^{K-K_s+1}} \\
&\times \left. \frac{{}_2F_1\left(1+i-K_s, K-K_s+1; K-K_s+2; \frac{1-\exp\left(-\frac{\min(\gamma T, \gamma)}{\bar{\gamma}}\right)}{1-\exp\left(-\frac{\gamma}{\bar{\gamma}}\right)}\right)}{{}_2F_1\left(1-K_s, K-K_s+1; K-K_s+2; 1-\exp\left(-\frac{\gamma T}{\bar{\gamma}}\right)\right)} \right\} \\
&+ \left\{ (1-U(\gamma-\gamma_T))(K-K_s+1) \times \frac{\left[\exp\left(-\frac{\gamma}{\bar{\gamma}}\right) \right]^{K_s} \left[1 - \exp\left(-\frac{\gamma}{\bar{\gamma}}\right) \right]^{K-K_s}}{\bar{\gamma} \times \left[1 - \exp\left(-\frac{\gamma T}{\bar{\gamma}}\right) \right]^{K-K_s+1}} \right. \\
&\times \left. \frac{1}{{}_2F_1\left(1-K_s, K-K_s+1; K-K_s+2; 1-\exp\left(-\frac{\gamma T}{\bar{\gamma}}\right)\right)} \right\} \\
&+ \sum_{K_a=K_s}^K \frac{K!}{(K-K_a)!K_a!} \left[\exp\left(-\frac{\gamma T}{\bar{\gamma}}\right) \right]^{K_a} \left[1 - \exp\left(-\frac{\gamma T}{\bar{\gamma}}\right) \right]^{K-K_a} \\
&\times \frac{1}{\bar{\gamma}} \exp\left(\frac{\gamma T - \gamma}{\bar{\gamma}}\right) U(\gamma - \gamma_T), \tag{4.34}
\end{aligned}$$

where ${}_2F_1(\alpha, \beta; \gamma; z)$ is the Hypergeometric function defined in [47, Eq. (9.100)] and [47, Eq. (9.111)]. As a validation of our analytical result, we compare in Fig. 11 the analytical PDF in (4.34) with an empirical PDF obtained by Monte-Carlo simulation. Note that our simulation results match perfectly our analytical results.

With the PDF of the output SNR of the scheduled user of the SBS scheme at hand, we can find the average BER, ASE, and AFL. In the following we provide some analytical formulas as well as some selected results illustrating the performance of our proposed SBS scheme.

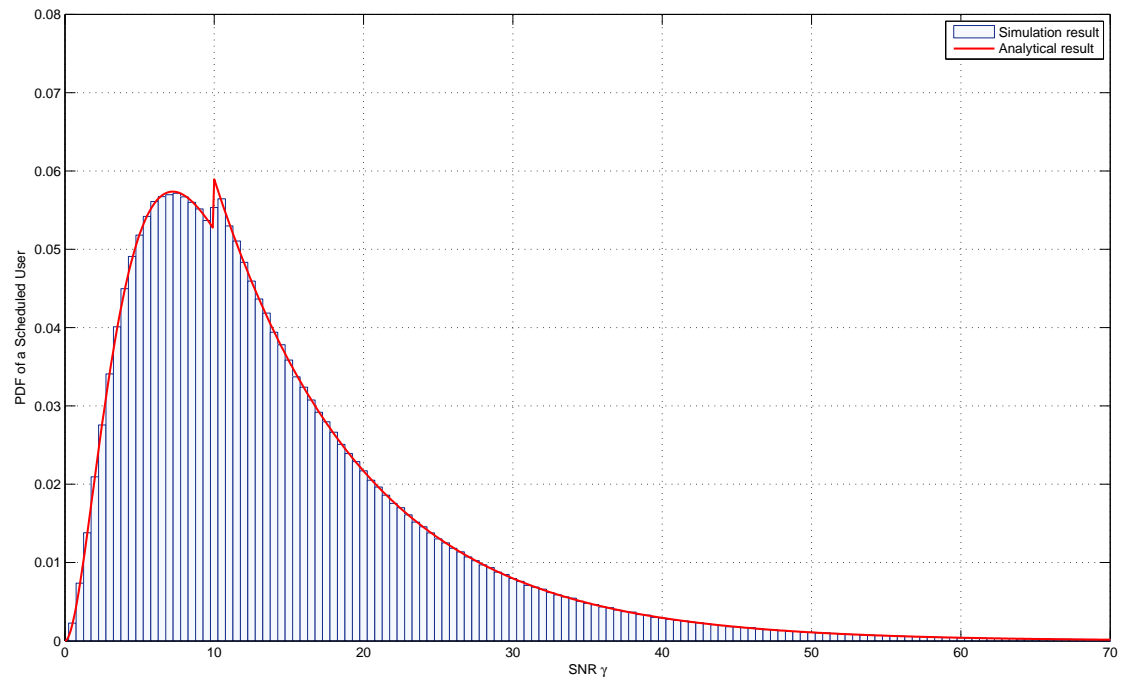


Fig. 11. PDF comparison between the analytical and the simulation results of the SBS scheme for $K = 5$, $K_s = 3$, $\gamma_T = 10$ dB, $\bar{\gamma} = 10$ dB, and i.i.d. Rayleigh fading condition.

b. AFL

In this section, we calculate the AFL for the SBS scheme during the guard period. This study allows a thorough comparison between the SBS scheme and the GSC based scheduling scheme. The scheduler asks for feedback of the channel state information from each user in a sequential manner. The BS terminates this SNR asking/checking process until either the BS finds K_s acceptable users or fails to find K_s acceptable users after checking all K users.

In the case that there are less than K_s acceptable users among the total K users, based on the mode of operation of the SBS, the BS needs to ask and check feedbacks of the all K users. As a result, the number of feedback becomes K and the number of unacceptable users is random and takes values from $(K - K_s + 1)$ to K and follows a binomial distribution. Since the diversity paths are assumed to be i.i.d. faded, the probability of number of feedback in this case that there are less than K_s acceptable users can be easily written as

$$P_B = \sum_{l=K-K_s+1}^K \binom{K}{l} [P_\gamma(\gamma_T)]^l [1 - P_\gamma(\gamma_T)]^{K-l}. \quad (4.35)$$

In the case that there are at least K_s acceptable users among the total K users, based on the mode of operation of the SBS scheme, the BS will terminate the process of asking and checking the feedback of the user. In this case, the number of feedback takes values from K_s to K and the probability of the number of required feedbacks follows a negative binomial (or Pascal) distribution given by

$$P_{K_a}(k) = \binom{k-1}{k-K_s} [1 - P_\gamma(\gamma_T)]^{K_s} [P_\gamma(\gamma_T)]^{k-K_s}, \quad k = K_s, \dots, K. \quad (4.36)$$

Finally, by combining these two mutually exclusive cases, we can obtain the overall average number of feedback during the guard period as

$$\begin{aligned}
\text{AFL} &= E [K_a] \\
&= \sum_{k=K_s}^K k P_{K_a}(k) + K P_B \\
&= \sum_{k=K_s}^K k \binom{k-1}{k-K_s} [1 - P_\gamma(\gamma_T)]^{K_s} [P_\gamma(\gamma_T)]^{k-K_s} \\
&\quad + K \sum_{l=K-K_s+1}^K \binom{K}{l} [P_\gamma(\gamma_T)]^l [1 - P_\gamma(\gamma_T)]^{K-l}. \tag{4.37}
\end{aligned}$$

Since we assumed that the diversity paths from all K users have the i.i.d. Rayleigh fading distribution, replacing $P_\gamma(\gamma)$ with $\left(1 - \exp\left(-\frac{\gamma}{\bar{\gamma}}\right)\right)$ we obtain the following closed form of AFL:

$$\begin{aligned}
\text{AFL} &= \sum_{k=K_s}^K k \binom{k-1}{k-K_s} \left[\exp\left(-\frac{\gamma_T}{\bar{\gamma}}\right) \right]^{K_s} \left[1 - \exp\left(-\frac{\gamma_T}{\bar{\gamma}}\right) \right]^{k-K_s} \\
&\quad + K \sum_{l=K-K_s+1}^K \binom{K}{l} \left[1 - \exp\left(-\frac{\gamma_T}{\bar{\gamma}}\right) \right]^l \left[\exp\left(-\frac{\gamma_T}{\bar{\gamma}}\right) \right]^{K-l}. \tag{4.38}
\end{aligned}$$

c. ASE

In this case, the ASE of a scheduled user is the same as (5.15). The P_n can be obtained by integrating $p_{\gamma_{SBS}}(\gamma)$ from γ_{T_n} to $\gamma_{T_{n+1}}$. To obtain the ASE of the scheduled users for each time-slot, we need also to multiply the average number of scheduled users by (5.15). Based on the SBS scheme, the number of the scheduled users for each time-slot has the same value K_s . Therefore, the ASE of scheduled users for each time-slot becomes

$$\begin{aligned}
\text{ASE}_{\text{time-slot} = K_s} &= \sum_{n=1}^N R_n \int_{\gamma_{T_n}}^{\gamma_{T_{n+1}}} p_{\gamma_{SBS}}(\gamma) d\gamma \\
&= K_s \left[\sum_{n=1}^{N-1} R_n \{ P_{\gamma_{SBS}}(\gamma_{T_{n+1}}) - P_{\gamma_{SBS}}(\gamma_{T_n}) \} + R_N \{ 1 - P_{\gamma_{SBS}}(\gamma_{T_N}) \} \right], \tag{4.39}
\end{aligned}$$

where $P_{\gamma_{SBS}}(\gamma_{T_n}) = \int_0^{\gamma_{T_n}} p_{\gamma_{SBS}}(\gamma) d\gamma$ is the CDF of (4.34) and which unfortunately cannot be found in a simple closed form.

d. $\overline{\text{BER}}$

In this case, the average BER for over all codes and SNRs of scheduled users is the same as (4.15) and using the summation part of (4.39), it can be re-written as

$$\overline{\text{BER}} = \frac{\sum_{n=1}^N R_n \overline{\text{BER}}_n}{\sum_{n=1}^N R_n P_n}, \quad (4.40)$$

$$= \frac{\sum_{n=1}^N R_n \int_{\gamma_{T_n}}^{\gamma_{T_{n+1}}} a_n \exp\left(-\frac{b_n \gamma}{M_n}\right) p_{\gamma_{SBS}}(\gamma) d\gamma}{\sum_{n=1}^{N-1} R_n [P_{\gamma_{SBS}}(\gamma_{T_{n+1}}) - P_{\gamma_{SBS}}(\gamma_{T_n})] + R_N [1 - P_{\gamma_{SBS}}(\gamma_{T_N})]}. \quad (4.41)$$

D. Numerical Examples

Since the number of scheduled users in the OOBS scheme is random and variable whereas in the GSC based scheduling scheme it is fixed and equal to K_s , and to allow a comparison between the two multiuser scheduling schemes, we must define an appropriate basis for this comparison. In the OOBS scheme, since the number of scheduled users is the same as the number probed users (i.e., feedback load), the average number of scheduled users, denoted by \overline{K}_s , becomes

$$\overline{K}_s = K [1 - P_\gamma(\gamma_T)]. \quad (4.42)$$

For the i.i.d. Rayleigh fading condition, (4.42) becomes

$$\overline{K}_s = K \exp\left(-\frac{\gamma_T}{\bar{\gamma}}\right). \quad (4.43)$$

For a fair basis of comparison, we need to choose the equivalent SNR threshold of the OOBS scheme, such that the average number of scheduled users \overline{K}_s is equal to K_s .

Thus, using (4.43), we have

$$K_s = K \exp\left(-\frac{\gamma_T^*}{\bar{\gamma}}\right), \quad (4.44)$$

or, equivalently,

$$\begin{aligned} \gamma_T^* &= -\bar{\gamma} \ln\left(\frac{K_s}{K}\right) \\ &= \bar{\gamma} \ln\left(\frac{K}{K_s}\right), \end{aligned} \quad (4.45)$$

where γ_T^* is the equivalent SNR threshold of the OOBS scheme and is varying with $\bar{\gamma}$. Note that for fair comparison purposes we choose an equivalent threshold of the OOBS scheme in a way that the average number of scheduled users equal to K_s .

Fig. 12 shows the average BER of adaptive coded M-QAM modulation with the OOBS scheme, the SBS scheme, and the GSC based scheduling scheme as a function of the average SNR $\bar{\gamma}$, and as a function of the SNR threshold γ_T over i.i.d. Rayleigh fading conditions with $K = 5$, $K_s = 3$, and using the equivalent threshold γ_T^* obtained from (4.45). Comparing the OOBS scheme with the GSC based scheduling scheme, the OOBS scheme has almost the same error performance as the GSC based scheme because by applying the equivalent threshold γ_T^* the OOBS schemes operates more like the GSC based scheme by selecting only the best K_s users among K users. However, in the range of very high SNR (especially over γ_{TN}) in Fig. 12 (a), the error performance of the OOBS scheme is decreasing faster because by applying the equivalent threshold, the average BER equation consists of only the function of $\frac{1}{\bar{\gamma}} \exp(-\bar{\gamma})$ and then this equation is decreasing faster as $\bar{\gamma}$ increases (the OOBS scheme outperforms the GSC based scheme). Note that the average BER of the OOBS scheme fluctuates around that of the GSC based scheme because the combined effect of the adaptive modulation and the equivalent threshold γ_T^* (the value of the SNR threshold γ_T is changing with the value of the average SNR). Fig. 12 also compares the average BER of adaptive

coded M-QAM modulation with SBS scheme and the GSC based scheduling scheme as a function of the average SNR $\bar{\gamma}$ and as a function of the SNR threshold γ_T over i.i.d. Rayleigh fading conditions with $K = 5$ and $K_s = 3$. Based on the mode of operation of the SBS scheme, as we increase γ_T , the SBS scheme starts operating in the same manner as the GSC based scheme because there are not enough acceptable users. When $\bar{\gamma}$ is less than γ_T , the average BER of the SBS scheme has the error performance of the GSC based scheme because the SBS scheme tends to select the K_s users in a GSC fashion. However, as $\bar{\gamma}$ increases in comparison with γ_T , the average BER performance of the SBS scheme exhibits some degradation in comparison with the GSC based scheme. In Fig. 12 (a), similar to the OOBS scheme, there is also a fluctuation due to the adaptive modulation. However, this fluctuation is very small in comparison with the OOBS scheme.

In Fig. 13, we present the AFL of the OOBS scheme, the SBS scheme, and the GSC based scheduling scheme over i.i.d. Rayleigh fading conditions with $K = 5$ and $K_s = 3$. In Fig. 13 (b), as expected by its mode of operation, the AFL of the SBS scheme is increasing and eventually converging to the number of full path feedback loads (K), as γ_T increases for a fixed $\bar{\gamma}$. Based on comparison between the OOBS scheme and the GSC based scheduling scheme, for fixed $\bar{\gamma}$, the AFL is decreasing from K and converging to 0 as γ_T increases because the feedback load is the same as the number of scheduled users in the OOBS scheme and the number of scheduled users is decreasing as γ_T increases. However, with the equivalent threshold γ_T^* , we can see from Fig. 13 that the AFL of the OOBS scheme does not depend on γ_T and $\bar{\gamma}$ and needs only K_s feedback loads while the GSC based scheme needs a full path feedback load of K . In Fig. 13, we also compare the AFL between the SBS scheme and the GSC based scheduling scheme. In Fig. 13 (a), based on the mode of operation of the SBS scheme, for fixed γ_T , the AFL of the SBS scheme is decreasing from K

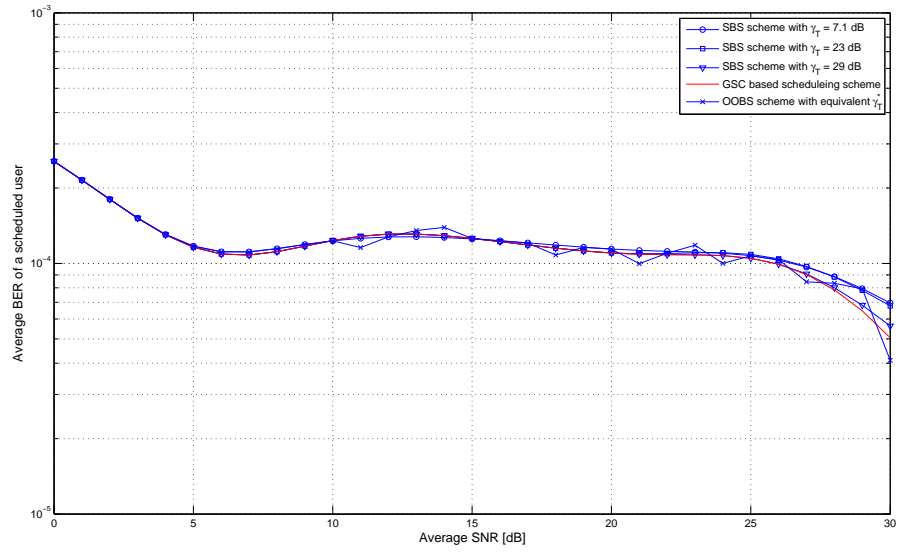
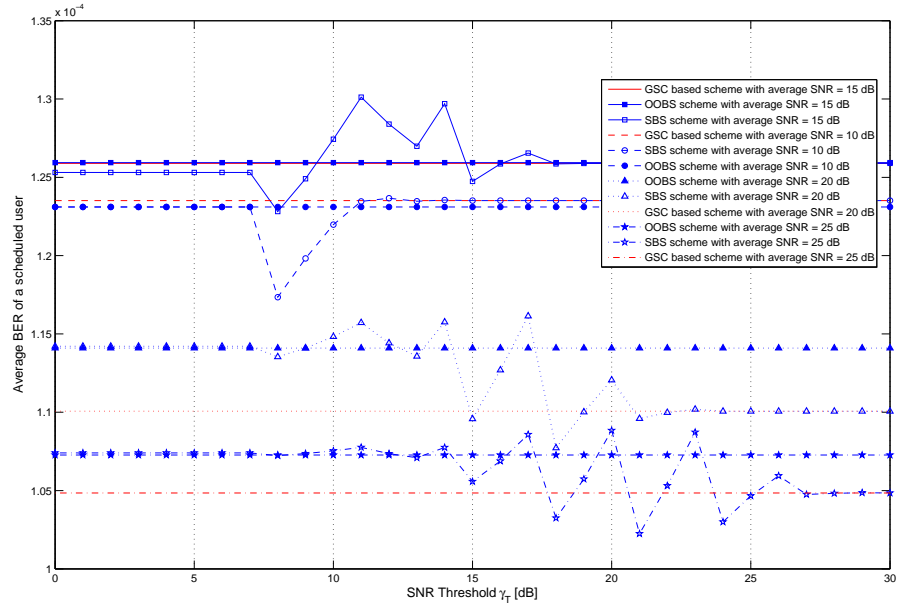
(a) Average BER as a function of average SNR $\bar{\gamma}$ (b) Average BER as a function of SNR threshold γ_T

Fig. 12. Average BER of adaptive coded M-QAM modulation with the (i) OOBS scheme, (ii) SBS scheme, and (iii) GSC based scheduling scheme for $K = 5$, $K_s = 3$, and i.i.d. Rayleigh fading conditions.

and eventually converging to K_s as $\bar{\gamma}$ increases while that of the GSC based scheme is always equal to K . As $\bar{\gamma}$ increases, the AFL with low γ_T is converging faster than that with high γ_T . This is because for a low threshold γ_T , the number of acceptable users is increasing and the target number of scheduled users is identified more quickly, which effectively reduces the AFL. In Fig. 13 (b), for fixed $\bar{\gamma}$, the AFL of the SBS scheme is increasing and when the γ_T is slightly higher than $\bar{\gamma}$, it is converging to that of the GSC based scheme as γ_T increases.

Fig. 14 presents the ASE of adaptive coded M-QAM modulation with the OOBS scheme, the SBS scheme, and the GSC based scheduling scheme as a function of average SNR $\bar{\gamma}$ and as a function of SNR threshold γ_T over the i.i.d. Rayleigh fading condition with $K = 5$ and $K_s = 3$. In Fig. 14 (a), with the fixed γ_T , the ASE of the OOBS scheme is increasing and eventually converging to $K \cdot R_N$ as $\bar{\gamma}$ increases because with fixed γ_T , i) as $\bar{\gamma}$ increases the number of scheduled users increases and eventually converges to K , ii) the total data rate depends on the number of scheduled users and each data rate depends on the its SNR. The ASE for low γ_T is converging faster than that for high γ_T because for the OOBS scheme, the AFL for the low γ_T is converging faster than that for high γ_T . When the channel condition is good, the ASE of the OOBS scheme is much larger than that of the GSC based scheme because the number of scheduled users with the OOBS scheme is converging to K while the number of scheduled users with GSC based scheme is always K_s . By applying the equivalent threshold γ_T^* in the OOBS scheme, when the channel condition is poor, the OOBS scheme has the almost same ASE of the GSC based scheme and the ASE of the OOBS scheme is slightly higher than that of the GSC based scheme from 5 dB to 35 dB. For high average SNR (above 35dB), the ASE of the OOBS scheme is re-converging to that of the GSC based scheme, $K_s \cdot R_N$. Comparing the ASE between the SBS scheme and the GSC based scheduling scheme, we can see that for

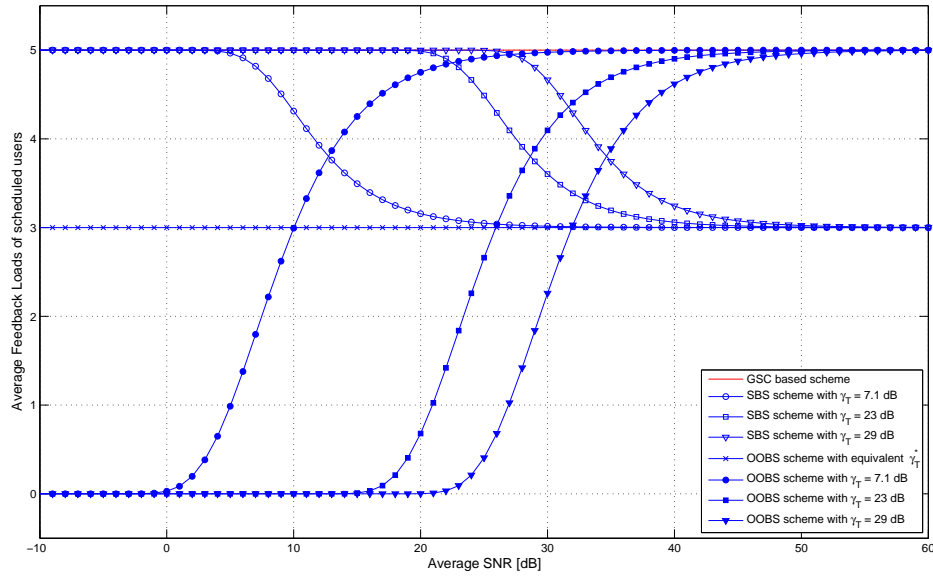
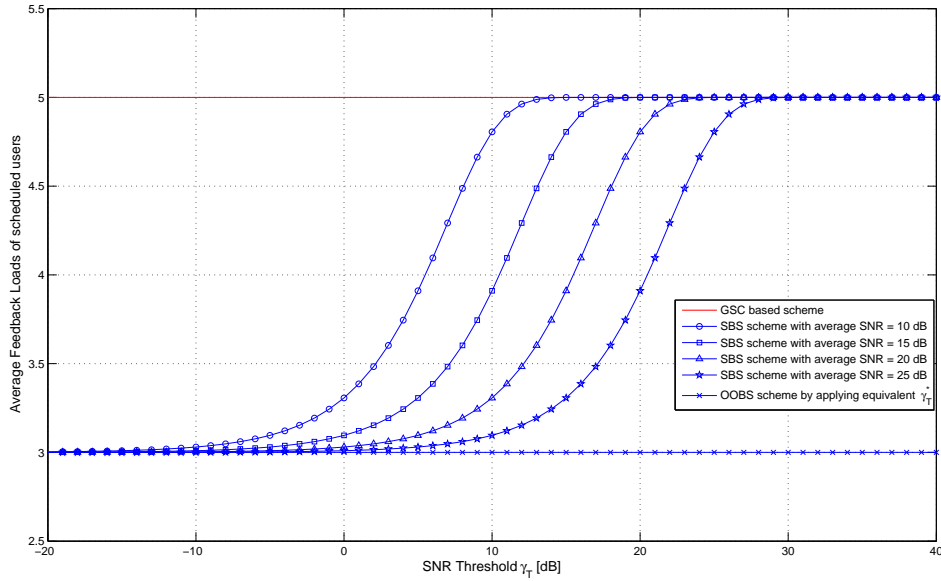
(a) AFL as a function of average SNR $\bar{\gamma}$ (b) AFL as a function of SNR threshold γ_T

Fig. 13. Average feedback loads for the (i) OOBS scheme, (ii) SBS scheme, and (iii) GSC based scheduling scheme ($K = 5$ and $K_s = 3$).

the fixed γ_T , when the channel condition is poor, the SBS scheme has the almost same ASE as the GSC based scheme and as $\bar{\gamma}$ increases, the GSC based scheme has a slightly better ASE and eventually these two schemes have the same ASE again. In Fig. 14 (b), for fixed $\bar{\gamma}$, as γ_T increasing, the ASE is improving and when the γ_T is slightly higher than $\bar{\gamma}$, the SBS scheme eventually has the same ASE as the GSC based scheme in the high average SNR range.

E. Conclusion

In this chapter, we proposed two new threshold-based parallel multiuser scheduling schemes. We analyzed the statistical characteristics, the average BER, the AFL, and the ASE of these two proposed schemes. We also showed a perfect match between our simulation results and our analytical results. The numerical results show that the OOBS scheme provides a slightly higher ASE without experiencing considerable BER loss in comparison with the GSC based scheme in the low to medium average SNR $\bar{\gamma}$ range. In the high average SNR range, the OOBS scheme provides a better error performance than the GSC based scheme for a similar AFL and ASE.

Comparing the SBS scheme with the GSC based scheme, we observed that when the threshold γ_T is slightly higher than $\bar{\gamma}$ then the SBS scheme has nearly the same average BER performance as the GSC based scheme but when γ_T is slightly lower than $\bar{\gamma}$, the SBS scheme suffers a minimal BER and ASE performance loss but offers a certain reduction in the AFL.

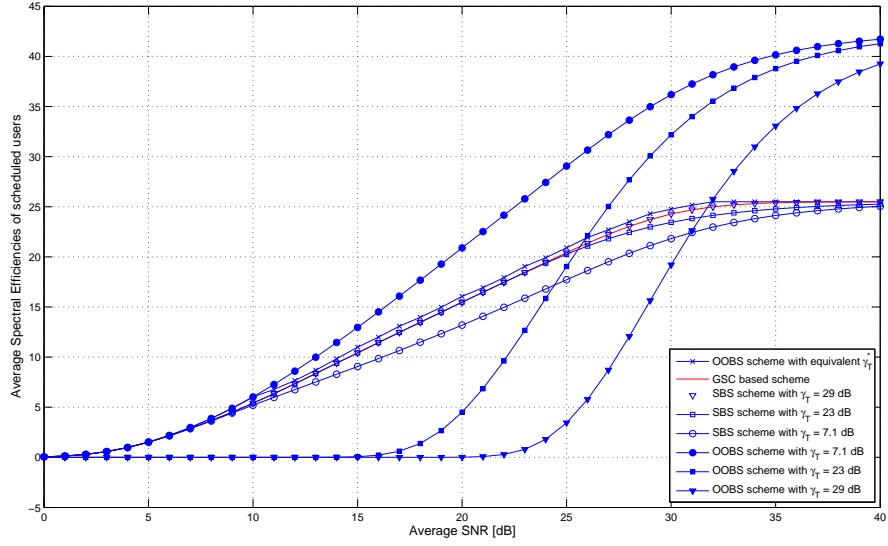
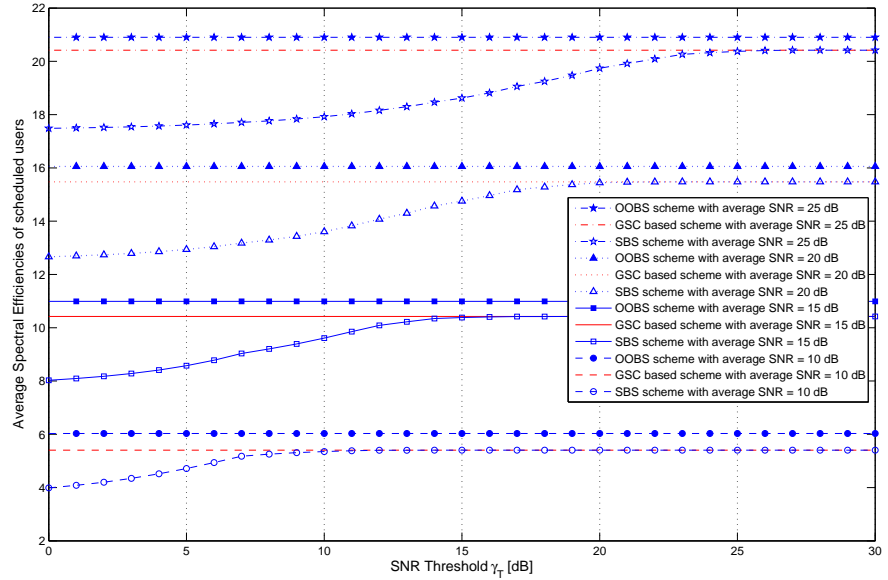
(a) ASE as a function of average SNR $\bar{\gamma}$ (b) ASE as a function of SNR threshold γ_T

Fig. 14. Average spectral efficiencies of adaptive coded M-QAM modulation for the (i) OOB scheme, (ii) SBS scheme, and (iii) GSC based scheduling scheme over i.i.d. Rayleigh fading conditions with $K = 5$ and $K_s = 3$.

CHAPTER V

PERFORMANCE EVALUATION OF THRESHOLD-BASED POWER
 ALLOCATION ALGORITHMS FOR DOWN-LINK SWITCHED-BASED
 PARALLEL SCHEDULING*

A. Introduction

Research in multiuser scheduling schemes for single user [49–51] and for multiple users [52, 56] has grown in recent years. Single user scheduling schemes [49–51] schedule only one user at a time. On the other hand, parallel scheduling schemes [52, 56] schedule multiple users at a time. The goal is to increase the average spectral efficiency (ASE) and to reduce the complexity of implementation. In the previous chapter, we proposed two new parallel multiuser scheduling schemes, namely (i) an on-off based scheduling (OOBS) scheme and (ii) a switched based scheduling (SBS) scheme to reduce the complexity of implementation without a considerable performance loss in comparison with conventional selection based scheduling [52]. While the OOBS scheme schedules all the users with a signal to noise ratio (SNR) above a pre-selected SNR threshold, the SBS scheme schedules only the K_s users among the K users with an acceptable SNR if there are enough acceptable users. Otherwise, the scheduler selects the best K_s users. Although the system with the SBS scheme increases the ASE and reduces the complexity of implementation, at least one user among the scheduled users may have an SNR below a pre-selected SNR threshold if there are not enough acceptable users.

*Reprinted with permission from “Performance Evaluation of Threshold-Based Power Allocation Algorithms for Down-Link Switched-based Parallel Scheduling” by S. S. Nam, 2008, *IEEE Trans Wireless Commun.*, Accepted, Copyright [2008] by IEEE.

In a down-link scenario, if the transmit power to the unacceptable users is increased, their SNRs increase as well and they can reach as such acceptable SNRs. However, the overall transmit power from the base station (BS) is typically limited by regulations and the level of interference to other out of cell users and devices. This limits the overall amount of power that the system can transmit. However, note that the acceptable users have SNRs above the pre-selected SNR threshold and acceptable users within the same SNR region will have the same ASE although they may have different SNRs because of the discrete nature of adaptive modulation. Therefore, if we re-allocate the excess SNR extracted from the acceptable users to the unacceptable users among the scheduled users, we can increase the number of acceptable users among the scheduled users without a considerable performance loss and without any additional down-link transmit power.

With the above motivation in mind, we propose in this chapter threshold-based power allocation algorithms for SBS type of scheduling. As its name indicates it, the system re-allocates the extracted excess SNR above the threshold from the acceptable users to the unacceptable users among the scheduled users. After the power allocation process, the unacceptable users can reach acceptable SNRs and then the number of effective acceptable users (which are the users with an SNR above a pre-selected SNR threshold for scheduling after power allocation process) among the scheduled users will be increased without any additional down-link transmit power.

The remainder of this chapter is organized as follows. Section B presents the system and channel models. In section C, details behind the mode of operation of our proposed power allocation algorithms are provided. While section D shows and discusses some simulation results via some selected figures, section E provides some analytical results for the algorithm which offers the best performance among the three proposed ones. Finally, section F offers some concluding remarks.

B. System and Channel Models

1. System Model

In our system model, we consider a code division multiple access (CDMA) system because the BS needs to schedule simultaneously K_s ($K_s = 0, 1, 2, \dots, K$) users among K potential users per time-slot. We assume that the multiuser signals are orthogonal and that there are no inter-cell interference and no co-interference among the users. We also assume that the schemes have a reliable feedback path between the receiver and transmitter and that they are implemented in a discrete-time fashion with a time-slot composed of a guard time period followed by a data transmitting time period. During the guard time period, the BS makes the necessary actions for proper power allocation after scheduling the K_s users. Finally, it is assumed that the channel estimation is perfect at the receiver and that the feedback to the transmitter is performed upon request without any error.

For the scheduled users and after power allocation, a rate-adaptive N multidimensional trellis coded M -quadrature amplitude modulation (M-QAM) modulation [34] for additive white Gaussian noise (AWGN) channels is employed to ensure a high system ASE. In [34, 50], the constellation size M_n is restricted to 2^{n+1} ($n = 1, 2, \dots, N$) different codes based on QAM signaling. In this case, rate adaptation is performed by dividing the SNR range into $N+1$ fading regions which are defined by the SNR thresholds, denoted by $0 < \gamma_{T_1} < \gamma_{T_2} < \dots < \gamma_{T_N} < \gamma_{T_{N+1}} = \infty$. When the estimated SNR of a scheduled user is in the n th region (*i.e.*, $\gamma_{T_n} \leq \gamma < \gamma_{T_{n+1}}$), the constellation size M_n (*i.e.*, $M_n = 4, 8, 16, 32, 64, 128, 256, 512$) with spectral efficiency R_n (*i.e.*, $R_n = 1.5, 2.5, 3.5, 4.5, 5.5, 6.5, 7.5, 8.5$) [bits/s/Hz] is transmitted. The lower SNR boundary γ_{T_n} of each fading region is set to the lowest SNR required to achieve a predefined target BER (say, $\text{BER}_0 = 10^{-3}$).

2. Channel Model

We denote by γ_i ($i = 1, 2, \dots, K$), the received SNR of the i th user and we adopt a block flat fading channel model. More specifically, assuming slowly-varying fading conditions, the different paths from users experience roughly the same fading conditions during the data burst and its preceding guard time period. In addition, the fading conditions are assumed to be independent across the paths from users and between guard time period and data burst pairs.

C. Power Allocation Algorithms

The main purpose of our proposed power allocation algorithms is to increase the number of the effective acceptable users without consuming any additional down-link transmit power. This is done by re-allocating the excess SNR extracted from the acceptable users to the unacceptable users among the scheduled users. Based on this, we propose three kinds of power allocation algorithms. For later reference, γ'_i denote the SNR of the scheduled user after power allocation. We also denote by K and K_s , the total number of users and the total number of scheduled users for the SBS scheme, respectively. K_a denotes the total original number of acceptable users before power allocation and γ_T and γ_{TP} denote the preselected SNR threshold for scheduling and for power allocation respectively. In this chapter, based on our motivation, we only consider the case of $\gamma_T = \gamma_{TP}$.

1. Algorithm 1

The main idea of the first power allocation algorithm is to extract only the required SNR from the acceptable users and then to allocate it to the unacceptable users sequentially from the strongest user to the weakest user. With this algorithm, the SNR

ranking information is maintained and sequential allocation of power to the unacceptable users from the strongest SNR users to the weakest SNR users is performed until the extracted excess power is exhausted. More specifically, Fig. 15 illustrates the detailed mode of operation of the first power allocation algorithm. With algorithm 1, during the guard time period, after SBS scheduling, the system estimates the required SNR from the unacceptable users $\gamma_{req} = \sum_{i=K_a+1}^{K_s} (\gamma_{TP} - \gamma_i)$. After dividing γ_{req} by the total number of acceptable users K_a , the system extracts this amount, $(\frac{\gamma_{req}}{K_a})$, from all the acceptable users to maintain the SNRs ranking information among the acceptable users. This yields:

- i) If $(\gamma_i - \frac{\gamma_{req}}{K_a}) \geq \gamma_{TP}$, then we subtract $\frac{\gamma_{req}}{K_a}$ from γ_i and then the modified SNR of the acceptable user is $\gamma'_i = \gamma_i - \frac{\gamma_{req}}{K_a}$, $i \in \{1, 2, \dots, K_a\}$.
- ii) If $(\gamma_i - \frac{\gamma_{req}}{K_a}) < \gamma_{TP}$, then we subtract $(\gamma_i - \gamma_{TP})$ from γ_i and then the modified SNR of the acceptable user is $\gamma'_i = \gamma_{TP}$, $i \in \{1, 2, \dots, K_a\}$.

After this first step, the system adds all extracted SNRs from the acceptable users yielding $\gamma_{excess} = \sum_{i=1}^{K_a} (\gamma_i - \gamma'_i)$. Then the system sequentially allocates γ_{excess} to the unacceptable users. More specifically, if $\gamma_{excess} = 0$, then all SNRs of the scheduled users are not changed after the power allocation process. If $\gamma_{excess} = \gamma_{req}$, then γ_{excess} is sequentially allocated to all unacceptable users as much as they need to have the minimum data rate and then all the SNRs of unacceptable users, γ'_i ($i \in \{K_a + 1, \dots, K_s\}$), are equal to the SNR threshold γ_{TP} . If $\gamma_{excess} < \gamma_{req}$, then γ_{excess} is sequentially allocated to the unacceptable users from the user with strongest SNR to the user with weakest SNR among the unacceptable users by exhausting the extracted power. More specifically, if $\gamma_{excess} \geq (\gamma_{TP} - \gamma_i)$, then the $(\gamma_{TP} - \gamma_i)$ is allocated to the unacceptable user and then $\gamma'_i = \gamma_{TP}$. If $\gamma_{excess} < (\gamma_{TP} - \gamma_i)$, then the γ_{excess} is allocated to the unacceptable user and then $\gamma'_i = (\gamma_i + \gamma_{excess})$ before

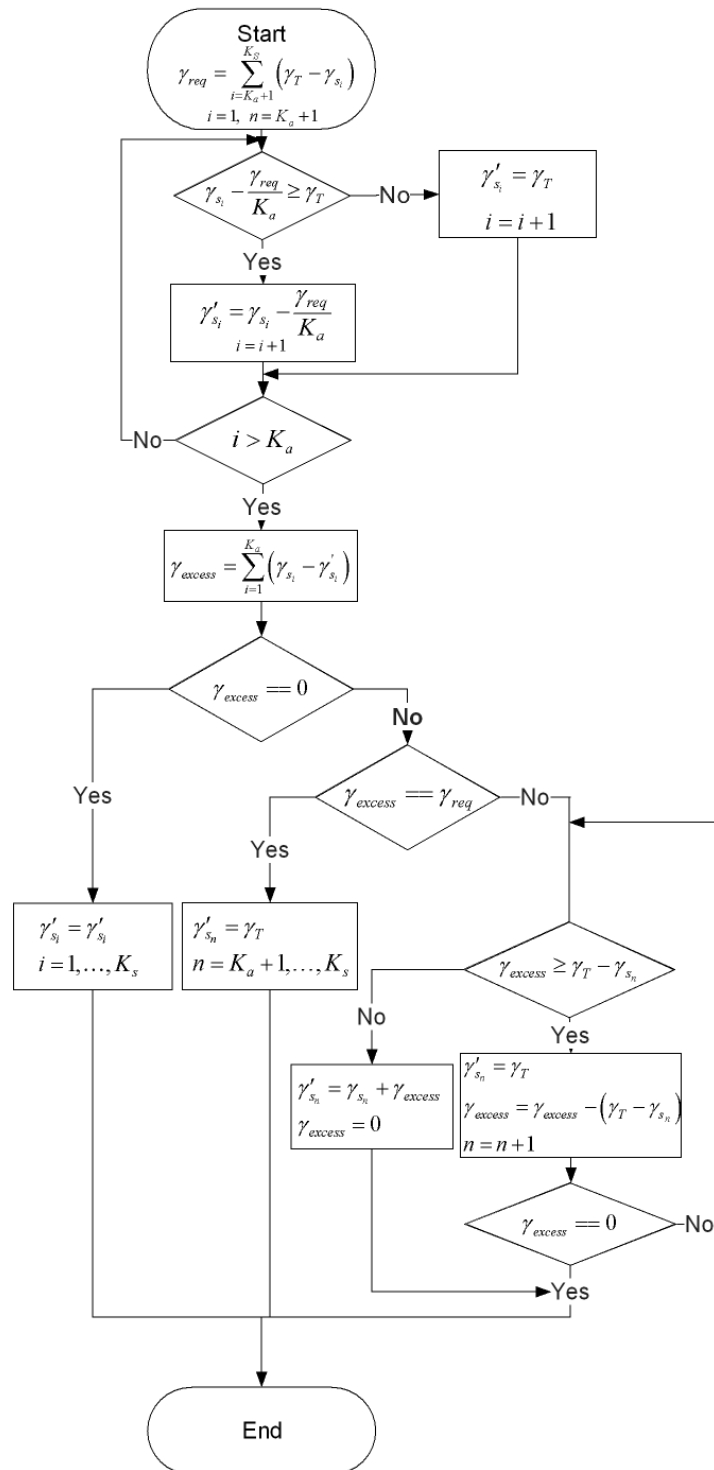


Fig. 15. Flowchart of the power allocation process for algorithm 1.

terminating the power allocation process. The power allocation process is continued and repeated until $\gamma_{excess} = 0$.

2. Algorithm 2

The main idea of the second algorithm is extracting only each user's excess SNR from the acceptable users and then allocating it to the unacceptable users sequentially from the strongest user to the weakest user. Because acceptable users have their own SNR regions due to the discrete nature of adaptive modulation and because the extraction of each user's excess SNR and re-allocating it to the unacceptable user, the system can increase the number of the effective acceptable users while maintaining the ASE of the acceptable users after power allocation. After the extraction process, and like in the first algorithm, the system sequentially allocates the excess power to the unacceptable users from the strongest SNR user to the weakest SNR user among the unacceptable users. More specifically, with algorithm 2, during the guard time period, after scheduling with SBS, the system estimates the excess SNR from the acceptable users. If the i -th acceptable user is placed in the j -th SNR region, then after power allocation, the excess SNR and modified SNR of the i -th acceptable user among the scheduled users becomes $\gamma_{excess,i} = \gamma_i - \gamma_{T_j}$ and $\gamma'_i = \gamma_{T_j}$, where $i = 1, 2, \dots, K_a$ and $j = 1, 2, 3, \dots, N$, respectively. After the extraction process, the system adds all the extracted excess SNRs from the acceptable users and then allocates it to the unacceptable users like the first power allocation algorithm. If some excess power remains after power allocation process, the system allocates it to all the scheduled users equally. Note that this algorithm has less complexity in comparison with the first one.

3. Algorithm 3

The main idea of the third algorithm is that after power allocation, the effective acceptable users end up with the same SNR. More specifically, after comparing the excess SNR to the required SNR and then estimating the number of effective acceptable users, the system equally allocates the total SNR of the effective acceptable users to only the effective acceptable users. After the power allocation process, all the effective acceptable users will have the same SNR and the SNRs of the remained users among the scheduled users will not be changed. This algorithm is more practical and has the lowest complexity of implementation among our proposed algorithms. More specifically, Fig. 16 illustrates the detailed mode of operation of the third power allocation algorithms. With algorithm 3, during the guard time period, and after SBS scheduling, the system estimates the excess SNR from the acceptable users and the required SNR from the unacceptable users where the excess SNR and the required SNR are given by $\gamma_{req} = \sum_{i=K_a+1}^{K_s} (\gamma_{TP} - \gamma_i)$ and $\gamma_{excess} = \sum_{i=1}^{K_a} (\gamma_i - \gamma_{TP})$ respectively. If $\gamma_{excess} = 0$, then all the SNRs of the scheduled users are not changed after power allocation, and $\gamma'_i = \gamma_i$ ($i = 1, 2, 3, \dots, K_s$). If $\gamma_{excess} \neq 0$ and $\gamma_{req} \leq \gamma_{excess}$, then all scheduled users are effective acceptable users and then they have the same SNRs $\gamma'_i = \frac{\gamma_{total}}{K_s}$. If $\gamma_{excess} \neq 0$ and $\gamma_{req} > \gamma_{excess}$, then the system estimates the number of the effective acceptable users, $K_{s,eff}$, and then equally allocates the effective total SNR, $\gamma_{total,eff}$, to the effective $K_{s,eff}$ users as explained in what follows:

- i) Let $K_{a,eff} = K_s - K_a$ and $K_{s,eff} = K_a + K_{a,eff}$.
- ii) Estimate the effective required SNR and the effective total SNR as $\gamma_{req,eff} = \sum_{i=K_a+1}^{K_{s,eff}} (\gamma_{TP} - \gamma_i)$ and $\gamma_{total,eff} = \sum_{i=1}^{K_{s,eff}} \gamma_i$, respectively.
- iii) If $\gamma_{req,eff} \leq \gamma_{excess}$, then $\gamma'_i = \frac{\gamma_{total,eff}}{K_{s,eff}}$ ($i = 1, 2, \dots, K_{s,eff}$) and $\gamma'_i = \gamma_i$ ($i = K_{s,eff} + 1, \dots, K_s$).

- iv) If $\gamma_{req,eff} > \gamma_{excess}$, then $K_{a,eff} = K_{a,eff} - 1$ and $K_{s,eff} = K_a + K_{a,eff}$ and then repeat step ii).

D. Simulation Results

In this section, the average number of the effective acceptable users, the ASE, and the average BER with our three proposed power allocation algorithms are investigated through Monte Carlo computer simulations. In our simulation, we use the SBS scheme with $K = 20$, $K_s = 15$, the coded adaptive modulation of [34] with $N = 8$, and independent and identically distributed (i.i.d.) Rayleigh fading conditions.

Fig. 17 presents the average number of effective acceptable users with our proposed power allocation algorithms over i.i.d. Rayleigh fading conditions with $K = 20$, $K_s = 15$, and $\gamma_T = \gamma_{TP} = 7.1$ dB. After power allocation with our proposed power allocation algorithms, as expected, the average number of effective acceptable users is increased. Also, as per our intuition, the third algorithm has the best performance among our proposed algorithms and the second algorithm has a better performance than the first algorithm.

Fig. 18 presents the ASE of SBS with our proposed power allocation algorithms over i.i.d. Rayleigh fading conditions with $K = 20$, $K_s = 15$, and $\gamma_T = \gamma_{TP} = 7.1$ dB. Based on their mode of operation, when the average SNR is close to the SNR threshold for power allocation, algorithm 2 acts like algorithm 1 and in the region of average SNR, $\bar{\gamma}$, higher than the SNR threshold, algorithm 2 acts like algorithm 3. As expected, after power allocation with algorithm 2, the ASE was increased because the acceptable users still have the same ASE and the ASE of the power allocated unacceptable users was increased. On the other hand, contrary to our original expectations, after power allocation with algorithm 1 and 3, the ASE

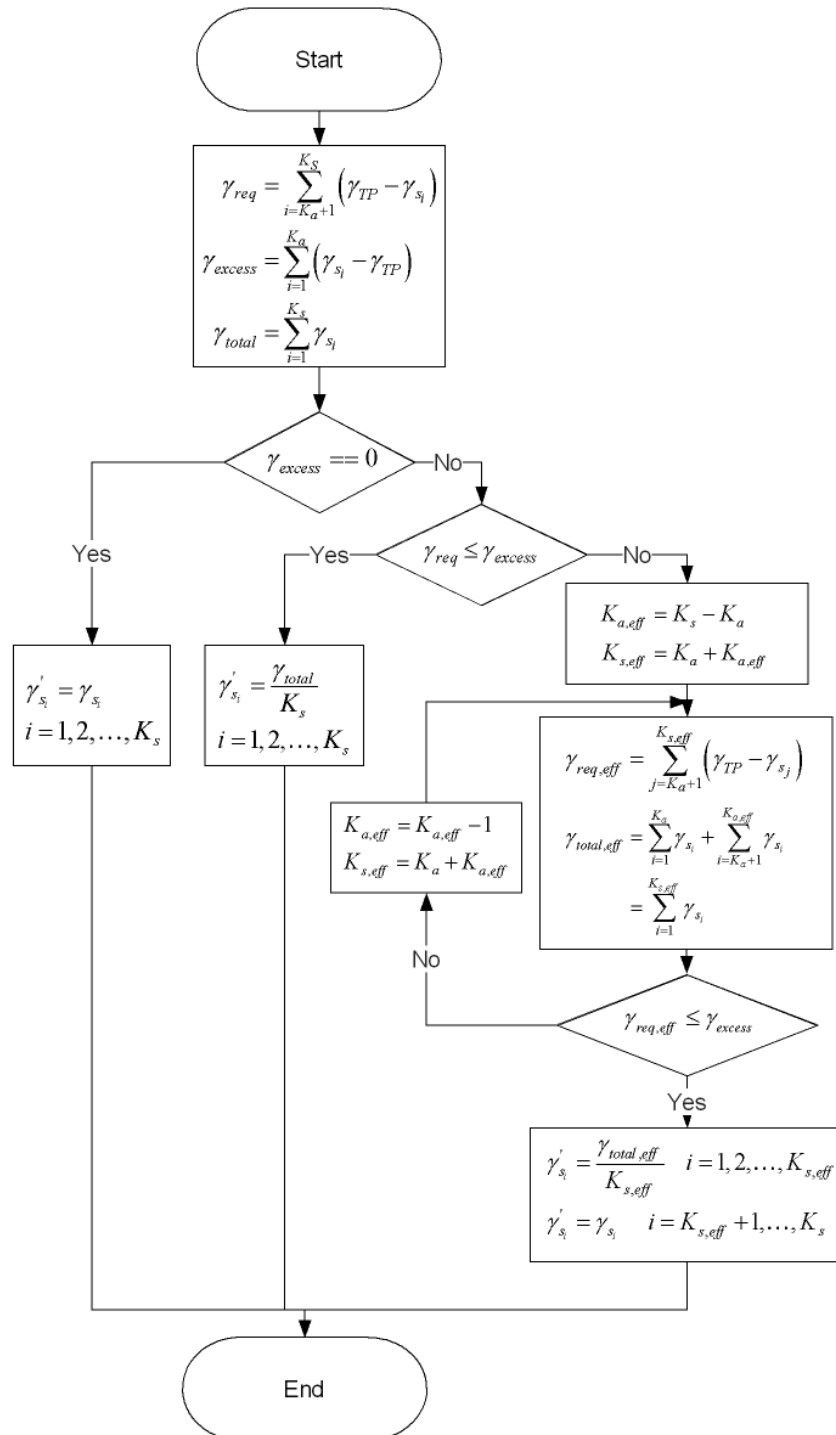


Fig. 16. Flowchart of the power allocation process for algorithm 3.

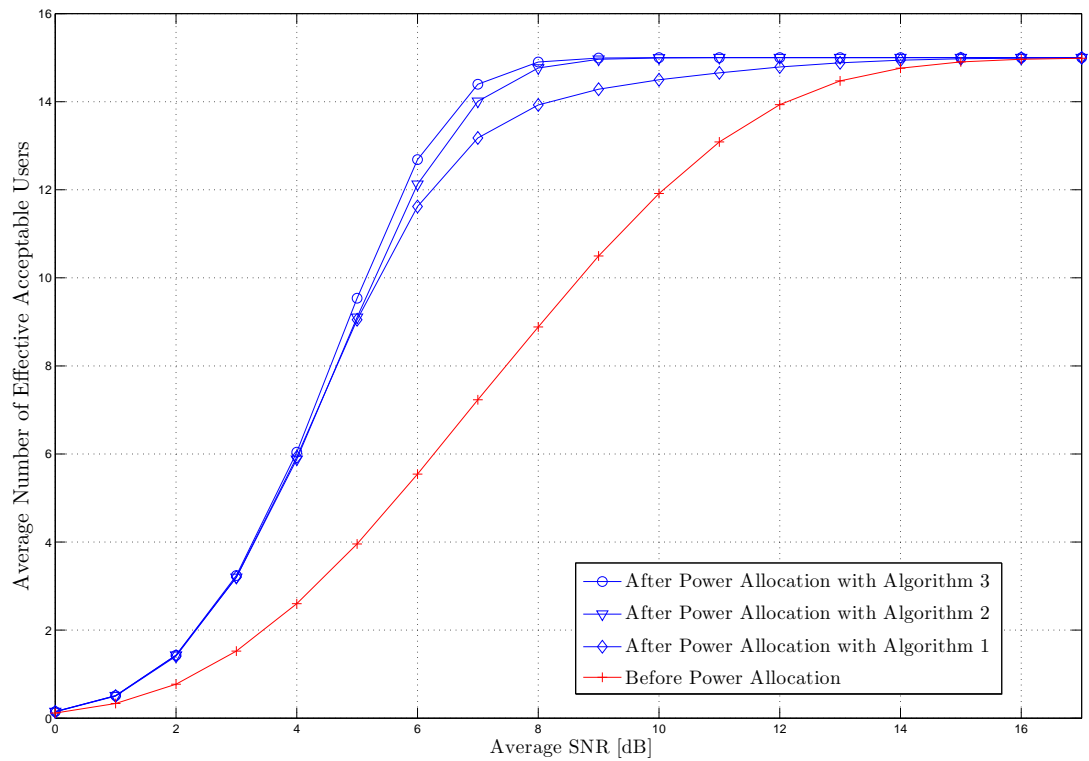


Fig. 17. Average number of effective acceptable users with SBS over i.i.d. Rayleigh fading conditions with $K = 20$, $K_s = 15$, and $\gamma_T = \gamma_{TP} = 7.1$ dB.

was also increased. This can be explained by the fact that based on the statistical property of the scheduled users with SBS, at least one of the acceptable users has very large SNR compared with others' among the scheduled users and then after power allocation, most of the acceptable users can still maintain their SNR regions after power allocation. The ASE with algorithm 1 was increased only when the average SNR is close to the SNR threshold for power allocation because in the region of high $\bar{\gamma}$, the required SNR is decreasing and the number of acceptable users is increasing and for that reason, most of the acceptable users can maintain their SNR regions. The ASE with algorithm 1 was increasing only in the region of low $\bar{\gamma}$. Based on the mode of operation of SBS, all the scheduled users with SBS may have acceptable SNRs in the region of high $\bar{\gamma}$. Therefore, based on the mode of operation of algorithm 1, the system did not need the power allocation process in the region of high $\bar{\gamma}$. The ASE with algorithm 2 is increasing when $\bar{\gamma}$ is slightly lower than the SNR threshold and finally approaching to the ASE prior to the application of the power allocation. Similar to algorithm 2, the ASE with algorithm 3 is also increasing when $\bar{\gamma}$ is slightly lower than the SNR threshold and finally it approaches to the ASE prior to the application of power allocation.

Fig. 19 presents the average BER of SBS with our proposed power allocation algorithms over i.i.d. Rayleigh fading conditions with $K = 5$, $K_s = 3$, and $\gamma_T = \gamma_{TP} = 7.1$ dB. After power allocation with algorithm 1, the average BER performance is degraded only when the average SNR is close to the SNR threshold for power allocation because the excess SNRs are extracted from the acceptable users. In the region of high $\bar{\gamma}$, the extracted SNR from the acceptable users is decreased and then the average BER is approaching the average BER prior to the application of the power allocation. Similar to the ASE results, the average BER of algorithm 2 acts like the ASE of algorithm 2 when the average SNR is close to the SNR threshold for

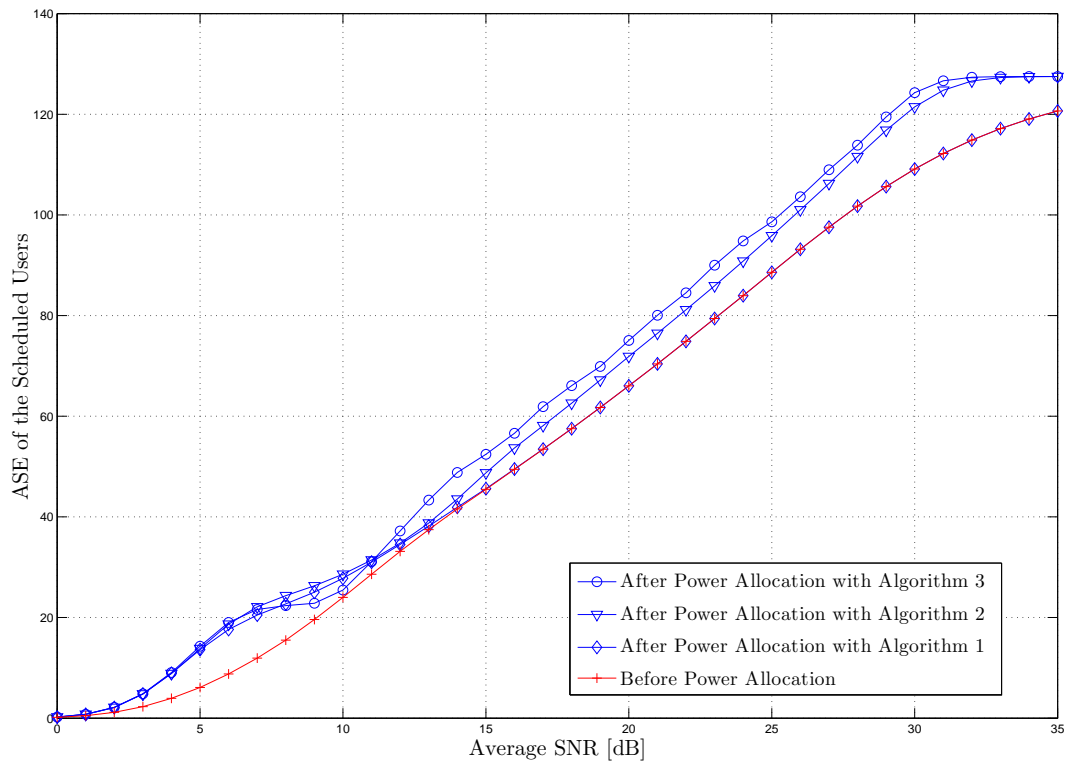


Fig. 18. ASE with SBS over i.i.d. Rayleigh fading conditions with $K = 20$, $K_s = 15$, and $\gamma_T = \gamma_{TP} = 7.1$ dB.

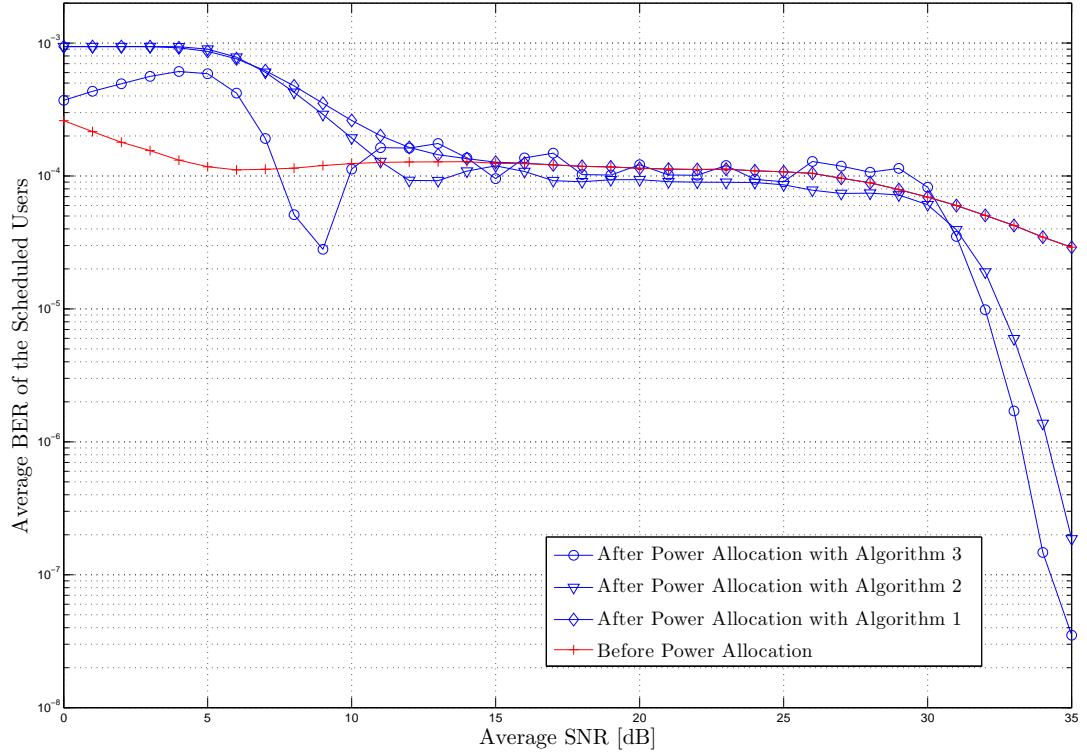


Fig. 19. Average BER with SBS over i.i.d. Rayleigh fading conditions with $K = 20$, $K_s = 15$, and $\gamma_T = \gamma_{TP} = 7.1$ dB.

power allocation.

E. Performance Analysis

Based on the simulation results presented in section IV, it is clear that algorithm 3 provides the best performance and the least complexity among our three proposed algorithms. Therefore, we analyze in this section the performance of the power allocation algorithm 3 with SBS scheduling in terms of average number of effective acceptable users, statistics of output SNR, ASE, and average BER over i.i.d. Rayleigh fading conditions. Based on the i.i.d. Rayleigh fading assumption, the received SNR γ_i will

have a probability density function (PDF), given by $p_\gamma(\gamma) = \frac{1}{\bar{\gamma}} \exp\left(-\frac{\gamma}{\bar{\gamma}}\right)$ and a corresponding cumulative distribution function (CDF) is given by $P_\gamma(\gamma) = 1 - \exp\left(-\frac{\gamma}{\bar{\gamma}}\right)$ where $\bar{\gamma}$ is the common average SNR for all users.

1. Average Number of Effective Acceptable Users

At first, we calculate the average number of effective acceptable users required by algorithm 3 with SBS during the guard period. This study allows a thorough comparison between before and after power allocation. To find the average number of effective acceptable users with SBS before power allocation with algorithm 3, we need to consider i) $K_a \geq K_s$ and ii) $K_a < K_s$, separately. In this case, $K_{s,eff}$ is equal to K_a . When $K_a \geq K_s$, there are enough acceptable users and $K_{s,eff}$ is always equal to K_s . Therefore, at least the K_s -th user should have a SNR larger than γ_{TP} . Otherwise, there are not enough acceptable users and the $K_{s,eff}$ takes K_a . In this case K_a takes a value from 0 to $K_s - 1$ but if $K_a = 0$, the average number of effective acceptable users is 0. Therefore, K_a can take a value from 1 to $K_s - 1$ and $\gamma_{(K_a)} \geq \gamma_{TP}$ & $\gamma_{(K_a+1)} < \gamma_{TP}$. From i) and ii) we can calculate the average number of effective acceptable users as the following:

$$\sum_{i=1}^{K_s-1} i \int_{\gamma_{TP}}^{\infty} \int_0^{\gamma_{TP}} p_{\gamma_{(i),\gamma_{(i+1)}}}(x,y) dy dx + K_s \int_{\gamma_{TP}}^{\infty} p_{\gamma_{(K_s)}}(z) dz, \quad (5.1)$$

where

$$p_{\gamma_{(i),\gamma_{(j)}}}(x,y) = \frac{K!}{(K-j)!(j-i-1)!(i-1)!} \times [P_\gamma(y)]^{K-j} [P_\gamma(x) - P_\gamma(y)]^{j-i-1} [1 - P_\gamma(x)]^{i-1} p_\gamma(x)p_\gamma(y), \quad (5.2)$$

$x > y$ & $1 \leq i < j \leq K$, and

$$p_{\gamma_{(K_s)}}(\gamma) = \binom{K}{K_s} K_s \cdot p_\gamma(\gamma) [1 - P_\gamma(\gamma)]^{K_s-1} [P_\gamma(\gamma)]^{K-K_s}. \quad (5.3)$$

After power allocation with algorithm 3, we need to consider i) $K_a \geq K_s$ and ii) $K_a < K_s$ separately. In case of $K_a \geq K_s$, there are enough acceptable users and $K_{s,eff}$ is always K_s . Therefore, because at least K_s -th user should have a SNR larger than γ_{TP} , the sum of the best K_s SNR is larger than $K_s\gamma_{TP}$. Otherwise, there are not enough acceptable users and the $K_{s,eff}$ takes a value from 0 to K_s . In case $K_{s,eff} = 0$, K_a should be 0 because if $K_a < K_s$ and $K_a = 0$, there are no acceptable users. In case of $1 \leq K_{s,eff} \leq K_s - 1$, $\gamma_{(K_{s,eff}+1)} < \gamma_{TP}$ & $K_{s,eff}\gamma_{TP} \leq \sum_{i=1}^{K_{s,eff}} \gamma_{(i)} < (K_{s,eff} + 1)\gamma_{TP} - \gamma_{(K_{s,eff}+1)}$. In case of $K_{s,eff} = K_s$, the sum of the best K_s SNR is larger than $K_s\gamma_{TP}$. From i) and ii) for the case of $K_{s,eff} = K_s$, we can calculate the total probability of $K_{s,eff}$ at once as the following:

$$\begin{aligned}
\Pr[K_{s,eff} = K_s] &= \Pr[K_a > K_s] + \Pr[K_a < K_s, \sum_{i=1}^{K_s} \gamma_{(i)} > K_s\gamma_{TP}] \\
&= \Pr[K_a > K_s, \sum_{i=1}^{K_s} \gamma_{(i)} > K_s\gamma_{TP}] + \Pr[K_a < K_s, \sum_{i=1}^{K_s} \gamma_{(i)} > K_s\gamma_{TP}] \\
&= \Pr[\sum_{i=1}^{K_s} \gamma_{(i)} > K_s\gamma_{TP}]
\end{aligned} \tag{5.4}$$

Therefore, if we consider the above two cases, the average number of effective acceptable users is given by

$$\begin{aligned}
\overline{K_{s,eff}} &= \Pr[K_{s,eff} < K_s] + \Pr[K_{s,eff} = K_s] \\
&= \sum_{j=1}^{K_s-1} j \int_0^{\gamma_{TP}} \int_{j\gamma_{TP}}^{(j+1)\gamma_{TP}-x} p_{\gamma_{(j+1), \sum_{i=1}^j \gamma_{(i)}}}(x, y) dy dx \\
&\quad + K_s \int_{K_s\gamma_{TP}}^{\infty} p_{\sum_{i=1}^{K_s} \gamma_{(i)}}(z) dz,
\end{aligned} \tag{5.5}$$

where

$$\begin{aligned}
p_{\gamma_{(j+1)}, \sum_{i=1}^j \gamma_{(i)}}(x, y) &= p_{\sum_{i=1}^j \gamma_{(i)}, \gamma_{(j+1)}}(y, x) \\
&= \frac{K!}{(K-j-1)!(j)!} [P_\gamma(x)]^{K-j-1} [1 - P_\gamma(x)]^j \\
&\quad \times p_\gamma(x) p_{\sum_{i=1}^j \gamma''_i}(y), \\
&\quad x > 0, y > jx,
\end{aligned} \tag{5.6}$$

and $p_{\sum_{i=1}^{K_s} \gamma_{(i)}}(\gamma)$ has the distribution of the sum of the first K_s order statistics and $p_{\sum_{i=1}^j \gamma''_i}(\gamma) = p_{\sum_{i=1}^j \gamma_{(i)} | \gamma_{(j+1)} = x}(y)$ has the distribution of the sum of j different i.i.d. random variables with a truncated PDF of the original variable on the left at x [57].

2. Statistics of Output SNR

To obtain other performance measures, we need to characterize the statistics of the output SNR γ_s of a scheduled user after power allocation with algorithm 3. Based on the mode of operation of algorithm 3, we can divide the PDF of the SNRs of scheduled users after power allocation by considering four cases as the following: i) $\gamma_{excess} = \sum_{i=1}^{K_a} (\gamma_{s_i} - \gamma_{TP}) = 0$, ii) $\gamma_{req} = \sum_{i=K_a+1}^{K_s} (\gamma_{TP} - \gamma_{s_i}) = 0$, iii) $\gamma_{excess} \geq \gamma_{req} > 0$, iv) $0 < \gamma_{excess} < \gamma_{req}$. Note that in the following analysis, we assume $\gamma_{TP} = \gamma_T$. Finally, we can write the PDF of the user SNR after combining all the four cases for the i.i.d. fading case as

$$p_{\gamma_{SBS,alloc}}(\gamma) = p_{\gamma_{SBS,i}}(\gamma) + p_{\gamma_{SBS,ii}}(\gamma) + p_{\gamma_{SBS,iii}}(\gamma) + p_{\gamma_{SBS,iv}}(\gamma). \tag{5.7}$$

If $\gamma_{excess} = \sum_{i=1}^{K_a} (\gamma_{s_i} - \gamma_{TP}) = 0$, no user is acceptable or all acceptable users have γ_{TP} (the largest SNR of the scheduled users is smaller or equal to γ_{TP}) and thus the scheduled users's SNRs will not be changed during the power allocation process. Since $\gamma_{TP} = \gamma_T$, $\gamma_{excess} = 0$ if and only if there is no acceptable users or all acceptable

users have γ_{TP} . However, statistically, the probability of $\gamma_i = \gamma_{TP}$ is zero and this will have no effect on the expression of the probability. Therefore, we show in Appendix D that we can easily write

$$p_{\gamma_{SBS,i}}(\gamma) = \Pr[\gamma_{excess} = 0] p_{\gamma_{SBS,1}}(\gamma). \quad (5.8)$$

If $\gamma_{req} = \sum_{i=K_a+1}^{K_s} (\gamma_{TP} - \gamma_{s_i}) = 0$, (i.e. $K_a > K_s$), power allocation in this case simply redistribute the power among K_s acceptable users. The user SNR after power allocation is the average of K_s user SNRs who has a truncated distribution from left at γ_{TP} . Also the probability of this case is equal to the probability that there are more than K_s acceptable users. Thus, we show in Appendix E that we can derive the PDF as

$$\begin{aligned} p_{\gamma_{SBS,ii}}(\gamma) &= \Pr[\gamma_{req} = 0] p_{\gamma_{SBS,2}}, \\ &= \Pr[\gamma_{req} = 0] p_{\frac{1}{K_s} \sum_{i=1}^{K_s} \gamma_i}(\gamma). \end{aligned} \quad (5.9)$$

If $\gamma_{excess} \geq \gamma_{req} > 0$, the scheduled users have the same amount SNR ($\frac{\gamma_{total}}{K_s}$) $> \gamma_{TP}$, but not every scheduled user is acceptable. The user SNR after power allocation in this case is equal to the average SNR of the sum of the largest K_s SNRs while the K_s th largest SNR is smaller than γ_{TP} , i.e. $\gamma_{SBS,3} = \frac{1}{K_s} \sum_{i=1}^{K_s} \gamma(i)$ given $\gamma_{(K_s)} < \gamma_{TP}$. The CDF of $\sum_{i=1}^{K_s} \gamma(i)$ given $\gamma_{(K_s)} < \gamma_{TP}$ can be derived in terms of the joint PDF of $\gamma_{(K_s)}$ and $\sum_{i=1}^{K_s-1} \gamma(i)$. Finally, we show in Appendix F that the PDF of $\gamma_{SBS,3}$ is obtained as the derivative of the CDF of $\gamma_{SBS,3}$ as

$$p_{\gamma_{SBS,iii}}(\gamma) = p_{\gamma_{SBS,3}}(\gamma). \quad (5.10)$$

If $0 < \gamma_{excess} < \gamma_{req}$, the number of acceptable users after power allocation $K_{s,eff}$ may take the value from 0 to $K_s - 1$ but we do not need to consider the case of $K_{s,eff} = 0$ because we did already deal with it in case of $\gamma_{req} = \sum_{i=K_a+1}^{K_s} (\gamma_{TP} - \gamma_{s_i}) = 0$.

For the PDF of user SNR after power allocation, we show in Appendix G that applying the total probability theorem that the PDF can be re-written as

$$p_{\gamma_{SBS,iv}}(\gamma) = \sum_{j=1}^{K_s-1} p_{\gamma_{SBS,A,K_s,eff=j}}(\gamma). \quad (5.11)$$

Therefore, as a result, we can re-write (5.7) as

$$\begin{aligned} p_{\gamma_{SBS,alloc}}(\gamma) &= \Pr[\gamma_{excess} = 0] p_{\gamma_{SBS,1}}(\gamma) + \Pr[\gamma_{req} = 0] p_{\frac{1}{K_s} \sum_{i=1}^{K_s} \gamma_i}(\gamma) \\ &+ p_{\gamma_{SBS,3}}(\gamma) + \sum_{j=1}^{K_s-1} p_{\gamma_{SBS,A,K_s,eff=j}}(\gamma). \end{aligned} \quad (5.12)$$

After some manipulations and with the help of results in [22,38,39,57], we can re-write (5.12) as the expression given at the bottom of this page. By inserting expressions for i.i.d Rayleigh fading into (5.13), we can get the analytical PDF of a scheduled user after power allocation with algorithm 3 over i.i.d. Rayleigh fading paths in (5.14) at the top of the next page. As a validation of our analytical result, we compare in Fig. 11 the analytical PDF in (5.14) with an empirical PDF obtained by Monte-Carlo simulation. Note that our simulation results match perfectly our analytical results.

$$\begin{aligned} & p_{\gamma_{SBS,alloc}}(\gamma) \\ &= [P_{\gamma}(\gamma_{TP})]^K \frac{1}{K_s} \left(\sum_{i=2}^{K_s} p_{\gamma(i)|\gamma(1)}(\gamma) + \frac{p_{\gamma(1)}(\gamma)}{P_{\gamma(1)}(\gamma_{TP})} (1 - U(\gamma - \gamma_{TP})) \right) + \left[\sum_{K_a=K_s}^K \frac{K!}{(K-K_a)!K_a!} [1 - P_{\gamma}(\gamma_{TP})]^{K_a} [P_{\gamma}(\gamma_{TP})]^{K-K_a} \right. \\ & \quad \left. \times K_s p_{\sum_{i=1}^{K_s} \gamma_i}(K_s \gamma) U(\gamma - \gamma_{TP}) \right] + \frac{d}{d\gamma} \int_0^{\min[\gamma_{TP}, \gamma]} \int_{\max[(K_s-1)y, K_s \gamma_{TP} - y]}^{K_s \gamma - y} p_{\gamma(K_s), \sum_{i=1}^{K_s-1} \gamma(i)}(y, z) U(\gamma - \gamma_{TP}) dz dy \\ &+ \frac{d}{d\gamma} \sum_{j=1}^{K_s-1} \left[\frac{j}{K_s} \int_0^{\gamma_{TP}} \int_{j\gamma_{TP}}^{\min[j\gamma, (j+1)\gamma_{TP}-y]} p_{\gamma(j+1), \sum_{i=1}^j \gamma(i)}(y, z) U(\gamma - \gamma_{TP}) dz dy \right. \\ &+ \frac{K_s - j}{K_s} \frac{1}{K_s - j} \left(\int_{j\gamma_{TP}}^{\infty} \int_0^{\min[(j+1)\gamma_{TP}-y, y/j, \gamma]} p_{\sum_{i=1}^j \gamma(i), \gamma(j+1)}(y, w) (1 - U(\gamma - \gamma_{TP})) dw dy \right. \\ & \left. \left. + \sum_{k=j+2}^{K_s} \int_{j\gamma_{TP}}^{\infty} \int_0^{\min[(j+1)\gamma_{TP}-y, y/j]} \int_0^{\min[\gamma, w]} p_{\sum_{i=1}^j \gamma(i), \gamma(j+1), \gamma(k)}(y, w, z) (1 - U(\gamma - \gamma_{TP})) dz dw dy \right) \right], \end{aligned} \quad (5.13)$$

$$\begin{aligned}
& p_{\gamma_{SBS,alloc}}(\gamma) \\
= & [P_{\gamma}(\gamma_{TP})]^K \frac{1}{K_s} \left(\sum_{i=2}^{K_s} \frac{\int_{\gamma}^{\gamma_{TP}} \frac{K!}{(K-i)!(i-2)!} [P_{\gamma}(\gamma)]^{K-i} [P_{\gamma}(y) - P_{\gamma}(\gamma)]^{i-2} p_{\gamma}(\gamma) p_{\gamma}(y) U(y-\gamma) dy}{\int_0^{\gamma_{TP}} K [P_{\gamma}(x)]^{K-1} p_{\gamma}(x) dx} \right. \\
& + \left. \frac{K [P_{\gamma}(\gamma)]^{K-1} p_{\gamma}(\gamma)}{\int_0^{\gamma_{TP}} K [P_{\gamma}(x)]^{K-1} p_{\gamma}(x) dx} (1 - U(\gamma - \gamma_{TP})) \right) \\
& + \left[\sum_{K_a=K_s}^K \frac{K!}{(K-K_a)!K_a!} [1 - P_{\gamma}(\gamma_{TP})]^{K_a} [P_{\gamma}(\gamma_{TP})]^{K-K_a} \frac{K_s}{(K_s-1)! \bar{\gamma}^{K_s}} (K_s \gamma - K_s \gamma_{TP})^{K_s-1} e^{-\frac{K_s \gamma - K_s \gamma_{TP}}{\bar{\gamma}}} U(\gamma - \gamma_{TP}) \right] \\
& + \frac{d}{d\gamma} \int_0^{\min[\gamma_{TP}, \gamma]} \int_{\max[(K_s-1)y, K_s \gamma_{TP} - y]}^{K_s \gamma - y} \sum_{j=0}^{K-K_s} \frac{(-1)^j K! [z - (K_s - 1)y]^{K_s-2}}{(K-K_s-j)!(K_s-1)!(K_s-2)!j! \bar{\gamma}^{K_s}} e^{-\frac{z+(j+1)y}{\bar{\gamma}}} U(z - (K_s - 1)y) U(\gamma - \gamma_{TP}) dz dy \\
& + \frac{d}{d\gamma} \sum_{j=1}^{K_s-1} \left[\frac{j}{K_s} \int_0^{\gamma_{TP}} \int_{j\gamma_{TP}}^{\min[j\gamma, (j+1)\gamma_{TP} - y]} \sum_{i=0}^{K-j-1} \frac{(-1)^i K! [z - jy]^{j-1}}{(K-j-1-i)!(j)!(j-1)!i! \bar{\gamma}^{j+1}} e^{-\frac{z+(i+1)y}{\bar{\gamma}}} U(z - jy) U(\gamma - \gamma_{TP}) dz dy \right. \\
& + \left. \frac{1}{K_s} \left(\int_{j\gamma_{TP}}^{\infty} \int_0^{\min[(j+1)\gamma_{TP} - y, y/j, \gamma]} \sum_{i=0}^{K-j-1} \frac{(-1)^i K! [y - jw]^{j-1}}{(K-j-1-i)!(j)!(j-1)!i! \bar{\gamma}^{j+1}} e^{-\frac{y+(i+1)w}{\bar{\gamma}}} U(y - jw) (1 - U(\gamma - \gamma_{TP})) dw dy \right) \right. \\
& + \left. \sum_{k=j+2}^{K_s} \int_{j\gamma_{TP}}^{\infty} \int_0^{\min[(j+1)\gamma_{TP} - y, y/j]} \int_0^{\min[\gamma, w]} \left(\frac{K!}{(K-j-1)!(j)!} [P_{\gamma}(w)]^{K-j-1} [1 - P_{\gamma}(w)]^j p_{\gamma}(w) \right) \right. \\
& \left. \left(\frac{(K-j-1)! [P_{\gamma}(z)]^{K-k} [P_{\gamma}(w) - P_{\gamma}(z)]^{k-j-2} p_{\gamma}(z) U(w-z)}{(K-k)!(k-j-2)! [P_{\gamma}(w)]^{K-j-1}} U(w-z) \right) \left(\frac{(y-jw)^{j-1}}{(j-1)! \bar{\gamma}^j} e^{-\frac{y-jw}{\bar{\gamma}}} U(y-jw) \right) (1 - U(\gamma - \gamma_{TP})) dz dw dy \right). \tag{5.14}
\end{aligned}$$

3. Average Spectral Efficiency

The ASE of a scheduled user is obtained as the sum of the all spectral efficiencies $\{R_n\}_{n=1}^N$ of the individual codes, weighted by the probability P_n that the SNR of a scheduled user after power allocation is assigned to the n th region:

$$\text{ASE} = \sum_{n=1}^N R_n P_n = \sum_{n=1}^N R_n \int_{\gamma_{T_n}}^{\gamma_{T_{n+1}}} p_{\gamma_{SBS,alloc}}(\gamma) d\gamma. \tag{5.15}$$

In this case, to obtain the ASE of the scheduled users for each time-slot, we just need to multiply the average number of scheduled users given in [56] by (5.15). Since the number of scheduled users after power allocation is the same as those before power allocation and the average number of scheduled users of SBS is also K_s , the ASE of the scheduled users for each time-slot becomes

$$\text{ASE}_{time-slot} = K_s \sum_{n=1}^N R_n \int_{\gamma_{T_n}}^{\gamma_{T_{n+1}}} p_{\gamma_{SBS,alloc}}(\gamma) d\gamma, \tag{5.16}$$

4. Average BER

The average BER for over all codes and SNRs of the scheduled users is given as the average number of bits in error divided by the average number of bits transmitted [34].

$$\overline{\text{BER}} = \frac{\sum_{n=1}^N R_n \overline{\text{BER}}_n}{\sum_{n=1}^N R_n P_n}, \quad (5.17)$$

where $\overline{\text{BER}}_n$ denotes the average BER when code n is used

$$\begin{aligned} \overline{\text{BER}}_n &= \int_{\gamma_{T_n}}^{\gamma_{T_{n+1}}} \text{BER}_n p_{\gamma_{SBS,alloc}}(\gamma) d\gamma \\ &= \int_{\gamma_{T_n}}^{\gamma_{T_{n+1}}} a_n \exp\left(-\frac{b_n \gamma}{M_n}\right) p_{\gamma_{SBS,alloc}}(\gamma) d\gamma, \end{aligned} \quad (5.18)$$

where a_n and b_n are code-dependent constants which were found by least square fitting to simulated data on AWGN channels [34, Table I].

F. Conclusion

In this chapter, we proposed threshold-based power allocation algorithms to increase the number of effective acceptable users among the scheduled users with SBS type of scheduling. The main idea is to re-allocate the extracted excess SNR from the acceptable users to the unacceptable users. We found that there exists a trade-off between the average BER, the ASE, and the average number of effective acceptable users with the SNR threshold after power allocation process. After power allocation, the unacceptable users can reach acceptable SNRs and as such the number of effective acceptable users with an acceptable SNR threshold among the scheduled users is increased without any additional power. Some selected numerical results, show that the proposed power allocation algorithms offer a certain improvement in ASE and an increase in the average number of effective acceptable users. Although the average

BER performance degrades especially when the average SNR is close to the SNR threshold for power allocation, this average BER performance still meets the average BER requirement because the average BER is still below the target BER.

CHAPTER VI

A MGF-BASED UNIFIED FRAMEWORK TO DETERMINE THE JOINT
STATISTICS OF PARTIAL SUMS OF ORDERED RANDOM VARIABLES

A. Introduction

The subject of order statistics deals with the properties and applications of the ordered random variables (RVs) and their functions. It has found applications in many areas of statistical theory and practice [58], with examples including life-testing, quality control, signal and image processing [59, 60]. Recently, order statistics makes a growing number of appearance in the analysis and design of wireless communication systems [39, 57, 61, 62]. For example, diversity techniques have been used for past half century to mitigate the effects of fading on wireless communication systems. These techniques improve the performance of wireless communication systems over fading channels by generating and combining multiple replicas of the same information bearing signal at the receiver. The analysis of a low-complexity selection combining scheme, which selects the best replica, requires some basic result of order statistics.

More recently, the design and analysis of adaptive diversity combining techniques and multiuser scheduling strategies call for some further results on order statistics. In particular, the joint statistics of several partial sums of ordered RVs are often necessary for the accurate characterization of the system performance. The major difficulty in obtaining the statistics of the sum of order statistics resides in the fact that while the original RVs are independently distributed, their ordered statistics are necessarily dependent due to the inequality relations among them. While previous works employ a successive conditioning approach to address this problem, in this chapter, we introduce a unified analytical framework to determine the joint statistics

of partial sums of order statistics based on the moment generating functions (MGF) by extending the approach used in [63–65].

In [63–65], the joint PDF of selected order statistics and the sum of all the remaining RVs was obtained. Here we generalize their method and solve the joint statistics of arbitrary partial sums of ordered RVs. With the proposed MGF-based approach, we can systematically derive the joint statistics in terms of the probability density function (PDF) not only when all the K ordered RVs are considered but also when only the K_s ($K_s < K$) best RVs are considered among K RVs. In addition, we derive the closed form expressions for the exponential special case. These closed-form results can apply to the performance analysis of various wireless communication systems over i.i.d. Rayleigh fading conditions.

The remainder of this chapter is organized as follows. In section II, we summarize the main idea of the proposed unified approach. In section III and IV, we present some selected examples on the derivation of joint PDF based on our proposed approach. Following this, we show some closed form expressions over i.i.d. Rayleigh fading conditions of these selected examples in section V. Finally, we discuss the application of these results in section VI.

B. The Main Idea

Let $\infty \geq \gamma_{1:K} \geq \gamma_{2:K} \geq \gamma_{3:K} \cdots \geq \gamma_{K:K} \geq 0$ be the order statistics obtained by arranging K nonnegative independent identically distributed (i.i.d.) RVs, $\{\gamma_i\}_{i=1}^K$, in decreasing order of magnitude. The objective is to derive the joint PDF of their partial sums involving either all K or the first K_s ($\leq K$) ordered RVs, e.g. joint PDF of $\gamma_{m:K}$ and $\sum_{\substack{n=1 \\ n \neq m}}^K \gamma_{n:K}$ or Joint PDF of $\sum_{n=1}^m \gamma_{n:K}$ and $\sum_{n=m+1}^{K_s} \gamma_{n:K}$. The proposed framework adopts a general two-step approach: i) obtain the analytical expressions

of the joint MGF of some partial sums (not necessarily the partial sums of interest as will be seen later), ii) apply inverse Laplace transform to derive the joint PDF of partial sums (additional integration may be required to obtain the desired joint PDF).

To facilitate the inverse Laplace transform calculation, the joint MGF from step i) should be made as compact as possible. An observation made in [63–65] involving the interchange of multiple integrals of ordered random variables becomes useful in the following analysis. Suppose for example that we need to evaluate a multiple integral over the range $\gamma_a \geq \gamma_1 \geq \gamma_2 \geq \gamma_3 \geq \gamma_4 \geq \gamma_b$. More specifically, let

$$I = \int_{\gamma_b}^{\gamma_a} d\gamma_1 \int_{\gamma_b}^{\gamma_1} d\gamma_2 \int_{\gamma_b}^{\gamma_2} d\gamma_3 \int_{\gamma_b}^{\gamma_3} d\gamma_4 p(\gamma_1, \gamma_2, \gamma_3, \gamma_4). \quad (6.1)$$

It can be shown by interchanging the order of integration while ensuring each pair of limits is chosen to be as tight as possible, the multiple integral in (6.1) can be rewritten into the following equivalent representations,

$$\begin{aligned} I &= \int_{\gamma_b}^{\gamma_a} d\gamma_4 \int_{\gamma_4}^{\gamma_a} d\gamma_3 \int_{\gamma_3}^{\gamma_a} d\gamma_2 \int_{\gamma_2}^{\gamma_a} d\gamma_1 p(\gamma_1, \gamma_2, \gamma_3, \gamma_4) \\ &= \int_{\gamma_b}^{\gamma_a} d\gamma_2 \int_{\gamma_b}^{\gamma_2} d\gamma_3 \int_{\gamma_b}^{\gamma_3} d\gamma_4 \int_{\gamma_2}^{\gamma_a} d\gamma_1 p(\gamma_1, \gamma_2, \gamma_3, \gamma_4) \\ &= \int_{\gamma_b}^{\gamma_a} d\gamma_3 \int_{\gamma_3}^{\gamma_a} d\gamma_1 \int_{\gamma_b}^{\gamma_3} d\gamma_4 \int_{\gamma_3}^{\gamma_1} d\gamma_2 p(\gamma_1, \gamma_2, \gamma_3, \gamma_4) \\ &= \int_{\gamma_b}^{\gamma_a} d\gamma_1 \int_{\gamma_b}^{\gamma_1} d\gamma_4 \int_{\gamma_4}^{\gamma_1} d\gamma_3 \int_{\gamma_3}^{\gamma_1} d\gamma_2 p(\gamma_1, \gamma_2, \gamma_3, \gamma_4) \\ &= \int_{\gamma_b}^{\gamma_a} d\gamma_4 \int_{\gamma_4}^{\gamma_a} d\gamma_1 \int_{\gamma_4}^{\gamma_1} d\gamma_3 \int_{\gamma_3}^{\gamma_1} d\gamma_2 p(\gamma_1, \gamma_2, \gamma_3, \gamma_4). \end{aligned} \quad (6.2)$$

The general rule is that if a potential limit variable has already been integrated, the next tightest limit variable that is still active should be selected.

After deriving the MGF in a compact form, we rely on the Bromwich contour integral which is the one of inverse Laplace transform solutions to derive joint PDF of selected partial sum. In most of the case, the result involves a single one-dimensional

contour integration, which can be easily and accurately evaluated numerically using standard mathematical packages such as Mathematica and Matlab and so on.

When only the best $K_s (\leq K)$ ordered RVs are considered, the joint PDF is more complicated to obtain than the case when all K RVs are considered. In this case, some new partial sums may be introduced to simplify the evaluation of joint MGF. In particular, the order statistics $\gamma_{K_s:K}$ should be considered separately. As an illustration, the example in Fig. 20 considers the partial sums of three group of RVs which are $\{\gamma_{1:K}, \gamma_{2:K}, \gamma_{3:K}\}$, $\{\gamma_{4:K}, \gamma_{5:K}, \gamma_{6:K}\}$, and $\{\gamma_{7:K}, \gamma_{8:K}\}$, with $K = 10$ and $K_s = 8$. With the proposed approach, we will derive the 4-dimensional joint MGF in step i) by considering $\gamma_{8:K}$ separately, i.e. the following four groups of RVs $\{\gamma_{1:K}, \gamma_{2:K}, \gamma_{3:K}\}$, $\{\gamma_{4:K}, \gamma_{5:K}, \gamma_{6:K}\}$, $\{\gamma_{7:K}\}$, and $\{\gamma_{8:K}\}$. In addition, if RVs involved in one partial sum is separated by the other groups of RVs, we will divide these RVs into smaller groups. The example in Fig. 21 illustrate this process. There are three partial sum of RVs $\{\gamma_{1:K}, \gamma_{2:K}, \gamma_{5:K}, \gamma_{6:K}\}$, $\{\gamma_{3:K}, \gamma_{4:K}\}$, and $\{\gamma_{7:K}, \gamma_{8:K}\}$. Note that the first group is splitted (dis-continued) by the second group of RVs. We also consider this splitted group as two smaller group. As a results, we will derive 5-dimensional joint MGF of $\{\gamma_{1:K}, \gamma_{2:K}\}$, $\{\gamma_{3:K}, \gamma_{4:K}\}$, $\{\gamma_{5:K}, \gamma_{6:K}\}$, $\{\gamma_{7:K}\}$, and $\{\gamma_{8:K}\}$ in step i). In both cases, after the joint PDF of the new substituted partial sums are derived with inverse Laplace transform in step ii), we can transform it to lower dimensional desired joint PDF with finite integration.

The proposed approach is summarized in the flowchart in Fig. 22, where we consider four different case separately. In the following sections, we present several examples to illustrate the proposed framework. Our focus is on how to obtain a compact expression of the joint MGFs, which can be greatly simplified with the application of the following function and relations.

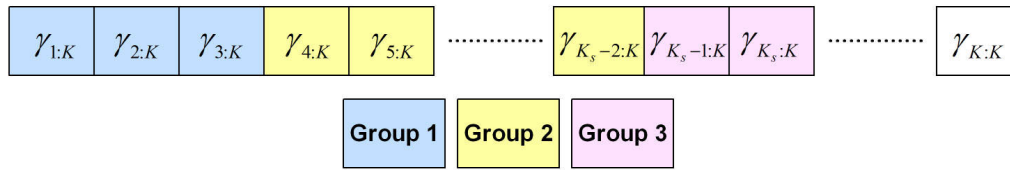
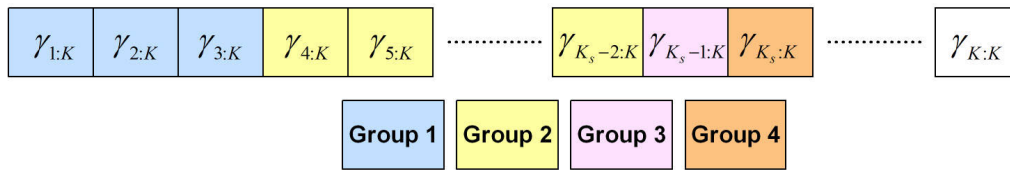
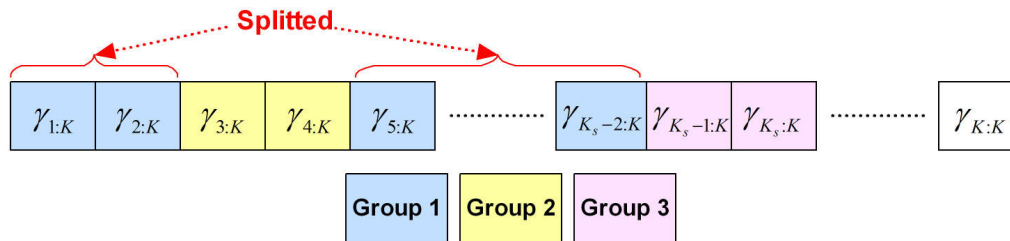
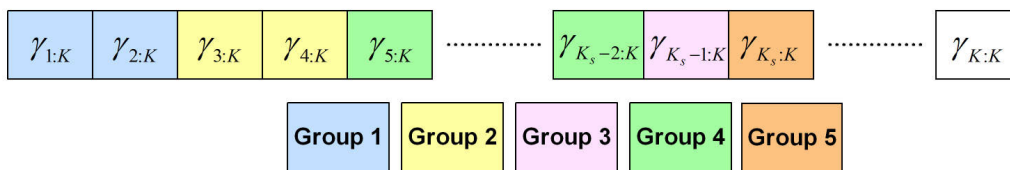
(a) Example of original M -dimensional groups(b) Example of substituted $(M + 1)$ -dimensional groups

Fig. 20. Examples for 3-dimensional joint PDF with non-splitting groups.

(a) Example of original M -dimensional groups

(b) Example of substituted splitted groups

Fig. 21. Examples for 3-dimensional joint PDF with splitted groups.

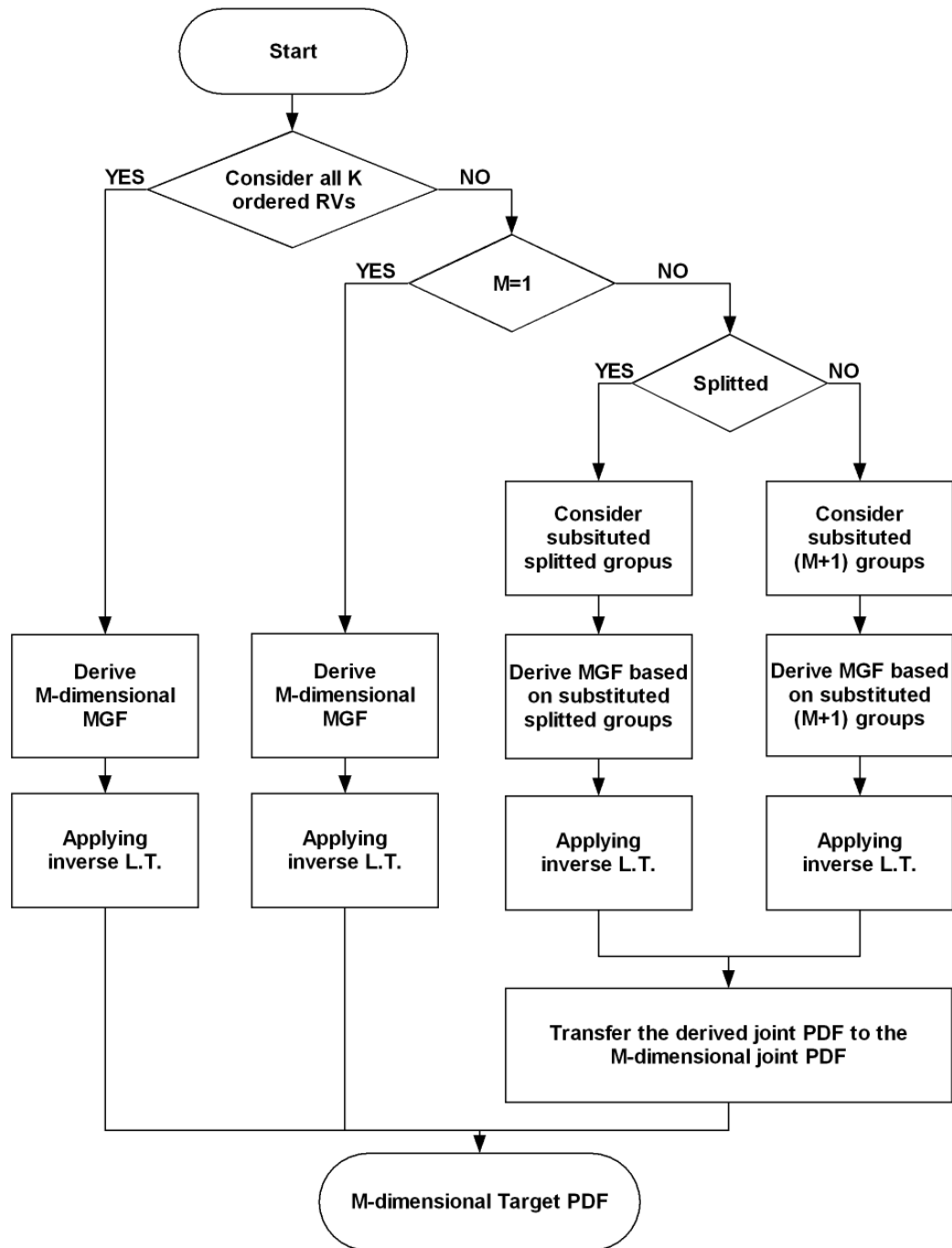


Fig. 22. Flow Chart.

1. Common Functions

i) A mixture of a CDF and an MGF $c(\gamma, \lambda)$:

$$c(\gamma, \lambda) = \int_0^\gamma dx p(x) \exp(\lambda x), \quad (6.3)$$

where $p(x)$ denotes the PDF of the RV of interest. Note that $c(\gamma, 0) = c(\gamma)$ is the CDF and $c(\infty, \lambda)$ leads to the MGF. Here, the variable γ is real, while λ can be complex.

ii) A mixture of an exceedance distribution function (EDF) and an MGF, $e(\gamma, \lambda)$:

$$e(\gamma, \lambda) = \int_\gamma^\infty dx p(x) \exp(\lambda x). \quad (6.4)$$

Note that $e(\gamma, 0) = e(\gamma)$ is the EDF which $e(0, \lambda)$ gives the MGF.

iii) An Interval MGF $\mu(\gamma_a, \gamma_b, \lambda)$:

$$\mu(\gamma_a, \gamma_b, \lambda) = \int_{\gamma_a}^{\gamma_b} dx p(x) \exp(\lambda x). \quad (6.5)$$

Note that $\mu(0, \infty, \lambda)$ gives the MGF.

Note that the functions defined in (6.3), (6.4) and (6.5) are related as following.

$$\begin{aligned} c(\gamma, \lambda) &= e(0, \lambda) - e(\gamma, \lambda) \\ &= c(\infty, \lambda) - e(\gamma, \lambda) \end{aligned} \quad (6.6)$$

$$\begin{aligned} e(\gamma, \lambda) &= c(\infty, \lambda) - c(\gamma, \lambda) \\ &= e(0, \lambda) - c(\gamma, \lambda) \end{aligned} \quad (6.7)$$

$$\begin{aligned} \mu(\gamma_a, \gamma_b, \lambda) &= c(\gamma_b, \lambda) - c(\gamma_a, \lambda) \\ &= e(\gamma_a, \lambda) - e(\gamma_b, \lambda). \end{aligned} \quad (6.8)$$

2. Simplifying Relationship

i) Integral I_m :

Based on the derivation given Appendix I, the integral I_m defined as:

$$\begin{aligned}
I_m &= \int_0^{\gamma_{m-1:K}} d\gamma_{m:K} p(\gamma_{m:K}) \exp(\lambda\gamma_{m:K}) \int_0^{\gamma_{m:K}} d\gamma_{m+1:K} p(\gamma_{m+1:K}) \exp(\lambda\gamma_{m+1:K}) \\
&\times \int_0^{\gamma_{m+1:K}} d\gamma_{m+2:K} p(\gamma_{m+2:K}) \exp(\lambda\gamma_{m+2:K}) \cdots \int_0^{\gamma_{K-1:K}} d\gamma_{K:K} p(\gamma_{K:K}) \exp(\lambda\gamma_{K:K}), \quad (6.9)
\end{aligned}$$

can be expressed in terms of function $c(\gamma, \lambda)$ as

$$I_m = \frac{1}{(K-m+1)!} [c(\gamma_{m-1:K}, \lambda)]^{(K-m+1)}. \quad (6.10)$$

ii) Integral I'_m :

Based on the derivation given in Appendix J, the integral I'_m defined as

$$\begin{aligned}
I'_m &= \int_{\gamma_{m+1:K}}^{\infty} d\gamma_{m:K} p(\gamma_{m:K}) \exp(\lambda\gamma_{m:K}) \int_{\gamma_{m:K}}^{\infty} d\gamma_{m-1:K} p(\gamma_{m-1:K}) \exp(\lambda\gamma_{m-1:K}) \\
&\times \int_{\gamma_{m-1:K}}^{\infty} d\gamma_{m-2:K} p(\gamma_{m-2:K}) \exp(\lambda\gamma_{m-2:K}) \cdots \int_{\gamma_{2:K}}^{\infty} d\gamma_{1:K} p(\gamma_{1:K}) \exp(\lambda\gamma_{1:K}), \quad (6.11)
\end{aligned}$$

can be expressed in terms of function $e(\gamma, \lambda)$ as

$$I'_m = \frac{1}{m!} [e(\gamma_{m+1:K}, \lambda)]^m. \quad (6.12)$$

iii) Integral $I''_{a,b}$:

Based on the derivation given in Appendix K, the integral $I''_{a,b}$ defined as

$$\begin{aligned}
I''_{a,b} &= \int_{\gamma_{a:K}}^{\gamma_{a:K}} d\gamma_{b-1:K} p(\gamma_{b-1:K}) \exp(\lambda\gamma_{b-1:K}) \int_{\gamma_{b-1:K}}^{\gamma_{a:K}} d\gamma_{b-2:K} p(\gamma_{b-2:K}) \exp(\lambda\gamma_{b-2:K}) \\
&\times \int_{\gamma_{b-2:K}}^{\gamma_{a:K}} d\gamma_{b-3:K} p(\gamma_{b-3:K}) \exp(\lambda\gamma_{b-3:K}) \cdots \int_{\gamma_{a+2:K}}^{\gamma_{a:K}} d\gamma_{a+1:K} p(\gamma_{a+1:K}) \exp(\lambda\gamma_{a+1:K}), \quad (6.13)
\end{aligned}$$

can be expressed in terms of function $\mu(\cdot, \cdot)$ as

$$I''_{a,b} = \frac{1}{(b-a-1)!} [\mu(\gamma_{b:K}, \gamma_{a:K}, \lambda)]^{(b-a-1)} \quad \text{for } b > a. \quad (6.14)$$

C. Sample Cases When All K Ordered RVs Are Considered

Assume the original RVs $\{\gamma_i\}$ are independent identically distributed (i.i.d.) with a common arbitrary probability density function (PDF) $p(\gamma)$, the K -dimensional joint

PDF of $\{\gamma_{i:K}\}_{i=1}^K$ is simply given by [58]

$$p(\gamma_{1:K}, \gamma_{2:K}, \dots, \gamma_{K:K}) = F \cdot \prod_{i=1}^K p(\gamma_{i:K}) \quad \text{for } \gamma_{1:K} \geq \gamma_{2:K} \geq \gamma_{3:K} \dots \geq \gamma_{K:K}, \quad (6.15)$$

where $F = K!$.

1. Joint PDF of $\gamma_{m:K}$ and $\sum_{\substack{n=1 \\ n \neq m}}^K \gamma_{n:K}$

Let $Z_1 = \gamma_{m:K}$ and $Z_2 = \sum_{\substack{n=1 \\ n \neq m}}^K \gamma_{n:K}$ for convenience. The second order MGF of $Z = [Z_1, Z_2]$ is given by the expectation

$$\begin{aligned} MGF_Z(\lambda_1, \lambda_2) &= E \{ \exp(\lambda_1 Z_1 + \lambda_2 Z_2) \} \\ &= F \int_0^\infty d\gamma_{1:K} p(\gamma_{1:K}) \exp(\lambda_2 \gamma_{1:K}) \int_0^{\gamma_{1:K}} d\gamma_{2:K} p(\gamma_{2:K}) \exp(\lambda_2 \gamma_{2:K}) \cdots \int_0^{\gamma_{m-2:K}} d\gamma_{m-1:K} p(\gamma_{m-1:K}) \exp(\lambda_2 \gamma_{m-1:K}) \\ &\quad \times \int_0^{\gamma_{m-1:K}} d\gamma_{m:K} p(\gamma_{m:K}) \exp(\lambda_1 \gamma_{m:K}) \\ &\quad \times \int_0^{\gamma_{m:K}} d\gamma_{m+1:K} p(\gamma_{m+1:K}) \exp(\lambda_2 \gamma_{m+1:K}) \cdots \int_0^{\gamma_{K-1:K}} d\gamma_{K:K} p(\gamma_{K:K}) \exp(\lambda_2 \gamma_{K:K}). \end{aligned} \quad (6.16)$$

We show in Appendix L that by applying (7.8), (6.2) and (7.11), we can obtain the second order MGF of $Z_1 = \gamma_{m:K}$ and $Z_2 = \sum_{\substack{n=1 \\ n \neq m}}^K \gamma_{n:K}$ as

$$\begin{aligned} MGF_Z(\lambda_1, \lambda_2) &= \frac{F}{(K-m)!(m-1)!} \int_0^\infty d\gamma_{m:K} p(\gamma_{m:K}) \exp(\lambda_1 \gamma_{m:K}) [c(\gamma_{m:K}, \lambda_2)]^{(K-m)} [e(\gamma_{m:K}, \lambda_2)]^{(m-1)}. \end{aligned} \quad (6.17)$$

With the MGF expression given in (6.17), we are now in the position to derive the 2-dimensional joint PDF of $Z_1 = \gamma_{m:K}$ and $Z_2 = \sum_{\substack{n=1 \\ n \neq m}}^K \gamma_{n:K}$. Letting $\lambda_1 = -S_1$ and $\lambda_2 = -S_2$, we can derive the 2-dimensional joint PDF by applying the inverse Laplace transform as

$$\begin{aligned}
p_Z(z_1, z_2) &= \mathcal{L}_{S_1, S_2}^{-1} \{MGF_Z(-S_1, -S_2)\} \\
&= \frac{K!}{(K-m)!(m-1)!} \int_0^\infty d\gamma_{m:K} \left[p(\gamma_{m:K}) \mathcal{L}_{S_1}^{-1} \{ \exp(-S_1 \gamma_{m:K}) \} \right. \\
&\quad \left. \times \mathcal{L}_{S_2}^{-1} \left\{ [c(\gamma_{m:K}, -S_2)]^{(K-m)} [e(\gamma_{m:K}, -S_2)]^{(m-1)} \right\} \right]. \tag{6.18}
\end{aligned}$$

Based on the inverse Laplace transform properties in Appendix H,

$$\mathcal{L}_{S_1}^{-1} \{ \exp(-S_1 \gamma_{m:K}) \} = \delta(z_1 - \gamma_{m:K}). \tag{6.19}$$

Therefore, substituting (6.19) in (7.6) we can obtain the 2-dimensional joint PDF of

$$Z_1 = \gamma_{m:K} \text{ and } Z_2 = \sum_{\substack{n=1 \\ n \neq m}}^K \gamma_{n:K} \text{ as}$$

$$\begin{aligned}
p_Z(z_1, z_2) &= p_{\gamma_{m:K}, \sum_{\substack{n=1 \\ n \neq m}}^K \gamma_{n:K}}(z_1, z_2) \\
&= \begin{cases} \frac{K!}{(K-1)!} p(z_1) \mathcal{L}_{S_2}^{-1} \left\{ [c(z_1, -S_2)]^{(K-1)} \right\} & \text{for } m=1, z_1 \geq \frac{1}{K-1} z_2 \\ \frac{K!}{(K-m)!(m-1)!} p(z_1) \mathcal{L}_{S_2}^{-1} \left\{ [c(z_1, -S_2)]^{(K-m)} [e(z_1, -S_2)]^{(m-1)} \right\} & \text{for } m \geq 2. \end{cases} \tag{6.20}
\end{aligned}$$

2. Joint PDF of $\sum_{n=1}^m \gamma_{n:K}$ and $\sum_{n=m+1}^K \gamma_{n:K}$

Let $Z_1 = \sum_{n=1}^m \gamma_{n:K}$ and $Z_2 = \sum_{n=m+1}^K \gamma_{n:K}$ for convenience. The second order MGF of $Z = [Z_1, Z_2]$ is given by the expectation

$$\begin{aligned}
MGF_Z(\lambda_1, \lambda_2) &= E \{ \exp(\lambda_1 Z_1 + \lambda_2 Z_2) \} \\
&= F \int_0^\infty d\gamma_{1:K} p(\gamma_{1:K}) \exp(\lambda_1 \gamma_{1:K}) \cdots \int_0^{\gamma_{m-1:K}} d\gamma_{m:K} p(\gamma_{m:K}) \exp(\lambda_1 \gamma_{m:K}) \tag{6.21}
\end{aligned}$$

$$\times \int_0^{\gamma_{m:K}} d\gamma_{m+1:K} p(\gamma_{m+1:K}) \exp(\lambda_2 \gamma_{m+1:K}) \cdots \int_0^{\gamma_{K-1:K}} d\gamma_{K:K} p(\gamma_{K:K}) \exp(\lambda_2 \gamma_{K:K}). \tag{6.22}$$

We show in Appendix M that by applying (7.8) and (6.2) and then (7.11), we can

obtain the second order MGF of $Z_1 = \sum_{n=1}^m \gamma_{n:K}$ and $Z_2 = \sum_{n=m+1}^K \gamma_{n:K}$ as

$$\begin{aligned}
& MGF_Z(\lambda_1, \lambda_2) \\
&= \frac{K!}{(K-m)!(m-1)!} \int_0^\infty d\gamma_{m:K} p(\gamma_{m:K}) \exp(\lambda_1 \gamma_{m:K}) [c(\gamma_{m:K}, \lambda_2)]^{(K-m)} [e(\gamma_{m:K}, \lambda_1)]^{(m-1)}. \quad (6.23)
\end{aligned}$$

Again, letting $\lambda_1 = -S_1$ and $\lambda_2 = -S_2$, we can derive the 2-dimensional joint PDF of $Z_1 = \sum_{n=1}^m \gamma_{n:K}$ and $Z_2 = \sum_{n=m+1}^K \gamma_{n:K}$ by applying the inverse Laplace transforms as

$$\begin{aligned}
p_Z(z_1, z_2) &= p_{\sum_{n=1}^m \gamma_{n:K}, \sum_{n=m+1}^K \gamma_{n:K}}(z_1, z_2) \\
&= \mathcal{L}_{S_1, S_2}^{-1} \{MGF_Z(-S_1, -S_2)\} \\
&= \frac{K!}{(K-m)!(m-1)!} \int_0^\infty d\gamma_{m:K} \left[p(\gamma_{m:K}) \mathcal{L}_{S_1}^{-1} \left\{ \exp(-S_1 \gamma_{m:K}) [e(\gamma_{m:K}, -S_1)]^{(m-1)} \right\} \right. \\
&\quad \left. \times \mathcal{L}_{S_2}^{-1} \left\{ [c(\gamma_{m:K}, -S_2)]^{(K-m)} \right\} \right] \quad \text{for } z_1 \geq \frac{m}{K-m} z_2. \quad (6.24)
\end{aligned}$$

D. Sample Cases When Only K_s Ordered RVs Are Considered

Let us now consider the cases where only the best $K_s (\leq K)$ ordered RVs are involved. Assuming the original $\{\gamma_i\}$ are i.i.d. RVs with a common arbitrary PDF $p(\gamma)$ and CDF $P(\gamma)$, the K_s -dimensional joint PDF of $\{\gamma_{i:K}\}_{i=1}^{K_s}$ is simply given by

$$p(\gamma_{1:K}, \gamma_{2:K}, \dots, \gamma_{K_s:K}) = F \cdot \prod_{i=1}^{K_s} p(\gamma_{i:K}) [P(\gamma_{K_s:K})]^{K-K_s}, \quad (6.25)$$

where $F = K_s! \binom{K}{K_s} = \frac{K!}{(K-K_s)!}$.

1. PDF of $\sum_{n=1}^{K_s} \gamma_{n:K}$

Let $Z_1 = \sum_{n=1}^{K_s} \gamma_{n:K}$ for convenience. The single order MGF of $Z = [Z_1]$ is given by the expectation

$$\begin{aligned}
MGF_Z(\lambda_1) &= E \{ \exp(\lambda_1 Z_1) \} \\
&= F \int_0^\infty d\gamma_{1:K} p(\gamma_{1:K}) \exp(\lambda_1 \gamma_{1:K}) \int_0^{\gamma_{1:K}} d\gamma_{2:K} p(\gamma_{2:K}) \exp(\lambda_1 \gamma_{2:K}) \\
&\quad \times \cdots \times \int_0^{\gamma_{K_s-1:K}} d\gamma_{K_s:K} p(\gamma_{K_s:K}) \exp(\lambda_1 \gamma_{K_s:K}) [c(\gamma_{K_s:K})]^{K-K_s}. \quad (6.26)
\end{aligned}$$

As in Appendix N by applying (6.2) and then (7.11), the single order MGF of $Z_1 = \sum_{m=1}^{K_s} \gamma_{m:K}$ can be obtained as

$$\begin{aligned}
MGF_Z(\lambda_1) \\
&= \frac{F}{(K_s - 1)!} \int_0^\infty d\gamma_{K_s:K} p(\gamma_{K_s:K}) \exp(\lambda_1 \gamma_{K_s:K}) [c(\gamma_{K_s:K})]^{K-K_s} [e(\gamma_{K_s:K}, \lambda_1)]^{(K_s-1)}. \quad (6.27)
\end{aligned}$$

With the MGF expression given in (6.27), we are now in the position to derive the PDF of $Z_1 = \sum_{m=1}^{K_s} \gamma_{m:K}$. Letting $\lambda_1 = -S_1$ we can derive the PDF of $Z_1 = \sum_{m=1}^{K_s} \gamma_{m:K}$ by applying the inverse Laplace transforms as

$$\begin{aligned}
p_Z(z_1) &= p_{\sum_{m=1}^{K_s} \gamma_{m:K}}(z_1) = \mathcal{L}_{S_1}^{-1} \{ MGF_Z(-S_1) \} \\
&= \frac{F}{(K_s - 1)!} \int_0^\infty d\gamma_{K_s:K} \left[p(\gamma_{K_s:K}) [c(\gamma_{K_s:K})]^{K-K_s} \right. \\
&\quad \left. \times \mathcal{L}_{S_1}^{-1} \left\{ \exp(-S_1 \gamma_{K_s:K}) [e(\gamma_{K_s:K}, -S_1)]^{(K_s-1)} \right\} \right]. \quad (6.28)
\end{aligned}$$

2. Joint PDF of $\gamma_{m:K}$ and $\sum_{\substack{n=1 \\ n \neq m}}^{K_s} \gamma_{n:K}$

To derive the joint PDF of $\gamma_{m:K}$ and $\sum_{\substack{n=1 \\ n \neq m}}^{K_s} \gamma_{n:K}$, we need to consider four cases i) $m = 1$, ii) $1 < m < K_s - 1$, iii) $m = K_s - 1$ and iv) $m = K_s$ separately based on our unified framework. While for case iv), we can start with the second order MGF

of $\gamma_{m:K}$ and $\sum_{\substack{n=1 \\ n \neq m}}^{K_s} \gamma_{n:K}$ directly, we should consider substituted groups instead of the original groups for cases i), ii), and iii). More specifically, for cases i) and iii), we need to consider $\gamma_{K_s:K}$ separately as shown in Fig. 23(a) and 23(c) whereas, for case ii), as one of original groups is splitted by $\gamma_{m:K}$, we should consider substituted groups for the splitted group instead of original groups as shown in Fig. 23(b). As a result, we will start by obtaining a four order MGF for case ii) and a three order MGF for case i) and case iii). In all these cases, the higher dimensional joint PDF can then be used to find the desired 2-dimensional joint PDF of interest by transformation.

Applying the results in (6.2), (7.8), (7.11) and (7.9), we derive in Appendix O the following joint MGF for different cases

a. $m = 1$

Let $Z_1 = \gamma_{1:K}$, $Z_2 = \sum_{n=2}^{K_s-1} \gamma_{n:K}$, and $Z_3 = \gamma_{K_s:K}$, then

$$\begin{aligned} & MGF_Z(\lambda_1, \lambda_2, \lambda_3) \\ &= F \int_0^\infty d\gamma_{K_s:K} p(\gamma_{K_s:K}) \exp(\lambda_3 \gamma_{K_s:K}) [c(\gamma_{K_s:K})]^{(K-K_s)} \\ & \quad \times \int_{\gamma_{K_s:K}}^\infty d\gamma_{1:K} p(\gamma_{1:K}) \exp(\lambda_1 \gamma_{1:K}) \frac{1}{(K_s-2)!} [\mu(\gamma_{K_s:K}, \gamma_{1:K}, \lambda_2)]^{(K_s-2)}. \end{aligned} \quad (6.29)$$

b. $1 < m < K_s - 1$

Let $Z_1 = \sum_{n=1}^{m-1} \gamma_{n:K}$, $Z_2 = \gamma_{m:K}$, $Z_3 = \sum_{n=m+1}^{K_s-1} \gamma_{n:K}$, and $Z_4 = \gamma_{K_s:K}$, then

$$\begin{aligned} & MGF_Z(\lambda_1, \lambda_2, \lambda_3, \lambda_4) \\ &= \frac{F}{(K_s - m - 1)! (m - 1)!} \int_0^\infty d\gamma_{K_s:K} p(\gamma_{K_s:K}) \exp(\lambda_4 \gamma_{K_s:K}) [c(\gamma_{K_s:K})]^{(K-K_s)} \\ & \quad \times \int_{\gamma_{K_s:K}}^\infty d\gamma_{m:K} p(\gamma_{m:K}) \exp(\lambda_2 \gamma_{m:K}) [e(\gamma_{m:K}, \lambda_1)]^{(m-1)} [\mu(\gamma_{K_s:K}, \gamma_{m:K}, \lambda_3)]^{(K_s-m-1)}. \end{aligned} \quad (6.30)$$

c. $m = K_s - 1$

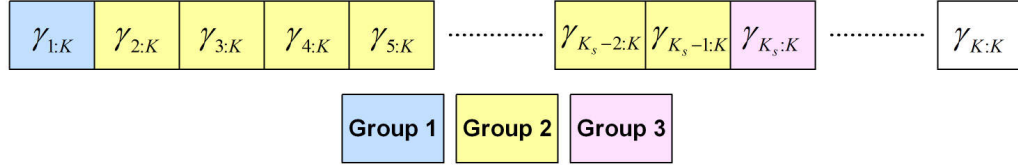
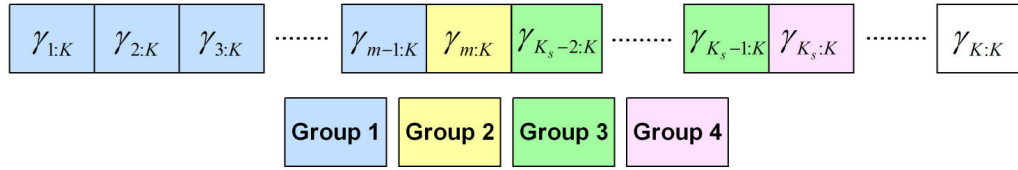
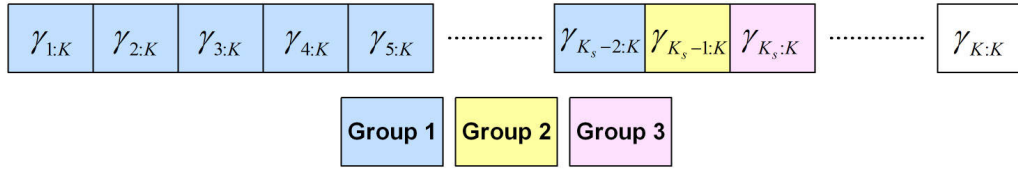
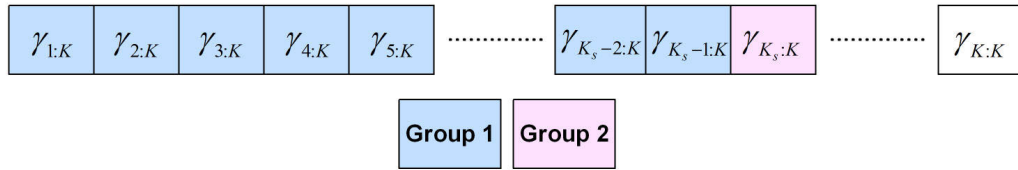
(a) For the case of $m = 1$ (b) For the case of $1 < m < K_s - 1$ (c) For the case of $m = K_s - 1$ (d) For the case of $m = K_s$

Fig. 23. Joint MGF of $\gamma_{m:K}$ and $\sum_{\substack{n=1 \\ n \neq m}}^{K_s} \gamma_{n:K}$.

Let $Z_1 = \sum_{n=1}^{K_s-2} \gamma_{n:K}$, $Z_2 = \gamma_{K_s-1:K}$ and $Z_3 = \gamma_{K_s:K}$, then

$$\begin{aligned}
& MGF_Z(\lambda_1, \lambda_2, \lambda_3) \\
&= F \int_0^\infty d\gamma_{K_s:K} p(\gamma_{K_s:K}) \exp(\lambda_3 \gamma_{K_s:K}) [c(\gamma_{K_s:K})]^{(K-K_s)} \\
&\quad \times \int_{\gamma_{K_s:K}}^\infty d\gamma_{K_s-1:K} p(\gamma_{K_s-1:K}) \exp(\lambda_2 \gamma_{K_s-1:K}) \frac{1}{(K_s-2)!} [e(\gamma_{K_s-1:K}, \lambda_1)]^{(K_s-2)}. \quad (6.31)
\end{aligned}$$

d. $m = K_s$

Let $Z_1 = \gamma_{K_s:K}$ and $Z_2 = \sum_{n=1}^{K_s-1} \gamma_{n:K}$, then

$$\begin{aligned}
MGF_Z(\lambda_1, \lambda_2) &= F \int_0^\infty d\gamma_{K_s:K} p(\gamma_{K_s:K}) \exp(\lambda_1 \gamma_{K_s:K}) [c(\gamma_{K_s:K})]^{(K-K_s)} \\
&\quad \times \frac{1}{(K_s-1)!} [e(\gamma_{K_s:K}, \lambda_2)]^{(K_s-1)}. \quad (6.32)
\end{aligned}$$

Starting from the MGF expressions given above, we apply inverse Laplace transforms in Appendix O in order to derive the following joint PDFs

a. $m = 1$

$$\begin{aligned}
p_Z(z_1, z_2, z_3) &= p_{\gamma_{1:K}, \sum_{n=2}^{K_s-1} \gamma_{n:K}, \gamma_{K_s:K}}(z_1, z_2, z_3) \\
&= \frac{F}{(K_s-2)!} p(z_1) p(z_3) [c(z_3)]^{(K-K_s)} U(z_1 - z_3) \mathcal{L}_{S_2}^{-1} \left\{ [\mu(z_3, z_1, -S_2)]^{(K_s-2)} \right\}, \\
&\quad \text{for } z_3 < z_1, (K_s-2)z_3 < z_2 < (K_s-2)z_1. \quad (6.33)
\end{aligned}$$

where $U(\cdot)$ is the unit step function.

b. $1 < m < K_s - 1$

$$\begin{aligned}
p_Z(z_1, z_2, z_3, z_4) &= p_{\sum_{n=1}^{m-1} \gamma_{n:K}, \gamma_{m:K}, \sum_{n=m+1}^{K_s-1} \gamma_{n:K}, \gamma_{K_s:K}}(z_1, z_2, z_3, z_4) \\
&= \frac{F}{(K_s-m-1)! (m-1)!} p(z_2) p(z_4) [c(z_4)]^{(K-K_s)} U(z_2 - z_4) \\
&\quad \times \mathcal{L}_{S_1}^{-1} \left\{ [e(z_2, -S_1)]^{(m-1)} \right\} \mathcal{L}_{S_3}^{-1} \left\{ [\mu(z_4, z_2, -S_3)]^{(K_s-m-1)} \right\}, \\
&\quad \text{for } z_4 < z_2, z_1 > (m-1)z_2 \text{ and } (K_s-m-1)z_4 < z_3 < (K_s-m-1)z_2. \quad (6.34)
\end{aligned}$$

c. $m = K_s - 1$

$$\begin{aligned}
p_Z(z_1, z_2, z_3) &= p_{\sum_{n=1}^{K_s-2} \gamma_{n:K}, \gamma_{K_s-1:K}, \gamma_{K_s:K}}(z_1, z_2, z_3) \\
&= \frac{F}{(K_s - 2)!} p(z_2) p(z_3) [c(z_3)]^{(K-K_s)} U(z_2 - z_3) \mathcal{L}_{S_1}^{-1} \left\{ [e(z_2, -S_1)]^{(K_s-2)} \right\}, \\
&\quad \text{for } z_3 < z_2, z_1 > (K_s - 2) z_2.
\end{aligned} \tag{6.35}$$

d. $m = K_s$

$$\begin{aligned}
p_Z(z_1, z_2) &= p_{\gamma_{K_s:K}, \sum_{n=1}^{K_s-1} \gamma_{n:K}}(z_1, z_2) \\
&= \frac{F}{(K_s - 1)!} p(z_1) [c(z_1)]^{(K-K_s)} \mathcal{L}_{S_2}^{-1} \left\{ [e(z_1, -S_2)]^{(K_s-1)} \right\}, \\
&\quad \text{for } z_2 \geq (K_s - 1) z_1.
\end{aligned} \tag{6.36}$$

Finally, the joint PDF of $\gamma_{m:K}$ and $\sum_{\substack{n=1 \\ n \neq m}}^{K_s} \gamma_{n:K}$ can be obtained as

$$\begin{aligned}
& p_{\gamma_{m:K}, \sum_{\substack{n=1 \\ n \neq m}}^{K_s} \gamma_{n:K}}(x, y) \\
&= \begin{cases} \int_{\left(\frac{K_s-2}{K_s-1}\right)y}^{(K_s-2)x} p_{\gamma_{1:K}, \sum_{n=2}^{K_s-1} \gamma_{n:K}, \gamma_{K_s:K}}(x, z_2, y - z_2) dz_2, & m = 1, \\ \int_0^x \int_{(m-1)x}^{y-(K_s-m)z_4} p_{\sum_{n=1}^{m-1} \gamma_{n:K}, \gamma_{m:K}, \sum_{n=m+1}^{K_s-1} \gamma_{n:K}, \gamma_{K_s:K}}(z_1, x, y - z_1 - z_4, z_4) dz_1 dz_4, & 1 < m < K_s - 1, \\ \int_{(K_s-2)x}^y p_{\sum_{n=1}^{K_s-2} \gamma_{n:K}, \gamma_{K_s-1:K}, \gamma_{K_s:K}}(z_1, x, y - z_1) dz_1, & m = K_s - 1, \\ p_{\gamma_{K_s:K}, \sum_{n=1}^{K_s-1} \gamma_{n:K}}(x, y), & m = K_s, \end{cases}
\end{aligned} \tag{6.37}$$

or equivalently

$$\begin{aligned}
 & p_{\gamma_{m:K}, \sum_{\substack{n=1 \\ n \neq m}}^{K_s} \gamma_{n:K}}(x, y) \\
 = & \begin{cases} \int_0^{(K_s-2)x} \int_{\left(\frac{K_s-2}{K_s-1}\right)y}^{(K_s-2)y} p_{\gamma_{1:K}, \sum_{n=2}^{K_s-1} \gamma_{n:K}, \gamma_{K_s:K}}(x, z_2, y - z_2) dz_2, & m = 1, \\ \int_0^x \int_{(K_s-m-1)z_4}^{(K_s-m-1)x} p_{\sum_{n=1}^{m-1} \gamma_{n:K}, \gamma_{m:K}, \sum_{n=m+1}^{K_s-1} \gamma_{n:K}, \gamma_{K_s:K}}(y - z_3 - z_4, x, z_3, z_4) dz_3 dz_4, & 1 < m < K_s - 1, \\ \int_0^x p_{\sum_{n=1}^{K_s-2} \gamma_{n:K}, \gamma_{K_s-1:K}, \gamma_{K_s:K}}(y - z_3, x, z_3) dz_3, & m = K_s - 1, \\ p_{\gamma_{K_s:K}, \sum_{n=1}^{K_s-1} \gamma_{n:K}}(x, y), & m = K_s. \end{cases}
 \end{aligned} \tag{6.38}$$

Note that (7.5) and (7.6) involve only finite integrations of joint PDFs. Therefore, while a generic closed-form expression is not possible, the desired joint PDF can be easily numerically evaluated using standard mathematical packages such as Mathematica or Matlab and so on.

3. Joint PDF of $\sum_{n=1}^m \gamma_{n:K}$ and $\sum_{n=m+1}^{K_s} \gamma_{n:K}$

We now consider the joint PDF of $X = \sum_{n=1}^m \gamma_{n:K}$ and $Y = \sum_{n=m+1}^{K_s} \gamma_{n:K}$. Noting that these two partial sum is related to those involved in (6.30) as $X = Z_1 + Z_2$ and $Y = Z_3 + Z_4$, we can simply obtain the joint PDF of $Z = [X, Y]$ using the 4-dimensional joint PDF given in (7.10) by integrating out z_2 and z_4 as

$$\begin{aligned}
 p_Z(x, y) &= p_{\sum_{n=1}^m \gamma_{n:K}, \sum_{n=m+1}^{K_s} \gamma_{n:K}}(x, y) \\
 &= \int_0^{\frac{y}{K_s-m}} \int_{\frac{y}{K_s-m}}^{\frac{x}{m}} p_{\sum_{n=1}^{m-1} \gamma_{n:K}, \gamma_{m:K}, \sum_{n=m+1}^{K_s-1} \gamma_{n:K}, \gamma_{K_s:K}}(x - z_2, z_2, y - z_4, z_4) dz_2 dz_4, \\
 &\text{for } x > \frac{m}{K_s - m} y.
 \end{aligned} \tag{6.39}$$

Note again that only the finite integrations of joint PDFs are involved.

E. Closed-form Expressions for Exponential RV Case

The above derived generic results apply to different distributions. If we limit ourselves to the i.i.d. exponential RV case with common PDF given by

$$p(\gamma) = \frac{1}{\bar{\gamma}} \exp\left(-\frac{\gamma}{\bar{\gamma}}\right), \quad (6.40)$$

where $\bar{\gamma}$ is the common average. The corresponding CDF is given by

$$P(\gamma) = 1 - \exp\left(-\frac{\gamma}{\bar{\gamma}}\right). \quad (6.41)$$

Therefore, (7.8), (7.11) and (7.9) specialize to

$$[e(z_a, -S_i)]^m = \frac{\left[\exp\left(-\left(S_i + \frac{1}{\bar{\gamma}}\right)z_a\right)\right]^m}{(\bar{\gamma})^m \left(S_i + \frac{1}{\bar{\gamma}}\right)^m} \quad (6.42)$$

$$[c(z_a, -S_i)]^m = \sum_{j=0}^m \frac{(-1)^j}{(\bar{\gamma})^m} \binom{m}{j} \left[\exp\left(-\frac{z_a}{\bar{\gamma}}\right)\right]^j \frac{[\exp(-z_a S_i)]^j}{\left(S_i + \frac{1}{\bar{\gamma}}\right)^m} \quad (6.43)$$

$$\begin{aligned} [\mu(z_a, z_b, -S_i)]^m &= \sum_{j=0}^m \left[\frac{(-1)^j}{(\bar{\gamma})^m} \binom{m}{j} \exp\left(-\frac{(m-j)}{\bar{\gamma}}z_a\right) \exp\left(-\frac{j}{\bar{\gamma}}z_b\right) \right. \\ &\quad \left. \times \frac{\exp(-((m-j)z_a + jz_b)S_i)}{\left(S_i + \frac{1}{\bar{\gamma}}\right)^m} \right]. \end{aligned} \quad (6.44)$$

After substituting (7.14), (7.15) and (7.16) into the derived expressions of the joint PDF of partial sums of ordered statistics presented in the previous sections, it is easy to derive the following closed-form expressions for the PDFs by applying the classical inverse Laplace transform pair given in (H.1) and the property given in (H.2) as:

1) PDF of $\sum_{n=1}^K \gamma_{n:K}$:

$$p_Z(z_1) = \frac{z_1^{K-1}}{(K-1)! \bar{\gamma}^K} \exp\left(-\frac{z_1}{\bar{\gamma}}\right). \quad (6.45)$$

2) Joint PDF of $\gamma_{m:K}$ and $\sum_{\substack{n=1 \\ n \neq m}}^K \gamma_{n:K}$:

$$p_Z(z_1, z_2) = \begin{cases} \frac{K!}{(K-1)!(K-2)!\bar{\gamma}^K} \exp\left(-\frac{z_1+z_2}{\bar{\gamma}}\right) \\ \times \sum_{j=0}^{K-1} (-1)^j \binom{K-1}{j} [z_2 - jz_1]^{K-2} U(z_2 - jz_1) & \text{for } m = 1, \\ \frac{K!}{(K-m)!(m-1)!(K-2)!\bar{\gamma}^K} \exp\left(-\frac{z_1+z_2}{\bar{\gamma}}\right) \\ \times \sum_{j=0}^{K-m} (-1)^j \binom{K-m}{j} [z_2 - (m+j-1)z_1]^{K-2} \\ \times U(z_2 - (m+j-1)z_1) & \text{for } m \geq 2. \end{cases} \quad (6.46)$$

3) Joint PDF of $\sum_{n=1}^m \gamma_{n:K}$ and $\sum_{n=m+1}^K \gamma_{n:K}$:

$$p_Z(z_1, z_2) = \begin{cases} \left[\frac{K!}{(K-m)!(K-m-1)!(m-1)!(m-2)!\bar{\gamma}^K} \exp\left(-\frac{z_1+z_2}{\bar{\gamma}}\right) \right. \\ \times \int_0^\infty d\gamma_{m:K} \left[[z_1 - m\gamma_{m:K}]^{m-2} U(z_1 - m\gamma_{m:K}) \right. \\ \left. \times \sum_{j=0}^{K-m} (-1)^j \binom{K-m}{j} [z_2 - j\gamma_{m:K}]^{K-m-1} U(z_2 - j\gamma_{m:K}) \right], & m \geq 2 \\ \left. \frac{K!}{(K-1)!(K-2)!\bar{\gamma}^K} \exp\left(-\frac{z_1+z_2}{\bar{\gamma}}\right) \right. \\ \left. \times \sum_{j=0}^{K-1} (-1)^j \binom{K-1}{j} [z_2 - jz_1]^{K-2} U(z_2 - jz_1), \right. & m = 1. \end{cases} \quad (6.47)$$

4) PDF of $\sum_{n=1}^{K_s} \gamma_{n:K}$:

$$p_Z(z_1) = \begin{cases} \left[\frac{K!}{(K-K_s)!(K_s-1)!(K_s-2)!\bar{\gamma}^{K_s}} \exp\left(-\frac{z_1}{\bar{\gamma}}\right) \right. \\ \left. \times \int_0^\infty d\gamma_{K_s:K} \left[1 - \exp\left(-\frac{\gamma_{K_s:K}}{\bar{\gamma}}\right) \right]^{K-K_s} [z_1 - K_s\gamma_{K_s:K}]^{K_s-2} \right. \\ \left. U(z_1 - K_s\gamma_{K_s:K}) \right], & K_s \geq 2 \\ \left. \frac{K}{\bar{\gamma}} \exp\left(-\frac{z_1}{\bar{\gamma}}\right) \left[1 - \exp\left(-\frac{z_1}{\bar{\gamma}}\right) \right]^{K-1}, \right. & K_s = 1 \end{cases} \quad (6.48)$$

where

$$\left[1 - \exp\left(-\frac{a}{\bar{\gamma}}\right) \right]^m = \sum_{i=0}^m (-1)^i \binom{m}{i} \left[\exp\left(-\frac{a}{\bar{\gamma}}\right) \right]^i. \quad (6.49)$$

5) Joint PDF of $\gamma_{m:K}$ and $\sum_{\substack{n=1 \\ n \neq m}}^{K_s} \gamma_{n:K}$:

a. For $m = 1$,

$$\begin{aligned}
 p_Z(z_1, z_2, z_3) &= \frac{K!}{(K - K_s)! (K_s - 2)! (K_s - 3)! \bar{\gamma}^{K_s}} \exp\left(-\frac{z_1 + z_2 + z_3}{\bar{\gamma}}\right) \\
 &\quad \times \left[1 - \exp\left(-\frac{z_3}{\bar{\gamma}}\right)\right]^{K - K_s} U(z_1 - z_3) \\
 &\quad \times \sum_{j=0}^{K_s - 2} \left[(-1)^j \binom{K_s - 2}{j} [z_2 - (K_s - 2 - j)z_3 - jz_1]^{K_s - 3} \right. \\
 &\quad \left. \times U(z_2 - (K_s - 2 - j)z_3 - jz_1)\right], \tag{6.50}
 \end{aligned}$$

b. For $1 < m < K_s - 1$,

$$\begin{aligned}
 p_Z(z_1, z_2, z_3, z_4) &= \frac{K!}{(K - K_s)! (K_s - m - 1)! (K_s - m - 2)! (m - 1)! (m - 2)! \bar{\gamma}^{K_s}} \\
 &\quad \times \exp\left(-\frac{z_1 + z_2 + z_3 + z_4}{\bar{\gamma}}\right) \left[1 - \exp\left(-\frac{z_4}{\bar{\gamma}}\right)\right]^{K - K_s} [z_1 - (m - 1)z_2]^{m - 2} \\
 &\quad \times \sum_{j=0}^{K_s - m - 1} \left[(-1)^j \binom{K_s - m - 1}{j} [z_3 - (K_s - m - 1 - j)z_4 - jz_2]^{K_s - m - 2} \right. \\
 &\quad \left. \times U(z_2 - z_4) U(z_1 - (m - 1)z_2) U(z_3 - (K_s - m - 1 - j)z_4 - jz_2)\right]. \tag{6.51}
 \end{aligned}$$

c. For $m = K_s - 1$,

$$\begin{aligned}
 p_Z(z_1, z_2, z_3) &= \frac{K!}{(K - K_s)! (K_s - 2)! (K_s - 3)! \bar{\gamma}^{K_s}} \exp\left(-\frac{z_1 + z_2 + z_3}{\bar{\gamma}}\right) \\
 &\quad \times \left[1 - \exp\left(-\frac{z_3}{\bar{\gamma}}\right)\right]^{K - K_s} U(z_2 - z_3) [z_1 - (K_s - 2)z_2]^{K_s - 3} \\
 &\quad \times U(z_1 - (K_s - 2)z_2). \tag{6.52}
 \end{aligned}$$

d. For $m = K_s$,

$$\begin{aligned}
 p_Z(z_1, z_2) &= \frac{K!}{(K - K_s)! (K_s - 1)! (K_s - 2)! \bar{\gamma}^{K_s}} \exp\left(-\frac{z_1 + z_2}{\bar{\gamma}}\right) \\
 &\quad \times \left[1 - \exp\left(-\frac{z_1}{\bar{\gamma}}\right)\right]^{K - K_s} [z_2 - (K_s - 1)z_1]^{K_s - 2} U(z_2 - (K_s - 1)z_1). \tag{6.53}
 \end{aligned}$$

F. Applications

The above derived joint PDFs of partial sums of ordered statistics in case of considering all K ordered RVs or only the best K_s ordered RVs can be applied to the performance analysis of various wireless communication systems. In this section, we discuss two examples.

1. Example i)

In conventional parallel multiuser scheduling schemes, a particular scheduled user's signal is detected by correlating signals of entire scheduled users at the receiver. Therefore, under these practical conditions, every scheduled user is interfering with every other scheduled user. This effect is called Multiple Access Interference (MAI) or Multiple User Interference (MUI). This MUI is a factor which limits the capacity and performance of multiuser systems and the level of interference becomes substantial as the number of scheduled users increases. To take into account the effect of MUI caused by the other scheduled users, the signal to interference plus noise ratio (SINR) which measures the ratio between the useful power and the amount of noise and interferences generated by all the other scheduled users is used. The level of interference becomes substantial as the number of the scheduled users increases because the SINR can decrease considerably in these conditions. This decrease in SINR can lead to a certain reduction of the rate allocated to each scheduled user. With the above motivation in mind, the impact of interference on the performance (throughput) of the scheduled users assuming a selection based parallel multiuser scheduling scheme is needed to investigate the total average sum rate capacity and the average spectral efficiency (ASE) based on the SINR of the scheduled users. The major difficulty in investigating this total average sum rate capacity and ASE resides

in the determination of the statistics of the SINR of the m -th scheduled user. Based on our approach, we can derive these results and then be applied to obtain the total average sum rate capacity and the ASE. Based on this system model, we need to derive the joint PDF of SNR of m -th desired scheduled user and the sum of the SNRs of the interfering $(K_s - 1)$ scheduled users among total $K(K > K_s)$ users. We will deal with this example in Chapter VII.

2. Example ii)

The first theoretical study of minimum selection minimum-selection generalized selection combining (MS-GSC) scheme was carried out in [57,66,67], where the distribution of the number of combined paths N with MS-GSC was derived and the error performance of MS-GSC was investigated. In [57, 66, 67], the average symbol error rate (SER) of MS-GSC was calculated as the weighted sum of the conditional average SER given that K_s paths are combined, with the weights being the probabilities of different possible values of N and the average SER of conventional GSC used as the conditional average SER. However, because the receiver with MS-GSC may combine N best paths only under the condition that the combined SNR of first K_s best paths is below the output threshold, the statistics of combined SNR with MS-GSC given that K_s paths are combined is different from that with corresponding conventional GSC. As such, the average SER result in [66, 67] should serve as an approximation. With this observation in mind, the author address the exact performance analysis of MS-GSC over fading channels in [57]. For that purpose, to investigate its performance analysis the joint PDF of the m -th order statistics and the partial sum of the first $(m - 1)$ order statistics is needed to be investigated. Based on our approach, we can investigate it easily. This new statistical result not only allows us to obtain distribution functions, including PDF and MGF, of the combined SNR with MS-GSC, but

leads also to a compact solution to the distribution of the number of combined paths.

CHAPTER VII

IMPACT OF INTERFERENCE ON THE PERFORMANCE OF SELECTION
BASED PARALLEL MULTIUSER SCHEDULING

A. Introduction

Research in multiuser scheduling schemes for single users [49–51] and for multiple users [52, 56, 68] has grown in recent years. Single user scheduling schemes [49–51] schedule only one user at a time. On the other hand, parallel multiuser scheduling schemes [52, 56, 68] schedule multiple users at a time. The goal is to increase the throughput and to reduce the complexity of implementation. The throughput of multiuser scheduling schemes for single user [49–51] and multiple users [52, 56, 68] was investigated assuming that the users are scheduled based on their signal to noise ratio (SNR).

In conventional parallel multiuser scheduling schemes, a particular scheduled user's signal is detected by correlating signals of entire scheduled users at the receiver. Therefore, under these practical conditions, every scheduled user is interfering with every other scheduled user. This effect is called Multiple Access Interference (MAI) or Multiple User Interference (MUI). This MUI is a factor which limits the capacity and performance of multiuser systems and the level of interference becomes substantial as the number of scheduled users increases. To take into account the effect of MUI caused by the other scheduled users, we use in this chapter the signal to interference plus noise ratio (SINR) which measures the ratio between the useful power and the amount of noise and interferences generated by all the other scheduled users. The level of interference becomes substantial as the number of the scheduled users increases because the SINR can decrease considerably in these conditions. This de-

crease in SINR can lead to a certain reduction of the rate allocated to each scheduled user.

With the above motivation in mind, we investigate in this chapter the impact of interference on the performance (throughput) of the scheduled users assuming a selection based parallel multiuser scheduling scheme [52]. In particular, we derive the total average sum rate capacity and the average spectral efficiency (ASE) based on the SINR of the scheduled users. The major difficulty in deriving this total average sum rate capacity and ASE resides in the determination of the statistics of the SINR of the m -th scheduled user. Fortunately, extending the approach used in [63–65] to derive some useful order statistics of interest, we accurately characterize the statistics of the SINR of the m -th scheduled user in terms of cumulative distribution function (CDF) and probability density function (PDF). These results are then applied to obtain the total average sum rate capacity and the ASE.

The remainder of this chapter is organized as follows. In section II, we describe the system and channel models. In section III, we derive the statistics of the ordered SINR of the m -th scheduled user. In section IV, a statistical analysis of our target joint PDF is presented. In particular, based on our extended approach, we derive the moment generating function (MGF) expression. Having this MGF expression in hand, we find our target joint PDF expression by taking the inverse Laplace transform of that MGF. Following this, these results are applied to the total average sum rate capacity and ASE analysis, and we then show and discuss some selected numerical results in section V. Finally, we offer some concluding remarks in section VI.

B. System and Channel Models

In our system model, we consider a code division multiple access (CDMA) system for the simultaneous scheduling of K_s ($K_s = 0, 1, 2, \dots, K$) users among K potential users per time-slot. We assume that there is some inter-user interference after the scheduling process. We also assume that the schemes have a reliable feedback path between the receiver and transmitter and that they are implemented in a discrete-time fashion with a time-slot composed of a guard time period followed by a data transmitting time period. During the guard time period, the system makes the necessary actions for scheduling the best K_s users based on SNR information then estimating the SINRs of these scheduled users for rate allocation. Finally, it is assumed that the channel estimation is perfect at the receiver and that the feedback to the transmitter is performed upon request without any error.

We denote by γ_i ($i = 1, 2, \dots, K$), the received SNR of the i th user and we adopt a block flat fading channel model. More specifically, assuming slowly-varying fading conditions, the different paths from users experience roughly the same fading conditions during the data burst and its preceding guard time period. In addition, the fading conditions are assumed to be independent across the paths from users and between guard time period and data burst pairs.

Based on the mode of operation of the proposed selection based parallel multiuser scheduling scheme, we select the best K_s users for scheduling among the K users. Therefore, if we consider a general communication system and we let $\gamma_{m:K}$ be a SNR of m -th scheduled user ($m = 1, 2, \dots, K_s$) then the SINR of this user can be written as

$$\begin{aligned}
SINR_m &= \gamma_{SINR_m} \\
&= \frac{\gamma_{m:K}}{1 + \alpha \sum_{\substack{n=1 \\ n \neq m}}^{K_s} \gamma_{n:K}},
\end{aligned} \tag{7.1}$$

where α is a multiuser interference cancellation coefficient which takes values between 0 to 1 and quantifies the level of MUI. In particular, when the MUI is canceled perfectly, the SINR reverts to the SNR. On the other hand when $\alpha = 1$, the MUI is fully present.

Let us consider only the best $K_s (\leq K)$ ordered random variables (RVs). Since the original $\{\gamma_i\}$ are i.i.d. RVs with a common arbitrary PDF $p(\gamma)$, the K_s -dimensional joint PDF of $\{\gamma_i\}_{i=1}^{K_s}$ is simply given by [58]

$$p(\gamma_{1:K}, \gamma_{2:K}, \dots, \gamma_{K_s:K}) = F \cdot \prod_{i=1}^{K_s} p(\gamma_{i:K}) [P(\gamma_{K_s:K})]^{K-K_s}, \tag{7.2}$$

where $F = K_s! \binom{K}{K_s} = \frac{K!}{(K-K_s)!}$.

For the scheduled users, a rate-adaptive N multidimensional uncoded M -quadrature amplitude modulation (M-QAM) modulation [38,69] for additive white Gaussian noise (AWGN) channels or a rate-adaptive N multidimensional coded M -quadrature amplitude modulation (M-QAM) modulation [34] can be employed to ensure a high system ASE. In this chapter, we use a rate-adaptive N multidimensional uncoded M -quadrature amplitude modulation (M-QAM) modulation [38,69]. In [38,69], the constellation size M_n is restricted to 2^n ($n = 1, 2, \dots, N$) different codes based on QAM signaling. In this case, rate adaptation is performed by dividing the SNR range into $N + 1$ fading regions which are defined by the SNR thresholds, denoted by $0 < \gamma_{T_1} < \gamma_{T_2} < \dots < \gamma_{T_N} < \gamma_{T_{N+1}} = \infty$. When the estimated SINR of a scheduled user is in the n th region (*i.e.*, $\gamma_{T_n} \leq \gamma < \gamma_{T_{n+1}}$), the constellation size M_n (*i.e.*, $M_n = 2, 4, 8, 16, 32, 64, 128, 256$) with spectral efficiency R_n (*i.e.*, $R_n = 1, 2, 3, 4, 5, 6, 7, 8$)

[bits/s/Hz] is transmitted. The lower SNR boundary γ_{T_n} of each fading region is set to the lowest SNR required to achieve a predefined target BER (for example, $\text{BER}_0 = 10^{-3}$ or 10^{-2}).

C. Statistics of the SINRs of the Scheduled Users

Starting from (7.1), the CDF of γ_{SINR_m} , denoted by $P_{\gamma_{\text{SINR}_m}}(\cdot)$, can be calculated in terms of the 2-dimensional joint PDF of SNR of m -th desired scheduled user, $\gamma_{m:K}$, and the sum of the SNRs of the interfering $K_s - 1$ scheduled users, $\sum_{\substack{n=1 \\ n \neq m}}^{K_s} \gamma_{n:K}$, denoted

by $p_{\gamma_{m:K}, \sum_{\substack{n=1 \\ n \neq m}}^{K_s} \gamma_{n:K}}(\cdot, \cdot)$ as

$$P_{\gamma_{\text{SINR}_m}}(\gamma) = \int_0^\infty \int_0^{\gamma(1+\alpha y)} p_{\gamma_{m:K}, \sum_{\substack{n=1 \\ n \neq m}}^{K_s} \gamma_{n:K}}(x, y) dx dy. \quad (7.3)$$

After taking the derivative of (7.3) with respect to γ , the PDF of γ_{SINR_m} , denoted by $p_{\gamma_{\text{SINR}_m}}(\cdot)$ can be obtained as

$$\begin{aligned} p_{\gamma_{\text{SINR}_m}}(\gamma) &= \frac{\partial}{\partial \gamma} P_{\gamma_{\text{SINR}_m}}(\gamma) \\ &= \int_0^\infty (1 + \alpha y) \cdot p_{\gamma_{m:K}, \sum_{\substack{n=1 \\ n \neq m}}^{K_s} \gamma_{n:K}}(\gamma(1 + \alpha y), y) dy. \end{aligned} \quad (7.4)$$

Therefore, to obtain the statistics of γ_{SINR_m} , we need to find the joint PDF $p_{\gamma_{m:K}, \sum_{\substack{n=1 \\ n \neq m}}^{K_s} \gamma_{n:K}}(\cdot, \cdot)$.

1. Joint PDF $\gamma_{m:K}$ and $\sum_{\substack{n=1 \\ n \neq m}}^{K_s} \gamma_{n:K}$

Applying our extended MGF-based approach we developed in Chapter VI and [70], we accurately derive the joint PDF of $\gamma_{m:K}$ and $\sum_{\substack{n=1 \\ n \neq m}}^{K_s} \gamma_{n:K}$, denoted by $p_{\gamma_{m:K}, \sum_{\substack{n=1 \\ n \neq m}}^{K_s} \gamma_{n:K}}(\cdot, \cdot)$, in terms of its MGF and PDF. Because of space limitations, we only present the final

results in this chapter. The specific details behind the derivation of these results can be found in Chapter VI and the mathematical paper [70].

Based on our extended method in Chapter VI and [70], we derive in Chapter VI and [70] the generic expression of the joint PDF of $\gamma_{m:K}$ and $\sum_{\substack{n=1 \\ n \neq m}}^{K_s} \gamma_{n:K}$, by considering four cases i) $m = 1$, ii) $1 < m < K_s - 1$, iii) $m = K_s - 1$ and iv) $m = K_s$ separately as

$$p_{\gamma_{m:K}, \sum_{\substack{n=1 \\ n \neq m}}^{K_s} \gamma_{n:K}}(x, y) = \begin{cases} \int \left(\frac{K_s-2}{K_s-1}\right)^x y^{\gamma_{1:K}, \sum_{n=2}^{K_s-1} \gamma_{n:K}, \gamma_{K_s:K}}(x, z_2, y - z_2) dz_2, & m = 1, \\ \int_0^x \int_{(m-1)x}^{y-(K_s-m)z_4} p_{\sum_{n=1}^{m-1} \gamma_{n:K}, \gamma_{m:K}, \sum_{n=m+1}^{K_s-1} \gamma_{n:K}, \gamma_{K_s:K}}(z_1, x, y - z_1 - z_4, z_4) dz_1 dz_4, & 1 < m < K_s - 1, \\ \int_{(K_s-2)x}^y p_{\sum_{n=1}^{K_s-2} \gamma_{n:K}, \gamma_{K_s-1:K}, \gamma_{K_s:K}}(z_1, x, y - z_1) dz_1, & m = K_s - 1, \\ p_{\gamma_{K_s:K}, \sum_{n=1}^{K_s-1} \gamma_{n:K}}(x, y), & m = K_s, \end{cases} \quad (7.5)$$

or equivalently

$$p_{\gamma_{m:K}, \sum_{\substack{n=1 \\ n \neq m}}^{K_s} \gamma_{n:K}}(x, y) = \begin{cases} \int \left(\frac{K_s-2}{K_s-1}\right)^x y^{\gamma_{1:K}, \sum_{n=2}^{K_s-1} \gamma_{n:K}, \gamma_{K_s:K}}(x, z_2, y - z_2) dz_2, & m = 1, \\ \int_0^x \int_{(K_s-m-1)z_4}^{(K_s-m-1)x} p_{\sum_{n=1}^{m-1} \gamma_{n:K}, \gamma_{m:K}, \sum_{n=m+1}^{K_s-1} \gamma_{n:K}, \gamma_{K_s:K}}(y - z_3 - z_4, x, z_3, z_4) dz_3 dz_4, & 1 < m < K_s - 1, \\ \int_0^x p_{\sum_{n=1}^{K_s-2} \gamma_{n:K}, \gamma_{K_s-1:K}, \gamma_{K_s:K}}(y - z_3, x, z_3) dz_3, & m = K_s - 1, \\ p_{\gamma_{K_s:K}, \sum_{n=1}^{K_s-1} \gamma_{n:K}}(x, y), & m = K_s. \end{cases} \quad (7.6)$$

Note that the operation in (7.5) involve only finite integrations of joint PDFs. Therefore, while a generic closed-form expression is not possible, the desired joint PDF can be easily numerically evaluated using standard mathematical packages such as Mathematica or Matlab and so on.

Further more, the joint PDFs for different cases in (7.5) and (7.6) are obtained as

a. $m = 1$

$$\begin{aligned} & p_{\gamma_{1:K}, \sum_{n=2}^{K_s-1} \gamma_{n:K}, \gamma_{K_s:K}}(z_1, z_2, z_3) \\ &= \frac{F}{(K_s - 2)!} p(z_1) p(z_3) [c(z_3, 0)]^{(K-K_s)} U(z_1 - z_3) \mathcal{L}_{S_2}^{-1} \left\{ [\mu(z_3, z_1, -S_2)]^{(K_s-2)} \right\}, \\ & \quad \text{for } z_3 < z_1, (K_s - 2)z_3 < z_2 < (K_s - 2)z_1. \end{aligned} \quad (7.7)$$

where $U(\cdot)$ is the unit step function,

$$\begin{aligned} & \frac{1}{(K - m + 1)!} [c(\gamma_{m-1:K}, \lambda)]^{(K-m+1)} \\ &= \int_0^{\gamma_{m-1:K}} d\gamma_{m:K} p(\gamma_{m:K}) \exp(\lambda \gamma_{m:K}) \int_0^{\gamma_{m:K}} d\gamma_{m+1:K} p(\gamma_{m+1:K}) \exp(\lambda \gamma_{m+1:K}) \\ & \quad \times \int_0^{\gamma_{m+1:K}} d\gamma_{m+2:K} p(\gamma_{m+2:K}) \exp(\lambda \gamma_{m+2:K}) \cdots \int_0^{\gamma_{K-1:K}} d\gamma_{K:K} p(\gamma_{K:K}) \exp(\lambda \gamma_{K:K}) \end{aligned} \quad (7.8)$$

, and

$$\begin{aligned} & \frac{1}{(b - a - 1)!} [\mu(\gamma_{b:K}, \gamma_{a:K}, \lambda)]^{(b-a-1)} \quad \text{for } b > a \\ &= \int_{\gamma_{a:K}}^{\gamma_{a:K}} d\gamma_{b-1:K} p(\gamma_{b-1:K}) \exp(\lambda \gamma_{b-1:K}) \int_{\gamma_{b-1:K}}^{\gamma_{a:K}} d\gamma_{b-2:K} p(\gamma_{b-2:K}) \exp(\lambda \gamma_{b-2:K}) \\ & \quad \times \int_{\gamma_{b-2:K}}^{\gamma_{a:K}} d\gamma_{b-3:K} p(\gamma_{b-3:K}) \exp(\lambda \gamma_{b-3:K}) \cdots \int_{\gamma_{a+2:K}}^{\gamma_{a:K}} d\gamma_{a+1:K} p(\gamma_{a+1:K}) \exp(\lambda \gamma_{a+1:K}) \end{aligned} \quad (7.9)$$

b. $1 < m < K_s - 1$

$$\begin{aligned} & p_{\sum_{n=1}^{m-1} \gamma_{n:K}, \gamma_{m:K}, \sum_{n=m+1}^{K_s-1} \gamma_{n:K}, \gamma_{K_s:K}}(z_1, z_2, z_3, z_4) \\ &= \frac{F}{(K_s - m - 1)! (m - 1)!} p(z_2) p(z_4) [c(z_4, 0)]^{(K-K_s)} U(z_2 - z_4) \\ & \quad \times \mathcal{L}_{S_1}^{-1} \left\{ [e(z_2, -S_1)]^{(m-1)} \right\} \mathcal{L}_{S_3}^{-1} \left\{ [\mu(z_4, z_2, -S_3)]^{(K_s-m-1)} \right\}, \\ & \quad \text{for } z_4 < z_2, z_1 > (m - 1)z_2 \text{ and } (K_s - m - 1)z_4 < z_3 < (K_s - m - 1)z_2. \end{aligned} \quad (7.10)$$

where

$$\begin{aligned} & \frac{1}{m!} [e(\gamma_{m+1:K}, \lambda)]^m \\ &= \int_{\gamma_{m+1:K}}^{\infty} d\gamma_{m:K} p(\gamma_{m:K}) \exp(\lambda\gamma_{m:K}) \int_{\gamma_{m:K}}^{\infty} d\gamma_{m-1:K} p(\gamma_{m-1:K}) \exp(\lambda\gamma_{m-1:K}) \\ & \quad \times \int_{\gamma_{m-1:K}}^{\infty} d\gamma_{m-2:K} p(\gamma_{m-2:K}) \exp(\lambda\gamma_{m-2:K}) \cdots \int_{\gamma_{2:K}}^{\infty} d\gamma_{1:K} p(\gamma_{1:K}) \exp(\lambda\gamma_{1:K}). \end{aligned} \quad (7.11)$$

c. $m = K_s - 1$

$$\begin{aligned} & p_{\sum_{n=1}^{K_s-2} \gamma_{n:K}, \gamma_{K_s-1:K}, \gamma_{K_s:K}}(z_1, z_2, z_3) \\ &= \frac{F}{(K_s - 2)!} p(z_2) p(z_3) [c(z_3, 0)]^{(K-K_s)} U(z_2 - z_3) \mathcal{L}_{S_1}^{-1} \left\{ [e(z_2, -S_1)]^{(K_s-2)} \right\}, \\ & \quad \text{for } z_3 < z_2, z_1 > (K_s - 2)z_2. \end{aligned} \quad (7.12)$$

d. $m = K_s$

$$\begin{aligned} p_{\gamma_{K_s:K}, \sum_{n=1}^{K_s-1} \gamma_{n:K}}(z_1, z_2) &= \frac{F}{(K_s - 1)!} p(z_1) [c(z_1, 0)]^{(K-K_s)} \mathcal{L}_{S_2}^{-1} \left\{ [e(z_1, -S_2)]^{(K_s-1)} \right\}, \\ & \quad \text{for } z_2 \geq (K_s - 1)z_1. \end{aligned} \quad (7.13)$$

2. I.I.D Rayleigh Fading Special Case

The generic non-closed form results presented in the previous sub-section apply to various fading environments. However for the i.i.d. Rayleigh fading environment both the joint MGF and PDF of interest can be found in closed-form expressions (i.e. expressions which do not involve any single integral). More specifically, assuming an i.i.d. Rayleigh fading assumption, in which the received SNRs γ_i s share a common PDF and common corresponding $p_\gamma(\gamma) = p(\gamma) = \frac{1}{\bar{\gamma}} \exp\left(-\frac{\gamma}{\bar{\gamma}}\right)$, where $\bar{\gamma}$ is the common average SNR for all users and common corresponding CDF $P_\gamma(\gamma) = P(\gamma) = 1 - \exp\left(-\frac{\gamma}{\bar{\gamma}}\right)$, we can obtain the following results

$$[e(z_a, -S_i)]^m = \frac{\left[\exp\left(-\left(S_i + \frac{1}{\bar{\gamma}}\right)z_a\right) \right]^m}{(\bar{\gamma})^m \left(S_i + \frac{1}{\bar{\gamma}}\right)^m} \quad (7.14)$$

$$[c(z_a, -S_i)]^m = \sum_{j=0}^m \frac{(-1)^j}{(\bar{\gamma})^m} \binom{m}{j} \left[\exp\left(-\frac{z_a}{\bar{\gamma}}\right) \right]^j \frac{[\exp(-z_a S_i)]^j}{\left(S_i + \frac{1}{\bar{\gamma}}\right)^m} \quad (7.15)$$

$$\begin{aligned} [\mu(z_a, z_b, -S_i)]^m &= \sum_{j=0}^m \left[\frac{(-1)^j}{(\bar{\gamma})^m} \binom{m}{j} \exp\left(-\frac{(m-j)z_a}{\bar{\gamma}}\right) \exp\left(-\frac{j}{\bar{\gamma}}z_b\right) \right. \\ &\quad \left. \times \frac{\exp\left(-((m-j)z_a + jz_b)S_i\right)}{\left(S_i + \frac{1}{\bar{\gamma}}\right)^m} \right]. \end{aligned} \quad (7.16)$$

Substituting (7.14), (7.15) and (7.16) into (7.7), (7.10), (7.12), and (7.13) and using the classical inverse Laplace transform pair (H.1) and property (H.2) given in Appendix H, we can obtain the formal joint PDF in (7.5) and (7.6) in closed-form as

a. $m = 1$

$$\begin{aligned} p_{\gamma_{1:K}, \sum_{n=2}^{K_s-1} \gamma_{n:K}, \gamma_{K_s:K}}(z_1, z_2, z_3) &= \frac{K!}{(K - K_s)! (K_s - 2)! (K_s - 3)! \bar{\gamma}^{K_s}} \exp\left(-\frac{z_1 + z_2 + z_3}{\bar{\gamma}}\right) \\ &\quad \times \left[1 - \exp\left(-\frac{z_3}{\bar{\gamma}}\right) \right]^{K - K_s} U(z_1 - z_3) \\ &\quad \times \sum_{j=0}^{K_s-2} \left[(-1)^j \binom{K_s-2}{j} [z_2 - (K_s - 2 - j)z_3 - jz_1]^{K_s-3} \right. \\ &\quad \left. \times U(z_2 - (K_s - 2 - j)z_3 - jz_1) \right], \end{aligned} \quad (7.17)$$

b. $1 < m < K_s - 1$

$$\begin{aligned}
& p_{\sum_{n=1}^{m-1} \gamma_{n:K}, \gamma_{m:K}, \sum_{n=m+1}^{K_s-1} \gamma_{n:K}, \gamma_{K_s:K}}(z_1, z_2, z_3, z_4) \\
&= \frac{K!}{(K - K_s)! (K_s - m - 1)! (K_s - m - 2)! (m - 1)! (m - 2)! \bar{\gamma}^{K_s}} \\
&\times \exp\left(-\frac{z_1 + z_2 + z_3 + z_4}{\bar{\gamma}}\right) \left[1 - \exp\left(-\frac{z_4}{\bar{\gamma}}\right)\right]^{K - K_s} [z_1 - (m - 1) z_2]^{m-2} \\
&\times \sum_{j=0}^{K_s - m - 1} \left[(-1)^j \binom{K_s - m - 1}{j} [z_3 - (K_s - m - 1 - j) z_4 - j z_2]^{K_s - m - 2}\right. \\
&\left. \times U(z_2 - z_4) U(z_1 - (m - 1) z_2) U(z_3 - (K_s - m - 1 - j) z_4 - j z_2)\right]. \quad (7.18)
\end{aligned}$$

c. $m = K_s - 1$

$$\begin{aligned}
& p_{\sum_{n=1}^{K_s-2} \gamma_{n:K}, \gamma_{K_s-1:K}, \gamma_{K_s:K}}(z_1, z_2, z_3) \\
&= \frac{K!}{(K - K_s)! (K_s - 2)! (K_s - 3)! \bar{\gamma}^{K_s}} \exp\left(-\frac{z_1 + z_2 + z_3}{\bar{\gamma}}\right) \\
&\times \left[1 - \exp\left(-\frac{z_3}{\bar{\gamma}}\right)\right]^{K - K_s} U(z_2 - z_3) [z_1 - (K_s - 2) z_2]^{K_s - 3} \\
&\times U(z_1 - (K_s - 2) z_2). \quad (7.19)
\end{aligned}$$

d. $m = K_s$

$$\begin{aligned}
& p_{\gamma_{K_s:K}, \sum_{n=1}^{K_s-1} \gamma_{n:K}}(z_1, z_2) \\
&= \frac{K!}{(K - K_s)! (K_s - 1)! (K_s - 2)! \bar{\gamma}^{K_s}} \exp\left(-\frac{z_1 + z_2}{\bar{\gamma}}\right) \\
&\times \left[1 - \exp\left(-\frac{z_1}{\bar{\gamma}}\right)\right]^{K - K_s} [z_2 - (K_s - 1) z_1]^{K_s - 2} U(z_2 - (K_s - 1) z_1). \quad (7.20)
\end{aligned}$$

or equivalently

$$\begin{aligned}
p_{\gamma_{K_s:K}, \sum_{n=1}^{K_s-1} \gamma_{n:K}}(z_1, z_2) &= \frac{K!}{(K - K_s)! (K_s - 1)! (K_s - 2)! \bar{\gamma}^{K_s}} \exp\left(-\frac{z_1 + z_2}{\bar{\gamma}}\right) \\
&\times [z_2 - (K_s - 1) z_1]^{K_s - 2} U(z_2 - (K_s - 1) z_1) \\
&\times \sum_{j=0}^{K - K_s} (-1)^j \binom{K - K_s}{j} \left[\exp\left(-\frac{z_1}{\bar{\gamma}}\right)\right]^j. \quad (7.21)
\end{aligned}$$

Note that we have derived the joint PDF of $\gamma_{m:K}$ and $\sum_{\substack{n=1 \\ n \neq m}}^{K_s} \gamma_{n:K}$, denoted by $p_{\gamma_{m:K}, \sum_{\substack{n=1 \\ n \neq m}}^{K_s} \gamma_{n:K}}(\cdot, \cdot)$, only for $m = K_s$. For other cases, the marginals need to be computed in order to get the desired results. We can now apply these results to obtain the PDF of γ_{SINR_m} in (7.4) and therefore assess the impact of the MUI on the performance of selection based parallel multiuser scheduling scheme.

D. Performance Analysis

In this section, we capitalize on the statistical results presented in the previous section to analyze the effect of interference on the throughput of the scheduled users assuming a selection based parallel multiuser scheduling scheme operating over i.i.d. Rayleigh fading conditions. In our simulation and numerical results, we use the selection based parallel multiuser scheduling scheme with $K = 20$ and different values of K_s and we assume i.i.d. Rayleigh fading conditions. To investigate the ASE, we also apply the conventional uncoded adaptive modulation of [34] with $N = 8$.

1. Total Average Sum Rate Capacity

a. Analysis

The achievable rate, R_m of the m -th scheduled user is limited by the individual instantaneous capacity C_m as

$$R_m \leq C_m = \log_2(1 + \gamma_{SINR_m}). \quad (7.22)$$

Therefore, the individual average sum rate capacity [60, 71, 72] can be obtained by averaging (7.22) with respect to $p_{\gamma_{SINR_m}}(\gamma)$ as

$$\begin{aligned}\bar{C}_m &= \text{E} \{ \log_2 (1 + \gamma_{SINR_m}) \} \\ &= \int_0^\infty \log_2 (1 + \gamma) p_{\gamma_{SINR_m}} (\gamma) d\gamma.\end{aligned}\quad (7.23)$$

By adding the individual average sum rate capacities of the K_s scheduled users, we can obtain the total average sum rate capacity as

$$\begin{aligned}\bar{R}_{total} \leq \bar{C}_{total} &= \bar{R}_{total,max} \\ &= \sum_{m=1}^{K_s} \bar{C}_m \\ &= \sum_{m=1}^{K_s} \int_0^\infty \log_2 (1 + \gamma) p_{\gamma_{SINR_m}} (\gamma) d\gamma.\end{aligned}\quad (7.24)$$

b. Numerical Examples

Fig. 24 and Fig. 25 show the total average sum rate capacity versus (i) the average SNR for different number of scheduled users with various values of α and (ii) the number of scheduled users with various values of α , respectively.

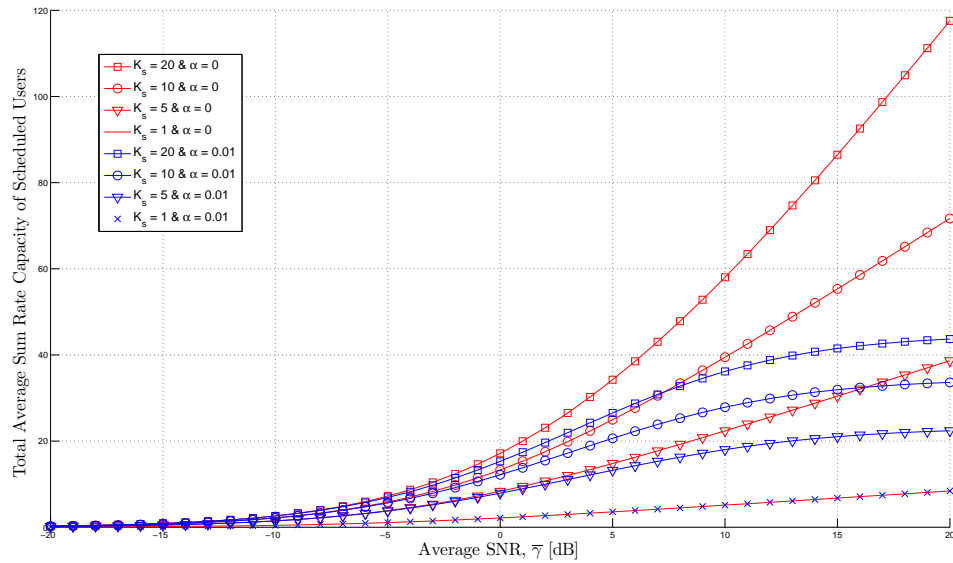
i) $\alpha = 0$

In this case, the SINRs of the scheduled users are constant as K_s increases. Therefore, the total average sum rate capacity is increasing continuously as K_s increases. As a result, the system can schedule as many users as possible.

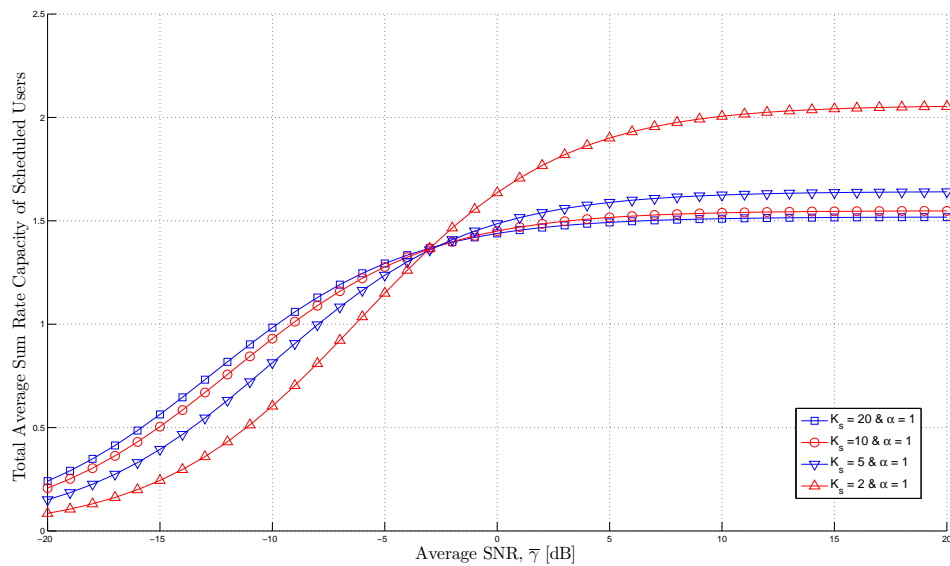
ii) $\alpha = 1$

In the region of low $\bar{\gamma}$, the SINRs of the scheduled users are decreasing and finally saturates as K_s increases but the values are almost constant. Therefore, the total average sum rate capacity is increasing as K_s increases. As a result, in the region of low $\bar{\gamma}$, the system can schedule as many users as possible.

In the region of high $\bar{\gamma}$, the SINRs of the scheduled users are decreasing consid-



(a) Total average sum rate capacity for $\alpha = 0$ and $\alpha = 0.01$ with various values of K_s .



(b) Total average sum rate capacity of scheduled users for $\alpha = 1$ with various values of K_s .

Fig. 24. Total average sum rate capacity as a function of the average SNR for selection based parallel multiuser scheduling over i.i.d. Rayleigh fading channels with $K = 20$ and various values of K_s and α .

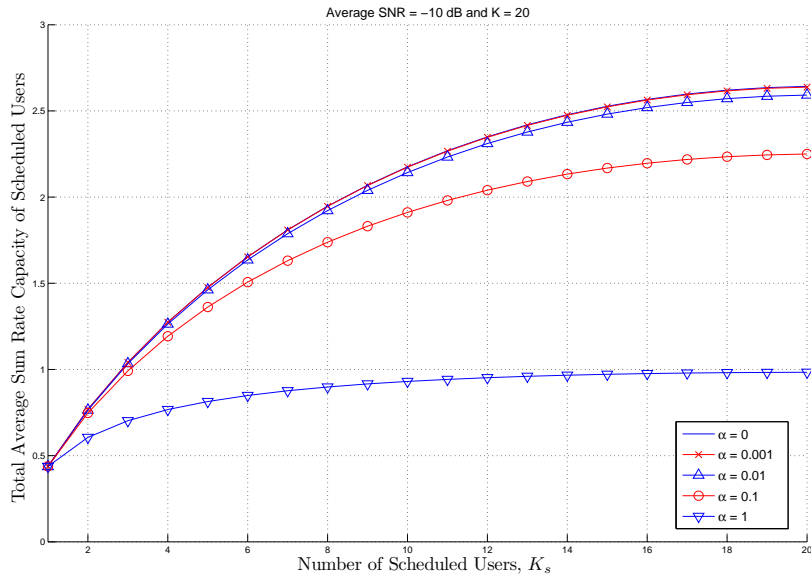
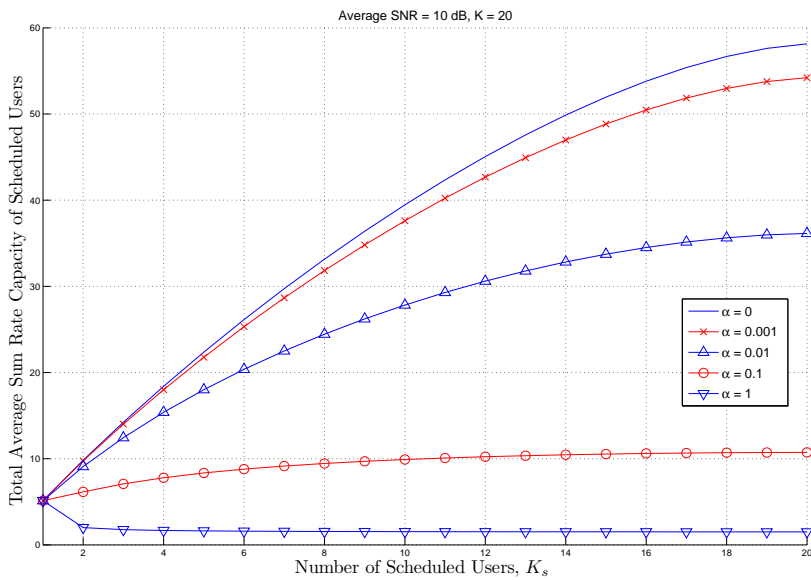
(a) Total average sum rate capacity for low average SNR $\bar{\gamma}$ (b) Total average sum rate capacity for high average SNR $\bar{\gamma}$

Fig. 25. Total average sum rate capacity of scheduled users as a function of the number of scheduled users for selection based parallel multiuser scheduling over i.i.d. Rayleigh fading channels with $K = 20$ and various values of α .

erably and finally saturated very quickly as K_s increases. Therefore, the total average sum rate capacity is decreasing and finally saturates as K_s increases. As a result, in the region of high $\bar{\gamma}$, there is no interest in scheduling multiple users simultaneously. If the fairness of access requires the simultaneous scheduling of multiple users in the region of high $\bar{\gamma}$, the system needs to select the number of scheduled users carefully by considering the total average sum rate capacity requirement and a channel status.

iii) $0 < \alpha < 1$

The SINRs of the scheduled users are decreasing as K_s increases. This decrement is increasing as $\bar{\gamma}$ increases. The SINR curve as a function of K_s for fixed value of $\bar{\gamma}$ approaches a straight line as α approaches 0. In the region of low $\bar{\gamma}$, the SINR curve as a function of K_s is almost straight regardless of the value of α . Therefore, in the region of low $\bar{\gamma}$, the total average sum rate capacity is increasing as K_s increases but for fixed value of K_s the gain is decreasing as α increases.

In the region of high $\bar{\gamma}$, in the case of very small α , the total average sum rate capacity is just increasing but in the case of very large α , the total average sum rate capacity is just decreasing as K_s increases. Otherwise, the total average sum rate capacity is increasing as K_s increases but the gain also depends on the value of α . Note that the total average sum rate capacity graph saturates more quickly and for fixed number of scheduled users, K_s , the gain is decreasing as α increases. Based on these facts, the system can schedule as many users as possible but the system needs to carefully select the number of scheduled users by considering the value of α , the total average sum rate capacity requirement, and the channel status.

2. Average Spectral Efficiency

a. Analysis

The ASE of the m -th scheduled user is obtained as the sum of the spectral efficiencies $\{R_n\}_{n=1}^N$ of the individual codes, weighted by the probability P_n that the SINR of this m -th scheduled user is assigned to the n -th region yielding

$$\text{ASE}_m = \sum_{n=1}^N R_n P_n = \sum_{n=1}^N R_n \int_{\gamma_{T_n}}^{\gamma_{T_{n+1}}} p_{\gamma_{\text{SINR}_m}}(\gamma) d\gamma. \quad (7.25)$$

To obtain the overall ASE of the scheduled users for each time-slot, we just need to add the individual ASE of the scheduled users yielding

$$\text{ASE}_{\text{time-slot}} = \sum_{m=1}^{K_s} \sum_{n=1}^N R_n \int_{\gamma_{T_n}}^{\gamma_{T_{n+1}}} p_{\gamma_{\text{SINR}_m}}(\gamma) d\gamma. \quad (7.26)$$

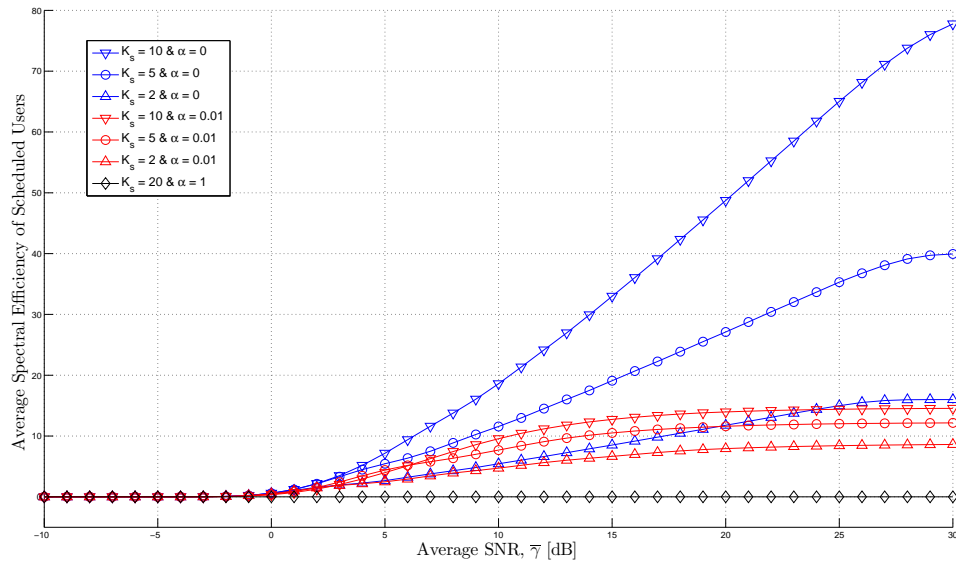
b. Numerical Examples

In Fig. 26 and Fig. 27, we plot the ASE of the scheduled users as a function of average SNR for different number of scheduled users and as a function of the number of scheduled users with various values of α respectively. As expected, we can see in Fig. 26 that the ASE is increasing as the average SNR increases before the ASE saturates on the spectral efficiency offered by the largest constellation.

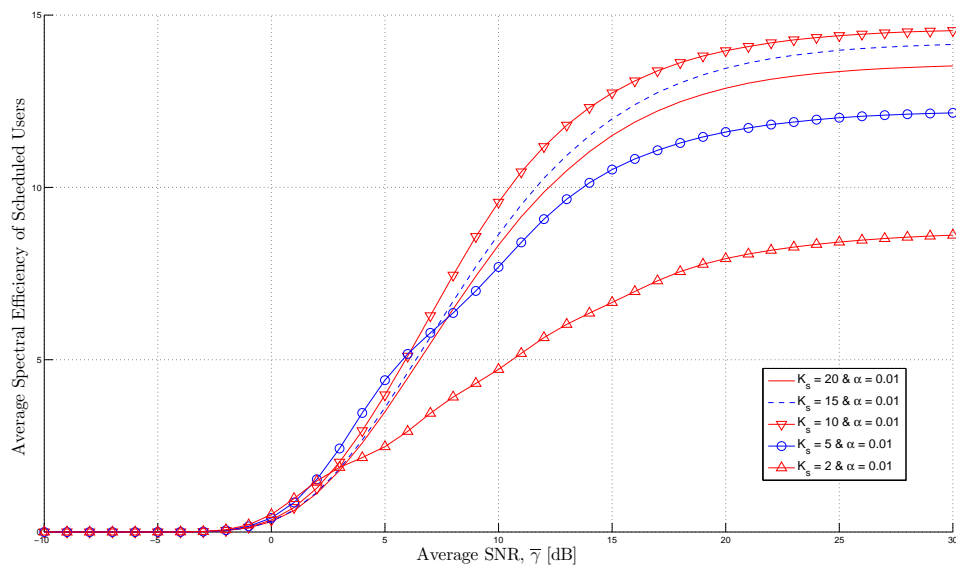
We can see from Fig 26 and Fig. 27 that there exists a trade-off between the ASE and the number of scheduled users.

i) $\alpha = 0$

In this case, the ASE does not depend on the type of adaptive modulation. The ASE always increases as K_s increases. Therefore, the system can schedule as many users as possible.



(a) Average spectral efficiency for $\alpha = 0$, $\alpha = 0.01$, and $\alpha = 1$ with various values of K_s



(b) Average spectral efficiency for $\alpha = 0.01$ with various values of K_s

Fig. 26. Average spectral efficiency of scheduled users as a function of the average SNR for selection based parallel multiuser scheduling over i.i.d. Rayleigh fading channels with $K = 20$ and various values of K_s and α .

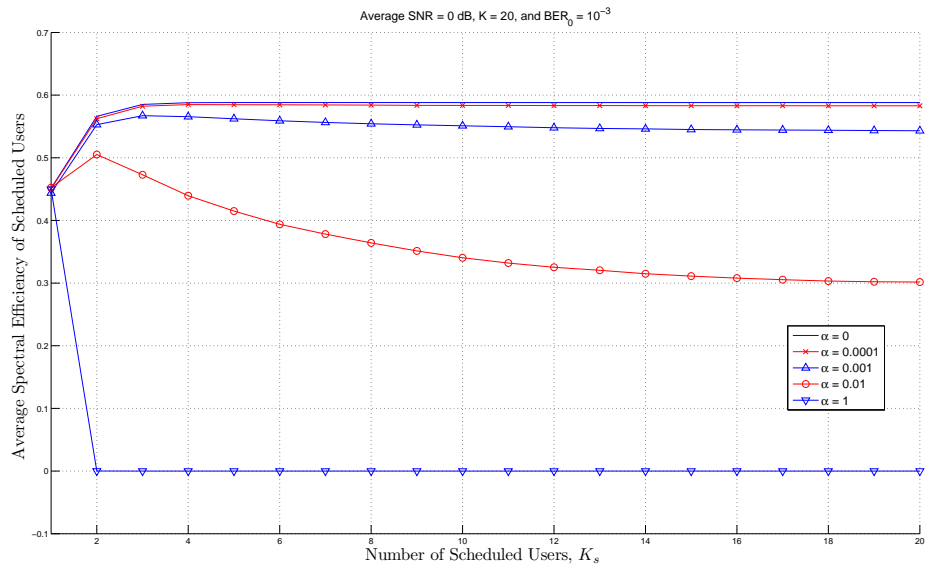
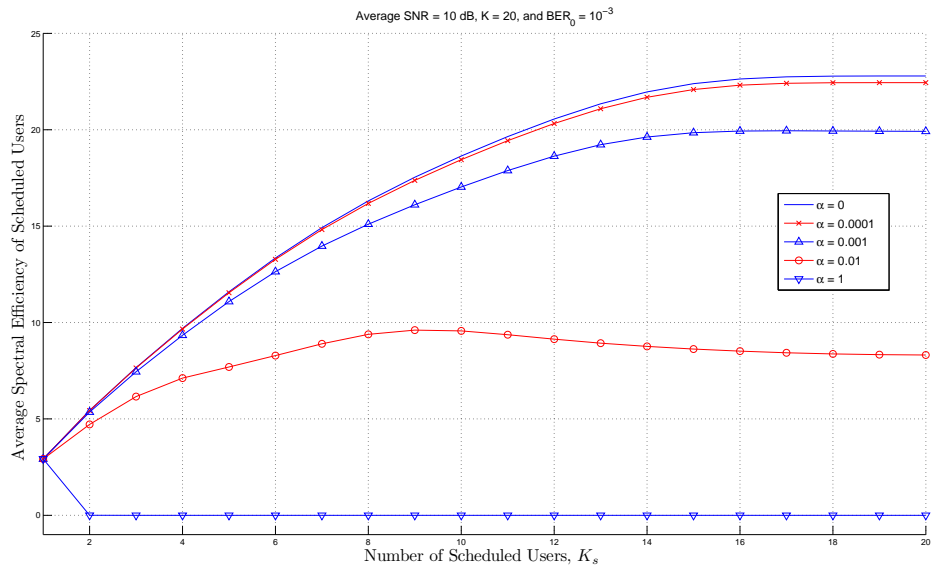
(a) Average spectral efficiency for low average SNR $\bar{\gamma}$ (b) Average spectral efficiency for high average SNR $\bar{\gamma}$

Fig. 27. Average spectral efficiency of scheduled users as a function of the number of scheduled users for selection based parallel multiuser scheduling over i.i.d. Rayleigh fading channels with $K = 20$ and various values of α .

ii) $\alpha = 1$

When $\alpha = 1$ and in the region of high $\bar{\gamma}$, the ASE decreases as K_s increases. Therefore, in the region of high $\bar{\gamma}$, there is no need to schedule multiple users. In case that multiple users scheduling is needed in the region of high $\bar{\gamma}$, the system needs to select the number of scheduled users carefully by considering a system capacity requirement and a channel status.

In the region of low $\bar{\gamma}$, the ASE of the scheduled users with conventional adaptive modulation [11, 30–38, 69] is decreasing and finally becomes zero due to the discrete nature of adaptive modulation. Note that the SINRs of the scheduled users is decreasing and finally saturated as K_s increases (but these values are almost constant although these values are changing) and almost of these values are very small compared with the minimum threshold of a conventional adaptive modulation. Therefore, for this case, the ASE is decreasing and finally becomes zero. However, if the system employs the appropriate type of adaptive modulation for low SNR $\bar{\gamma}$, in the region of low $\bar{\gamma}$, the ASE may have a similar behavior as the total average sum rate capacity.

iii) $0 < \alpha < 1$

When $0 < \alpha < 1$, in the region of high $\bar{\gamma}$, the ASE with very small α is increasing but the ASE with very large α is decreasing as K_s increases. Otherwise, the ASE is increasing and then decreasing and finally saturates as K_s increases. The trade-off point is moving to left side as α increases. This means that when α is large, a trade-off happens for the smaller value of K_s .

Note that based on the theoretical background, in the region of low $\bar{\gamma}$, the ASE may have a similar behavior as the total average sum rate capacity. More specifically, in the region of low $\bar{\gamma}$, the ASE of the scheduled users may be

increasing as K_s increases. Therefore, in the region of low $\bar{\gamma}$, the system with the appropriate type of adaptive modulation for low SNR $\bar{\gamma}$ may schedule as many users as possible.

However, as you can see the results from Fig. 26 and Fig. 27, in the region of low $\bar{\gamma}$, the ASE of the scheduled users with conventional adaptive modulation with very large α is just decreasing. Otherwise, the ASE is increasing a little bit and then suddenly decreasing and finally saturates as K_s increases due to the discrete nature of adaptive modulation.

Note that the ASE depends on both the value of α and the type of adaptive modulation especially in the low average SNR region. Therefore, if the system employs the appropriate type of adaptive modulation, in the region of low $\bar{\gamma}$, the system can schedule as many users as possible but in the region of high $\bar{\gamma}$, due to the trade-off between the ASE and the number of scheduled users, the system needs to select the number of scheduled users carefully by considering a system requirement and the channel status.

E. Conclusion

In this chapter, we investigated the impact of interference on the performance of selection based parallel multiuser scheduling. The major difficulty in deriving the total average sum rate capacity and the ASE analysis resided in the determination of the statistics of the SINR of the m -th scheduled user. Fortunately, we could derive an accurate statistical characterization of the SINR of the m -th scheduled user in terms of MGF and PDF by extending the approach presented in [63–65]. Based on these accurate statistical analysis, we can accurately evaluate the total average sum rate capacity and the average spectral efficiency based on the SINR. Based

on the total average sum rate capacity and the ASE analysis with the appropriate type of adaptive modulation, we can find the following results. In the case of the total average sum rate capacity, when $\alpha = 1$ and α is very large in the region of high $\bar{\gamma}$, there exists a trade-off between the total average sum rate capacity and the number of scheduled users. Otherwise, the system can schedule simultaneously as many multiple users as possible but the gain depends on the value of α . For the ASE with conventional adaptive modulation, when $\alpha = 0$, the system can schedule simultaneously as many multiple users as possible. When $\alpha = 1$ in the region of low $\bar{\gamma}$, the system can schedule as many users as possible also but in the region of high $\bar{\gamma}$, scheduling multiple users lead to a decrease in the ASE. When $0 < \alpha < 1$ except a very large and very small value of α , there exists a trade-off between the ASE with conventional adaptive modulation and the number of scheduled users. Hence, based on the trade-off between the ASE and the number of scheduled users, the system should carefully select the appropriate number of scheduled users to maximize the overall throughput while maintaining an acceptable quality of service.

CHAPTER VIII

CONCLUSION AND FUTURE WORK

A. Summary of Conclusions

In this dissertation, we looked into adaptive power control for single and multiuser opportunistic systems. First, we proposed a new adaptive power-controlled diversity combining scheme for single user systems. We then extended it to the multiusers case. In the multiuser case, we first proposed two new threshold based parallel multiuser scheduling schemes without power control. The first scheme is named OOBS scheme and the second scheme is named SBS scheme. Next, we proposed three threshold-based power allocation algorithms for the SBS scheme which is one of our proposed scheduling schemes. Finally, we introduced a unified analytical framework to determine the joint statistics of partial sums of ordered RVs with i.i.d and then we investigated the impact of interference on the performance of parallel multiuser scheduling based on our unified analytical framework to determine the joint statistics of partial sums of ordered RVs with i.i.d.

In chapter III, we proposed a new adaptive up-link diversity combining scheme that reduces the average transmitted power of the mobile units while meeting a certain minimum required quality of service. More specifically, four power control variants accounting for practical implementation constraints including discrete power levels and transmitter gain saturation were proposed and studied. The key idea was to take advantage of all the diversity offered by the channel and then request the transmitter (i) to increase its power level during very adverse channel conditions in order to reach the target SNR and (ii) to decrease its power level during favorable channel conditions just to keep the SNR level at the target required SNR. Based on some selected results,

we showed that our proposed scheme makes the system meet the target BER over the whole SNR range but the amplifier saturation leads to a violation of the target BER requirement in the low average SNR range. Additional numerical examples, show that the power control variants that take into account practical implementation constraints conserve the main features of the ideal continuous power algorithm.

In chapter IV, we proposed two new threshold-based parallel multiuser scheduling schemes, namely (i) an OOBS scheme and (ii) a SBS scheme. The objective is to reduce the complexity of implementation without a considerable performance loss in comparison with conventional selection based scheduling. We analyzed the statistical characteristics, the average BER, the AFL, and the ASE of these two proposed schemes. We also showed a perfect match between our simulation results and our analytical results. The numerical results show that the OOBS scheme provides a slightly higher ASE without experiencing considerable BER loss in comparison with the GSC based scheme in the low to medium average SNR $\bar{\gamma}$ range. In the high average SNR range, the OOBS scheme provides a better error performance than the GSC based scheme for a similar AFL and ASE. Comparing the SBS scheme with the GSC based scheme, we observed that when the threshold γ_T is slightly higher than $\bar{\gamma}$ then the SBS scheme has nearly the same average BER performance as the GSC based scheme but when γ_T is slightly lower than $\bar{\gamma}$, the SBS scheme suffers a minimal BER and ASE performance loss but offers a certain reduction in the AFL.

In chapter V, we proposed threshold-based power allocation algorithms to increase the number of effective acceptable users among the scheduled users with SBS type of scheduling. As its name indicates it, the system re-allocates the extracted excess SNR from some acceptable users to unacceptable users among the scheduled users. After the power allocation process, the unacceptable users can reach acceptable SNRs and as such the number of effective acceptable users with an acceptable

SNR threshold among the scheduled users is increased without any additional down-link transmit power. Some selected numerical results, show that the proposed power allocation algorithms offer a certain improvement in ASE and an increase in the average number of effective acceptable users. Although the average BER performance degrades especially when the average SNR is close to the SNR threshold, this average BER performance still meets the average BER requirement.

Order statistics find applications in various areas of communications and signal processing. In chapter VI, we introduced a unified analytical framework to determine the joint statistics of partial sums of ordered RVs with i.i.d. With the proposed approach, we can systematically derive the joint statistics of any partial sums of ordered statistics, in terms of the MGF and PDF, not only when all the K ordered RVs are considered but also when only the K_s ($K_s < K$) best RVs are considered among K RVs. In addition, we derived the closed form expressions for the exponential special case. These derived results of joint PDFs of partial sums of ordered statistics in case of considering all K ordered RVs or only the best K_s ordered RVs can be applied to the performance analysis of various wireless communication systems.

In chapter VII, we investigated the impact of interference on the performance of selection based parallel multiuser scheduling based on our unified analytical framework to determine the joint statistics of partial sums of ordered RVs with i.i.d. In particular, we derived the total average sum rate capacity and the ASE. The major difficulty in deriving the total average sum rate capacity and the ASE analysis resided in the determination of the statistics of the SINR of the m -th scheduled user. Fortunately, we could derive the accurate statistical characterization of the SINR of the m -th scheduled user in terms of MGF and PDF based on our unified analytical framework. With these accurate statistical analysis, we derived the total average sum rate capacity and the average spectral efficiency based on the SINR. Some selected

numerical results, show that there is trade-off between interference and throughput among the scheduled users when interference is taken into account after the scheduling process. If the system increases the number of scheduled users, interferences caused by the scheduled users were increasing and these increased interferences had a minor influence on the throughput of the scheduled users. Hence, based on the results of trade-off between the throughput and the number of scheduled users, the system needs to select the appropriate number of scheduled users to maximize the overall throughput while maintaining an acceptable quality of service and considering a channel status.

B. Future Research Directions

We investigated the impact of interference on the performance of selection based parallel multiuser scheduling. If the system increased the number of scheduled users, the throughput was increasing but the interference among the scheduled users was also increasing. Hence, there existed the trade-off between the interference and the throughput among the scheduled users. Therefore, we need to find the optimal number of scheduled users that maximizes the overall throughput while maintaining an acceptable quality of service.

Additionally, it is important to note that in this dissertation we made the assumption that all channel estimation is perfect and all feedback occurs without error. However, for practical cases, there should be performance degradations (ASE and BER degradations) due to imperfections. Adaptive transmission techniques optimize the spectral efficiency of a communication system by varying transmission parameters in consonance with the channel realization. Given perfect CSI at the transmitter and receiver, a significant gain in throughput is achievable, compared with non-adaptive

schemes. However, there are the factors affecting CSI acquisition, namely, channel estimation error, feedback delay, quantization error due to bandwidth constraint, and feedback error. A practical feedback channel is characterized by noise and fading. However, it is commonly assumed in most adaptive transmission schemes that the feedback channel is error-free. This is justified by assuming that a sufficiently powerful error control code can be employed since a low data rate is usually employed for the feedback channel. However, it should be pointed out that for practical feedback schemes, the CSI knowledge is usually imperfect due to noisy feedback channels, channel-estimation error at the receiver, and feedback delays in closed-loop adaptive transmission systems. From this point, we can further consider feedback errors based on our proposed schemes. It would be nice if we investigate what effect imperfections in either process would have on the performance of our schemes and algorithms.

REFERENCES

- [1] B. Sklar, “Rayleigh fading channels in mobile digital communication systems Part I: Characterization,” *IEEE Commun. Mag.*, pp. 90–100, July 1997.
- [2] J. G. Proakis, *Digital Communications*, 3rd ed. New York: McGraw-Hill, 1995.
- [3] B. Sklar, *Digital Communications: Fundamentals of Applications*, 2nd ed. Upper Saddle River, NJ: Prentice Hall, 2001.
- [4] T. S. Rapaport, *Wireless Communications: Principles and Practice*, 2nd ed. Upper Saddle River, NJ: Prentice Hall, 2002.
- [5] ———, *Wireless Communications: Principles and Practice*, 2nd ed. Upper Saddle River, NJ: Prentice Hall, 2002.
- [6] M. K. Simon and M. -S. Alouini, *Digital Communications over Generalized Fading Channels*, 2nd ed. New York : John Wiley & Sons, 2004.
- [7] G. L. Stüber, *Principles of Mobile Communications*, 2nd ed. Norwell, MA: Kluwer Academic Publishers, 2001.
- [8] B. Sklar, “Rayleigh fading channels in mobile digital communication systems Part I: Mitigation,” *IEEE Commun. Mag.*, pp. 102–109, July 1997.
- [9] G. Kaplan and S. Shamai, “Error probabilities for the Block-Fading Gaussian channel,” *A.E.U.*, vol. 49, no. 4, pp. 192–205, 1995.
- [10] L. Ozarow, S. Shamai, and A. Wyner, “Information theoretic considerations for cellular mobile radio,” *IEEE Trans. Veh. Technol.*, vol. 43, no. 2, pp. 359–378, May 1994.

- [11] M. -S. Alouini and A. Goldsmith, "Capacity of Rayleigh fading channels under different adaptive transmission and diversity techniques," *IEEE Trans. Veh. Technol.*, vol. 48, no. 4, pp. 1165–1181, July 1999.
- [12] W. C. Jakes, *Microwave Mobile Communications*, 2nd ed. Piscataway, NJ: IEEE Press, 1994.
- [13] T. Eng, N. Kong, and L. B. Milstein, "Comparison of diversity combining techniques for Rayleigh-fading channels," *IEEE Trans. Commun.*, vol. 44, no. 9, pp. 1117–1129, September 1996, see also "Correction to "Comparison of diversity combining techniques for Rayleigh-fading channels", *IEEE Trans. Commun.*, vol. COM-46, p. 1111, September 1998.
- [14] —, "Correction to "Comparison of diversity combining techniques for Rayleigh-fading channels", *IEEE Trans. Commun.*, vol. 46, no. 9, p. 1111, September 1998.
- [15] M. Z. Win and J. H. Winters, "Analysis of hybrid selection/maximal-ratio combining in Rayleigh fading," in *Proc. IEEE Int. Conf. on Commun. (ICC'99)*, Vancouver, BC, Canada, June 1999, pp. 6–10.
- [16] M. Z. Win and Z. Kostic, "Impact of spreading bandwidth on Rake reception in dense multipath channels," in *Proc. Communication Theory Mini-Conference in Conjunction with IEEE Int. Conf. on Commun. (ICC'99)*, Vancouver, BC, Canada, June 1999, pp. 78–82.
- [17] M. K. Simon and M. -S. Alouini, "Exponential-type bounds on the generalized Marcum q -function with application to the error probability analysis over fading channels," *IEEE Trans. Commun.*, vol. COM-48, no. 3, pp. 359–366, March 2000.

- [18] Y. Ma and C. C. Chai, "Unified error probability analysis for generalized selection combining in nakagami fading channels," *IEEE J. Select. Areas Commun.*, vol. 18, no. 11, pp. 2198–2210, November 2000.
- [19] A. Annamalai and C. Tellambura, "Analysis of hybrid selection/maximal-ratio diversity combiner with Gaussian errors," *IEEE Trans. Wireless Commun.*, vol. TWC-1, no. 3, pp. 498–512, July 2002.
- [20] H. C. Yang and M. S. Alouini, "Performance analysis of generalized switch and examine combining," in *Proc. of IEEE Int. Conf. on Commun. (ICC'03)*, Anchorage, Alaska, May 2003, pp. 2218–2222.
- [21] —, "Generalized switch-and-examine combining (GSEC): A low-complexity combining scheme for diversity-rich environments," *IEEE Trans. Commun.*, vol. 52, no. 10, pp. 1711–1721, 2004.
- [22] —, "Generalized switch-and-examine combining (GSEC) over fading paths with unequal average SNR," *IEEE Trans. Commun.*, vol. 53, no. 7, pp. 1132–1135, 2005.
- [23] S. W. Kim, D. S. Ha, and J. H. Reed, "Minimum selection GSC and adaptive low-power RAKE combining scheme," in *IEEE Int. Symp. on Circuits and Systems (ISCAS'03)*, Bangkok, Thailand, May 2003, pp. 357–360.
- [24] H. -C. Yang, "Exact performance analysis of minimum-selection generalized selection combining (GSC)," in *IEEE Int. Conf. on Commun. (ICC'05)*, Seoul, Korea, June 2005.
- [25] H. C. Yang, "New results on ordered statistics and analysis of minimum-selection generalized selection combining (GSC)," *IEEE Trans. Wireless Commun.*, vol. 5, no. 7, pp. 1876–1885, July 2006.

- [26] R. K. Mallik, D. Gupta, and Q. T. Zhang, "Minimum selection GSC in independent Rayleigh fading," *IEEE Trans. Veh. Technol.*, vol. 54, no. 3, pp. 1013–1021, May 2005.
- [27] M. S. Alouini and H. C. Yang, "Minimum estimation and combining generalized selection combining (NEC-GSC)," in *Proc. IEEE Int. Symp. on Information Theory (ISIT'05)*, Adelaide, Australia, Sept. 2005.
- [28] H. C. Yang and M. S. Alouini, "MRC and GSC diversity combining with an output threshold," *IEEE Trans. Veh. Technol.*, vol. 54, no. 3, pp. 1081–1090, May 2005.
- [29] ———, "Performance analysis of output-threshold generalized selection combining (OT-GSC)," in *Proc. IEEE Wireless Commun. & Networking Conf. (WCNC'06)*, Las Vegas, NV, Apr. 2006.
- [30] S. -G. Chua and A. J. Goldsmith, "Variable-rate variable-power M-QAM for fading channels," in *Proc. IEEE Veh. Technol. Conf. (VTC'96)*, Atlanta, GA, April 1996, pp. 815–819.
- [31] A. J. Goldsmith and S. -G. Chua, "Variable-rate variable-power M-QAM for fading channels," *IEEE Trans. Commun.*, vol. 45, no. 10, pp. 1218–1230, October 1997.
- [32] M. S. Alouini and A. Goldsmith, "Adaptive modulation over Nakagami fading channels," *Wireless Personal Communications*, vol. 13, pp. 119–143, 2000.
- [33] A. J. Goldsmith and S. -G. Chua, "Adaptive coded modulation for fading channels," *IEEE Trans. Commun.*, vol. 46, no. 5, pp. 595–602, May 1998.

- [34] K. J. Hole, H. Holm, and G. E. Øien, “Adaptive multidimensional coded modulation on flat fading channels,” *IEEE J. Select. Areas Commun.*, vol. 18, no. 7, pp. 1153–1158, 2000.
- [35] —, “Analysis of adaptive coded modulation with antenna diversity and feedback delay,” in *Proc. IST Mobile Communications Summit*, Barcelona, Spain, Oct. 2001.
- [36] G. E. Øien, H. Holm, and K. J. Hole, “Impact of channel prediction on adaptive coded modulation performance in Rayleigh fading,” *IEEE Trans. Veh. Technol.*, vol. 53, no. 3, pp. 758–769, May 2004.
- [37] Q. Liu, S. Zhou, and G. B. Giannakis, “Cross-layer combining of adaptive modulation and coding with truncated ARQ over wireless links,” *IEEE Trans. Wireless Commun.*, vol. 3, no. 5, pp. 1746–1755, Sept 2004.
- [38] Y. C. Ko, H. C. Yang, and M. S. Alouini, “Adaptive modulation and diversity combining based on output-threshold MRC,” in *Proc. IEEE Vehicular Technology Conf. (VTC’06-Spring)*, Melbourne, Australia, May 2006, pp. 1693–1697.
- [39] —, “Adaptive modulation and diversity combining based on output-threshold MRC,” *IEEE Trans. Wireless Commun.*, vol. 6, no. 10, pp. 3727–3737, Oct. 2007.
- [40] “3 GPP technical specification group radio access network: Physical layer procedures (FDD) specifications, 1999,” TS 25.214 V4.6.0 (2003-03).
- [41] N. Kong, T. Eng, and L. B. Milstein, “A selection combining scheme for RAKE receivers,” in *Proc. IEEE Int. Conf. Univ. Personal Comm. (ICUPC’95)*, Tokyo, Japan, Nov. 1995, pp. 426–429.

- [42] M. Z. Win and Z. A. Kostić, “Virtual path analysis of selective RAKE receiver in dense multipath channels,” *IEEE Commun. Letters*, vol. 3, no. 11, pp. 308–310, November 1999.
- [43] M. -S. Alouini and M. K. Simon, “An MGF-based performance analysis of generalized selective combining over Rayleigh fading channels,” *IEEE Trans. Commun.*, vol. 48, no. 3, pp. 401–415, March 2000.
- [44] Y. Roy, J. -Y. Chouinard, and S. Mahmoud, “Selection diversity combining with multiple antennae for mm-wave indoor wireless channels,” *IEEE Journal of Selected Areas in Communications*, vol. SAC-14, no. 4, pp. 674–682, May 1996.
- [45] G. L. Turin, F. D. Clapp, T. L. Johnston, S. B. Fine, and D. Lavry, “A statistical model of urban multipath propagation,” *IEEE Trans. Veh. Technol.*, vol. VT-21, no. 1, pp. 1–9, February 1972.
- [46] L. Yuanqing, “A theoretical formulation for the distribution density of multipath delay spread in a land mobile radio environment,” *IEEE Trans. Veh. Technol.*, vol. 43, no. 5, pp. 379–388, 1994.
- [47] I. S. Gradshteyn and I. M. Ryzhik, *Table of Integrals, Series, and Products*, 5th ed. San Diego, CA: Academic Press, 1994.
- [48] D. N. Tse, “Multiuser diversity in wireless networks,” presented at Stanford University, 2001.
- [49] R. Knopp and P. A. Humblet, “Information capacity and power control in single cell multiuser communications,” in *Proc. IEEE Int. Confs. on Commun. (ICC’95)*, Seattle, WA, June 1995, pp. 331–335.
- [50] G. B. Holter, M.-S. Alouini, G. E. Øien, and H.-C. Yang, “Multiuser switched

- diversity transmissions,” in *Proc. IEEE Vehicular Technology Conf. (VTC'04-Fall)*, Los Angeles, CA, Sept. 2004, pp. 2038–2043.
- [51] D. Gesbert and M. S. Alouini, “How much feedback is multi-user diversity really worth?” in *Proc. of IEEE Int. Conf. on Commun. (ICC'04)*, Paris, France, June 2004, pp. 234–238.
- [52] Y. Ma and D. Zhang, “Performance of generalized selection multiuser scheduling over generalized fading channels,” in *Proc. IEEE Int. Wireless Commun. and Mobile Comput. Conf. (IWCMC'06)*, Vancouver, Canada, July 2006.
- [53] M. K. Simon and M. S. Alouini, “Performance analysis of generalized selection combining with threshold test per branch (T-GSC),” *IEEE Trans. Veh. Technol.*, vol. 51, no. 5, pp. 1018–1029, 2002.
- [54] J. Hömläinen and R. Wichman, “Capacities of physical layer scheduling strategies on a shared link,” *Wireless Personal Communications*, vol. 39, no. 1, pp. 115–134, 2006.
- [55] L. Yang and H.-C. Yang, “GSECps: A diversity technique with improved performance-complexity tradeoff,” in *Proc. of IEEE Global Telecomm. Conf. (GLOBECOM'05)*, St. Louis, Mo, Nov. 2005.
- [56] S. S. Nam, M. S. Alouini, K. A. Qaraqe, and H. C. Yang, “Threshold based parallel multiuser scheduling,” in *Proc. IEEE International Symposium on Personal, Indoor and Mobile Radio Communications (PIMRC'07)*, Athens, Greece, Sept. 2007.
- [57] H.-C. Yang, “New results on ordered statistics and analysis of minimum-selection generalized selection combining (GSC),” *IEEE Trans. Wireless Commun.*, vol. 5, no. 7, pp. 1876–1885, 2006.

- [58] H. A. David, *Order Statistics*. New York: John Wiley & Sons, Inc., 1981.
- [59] N. Balakrishnan and C. R. Rao, *Handbook of Statistics 17: Order Statistics: Applications*, 2nd ed. North-Holland: Elsevier, 1998.
- [60] A. Goldsmith, *Wireless Communications*. New York: Cambridge University Press, 2005.
- [61] S. Choi, M.-S. Alouini, K. A. Qaraqe, and H.-C. Yang, "Finger replacement method for RAKE receivers in the soft handover region," *IEEE Trans. Wireless Commun.*, vol. TWC-7, no. 4, pp. 1152–1156, 2008.
- [62] P. Lu, H.-C. Yang, and Y.-C. Ko, "Sum-rate analysis of MIMO broadcast channel with random unitary beamforming," in *Proc. of IEEE Wireless Commun. and Networking Conf. (WCNC'08)*, Las Vegas, NV, Mar. 2008.
- [63] A. H. Nuttall, "An integral solution for the joint PDF of order statistics and residual sum," *NUWC-NPT, Technical Report*, Oct. 2001.
- [64] ———, "Joint probability density function of selected order statistics and the sum of the remaining random variables," *NUWC-NPT, Technical Report*, Jan. 2002.
- [65] A. H. Nuttall and P. M. Baggenstoss, "Joint distributions for two useful classes of statistics, with applications to classification and hypothesis testing," *IEEE Trans. Signal Processing*, submitted for publication. [Online]. Available: <http://www.npt.nuwc.navy.mil/Csf/papers/order.pdf>
- [66] S. W. Kim, D. S. Ha, and J. H. Reed, "Minimum selection GSC and adaptive low-power RAKE combining scheme," in *Proc. of IEEE Int. Symp. on Circuits and Systems. (ISCAS'03)*, Bangkok, Thailand, May 2003, pp. 357–360.

- [67] P. Gupta, N. Bansal, and R. K. Mallik, "Analysis of minimum selection H-S/MRC in Rayleigh fading," *IEEE Trans. Commun.*, vol. COM-53, no. 5, pp. 780–784, 2005.
- [68] Y. Ma, D. Zhang, and R. Schober, "Rate-maximizing multiuser scheduling for parallel channel access," *IEEE Signal Processing Lett.*, vol. 14, pp. 441–444, July 2007.
- [69] M. -S. Alouini and A. Goldsmith, "Adaptive M-QAM modulation over Nakagami fading channels," in *Proc. Communication Theory Mini-Conference (CTMC-VI) in conjunction with IEEE Global Commun. Conf. (GLOBECOM'97)*, Phoenix, AZ, Nov. 1997, pp. 218–223.
- [70] S. S. Nam, M. S. Alouini, and H. C. Yang, "A Unified Framework to determine the Joint Statistics of Ordered Random Variables," *IEEE Trans. Inform. Theory*, p. submitted, 2008.
- [71] M. Sharif and B. Hassibi, "On the capacity of MIMO broadcast channels with partial side information," *IEEE Trans. Inform. Theory*, vol. 51, no. 2, pp. 506–522, Feb. 2005.
- [72] N. Jindal, "MIMO broadcast channels with finite rate feedback," *IEEE Trans. Inform. Theory*, vol. 52, no. 11, pp. 5054–5059, Nov. 2006.
- [73] M. Abramowitz and I. A. Stegun, *Handbook of Mathematical Functions*. New York: Dover Publications, 1972.

APPENDIX A

A USEFUL IDENTITY

In what follows, we give a useful formula that is used in our derivations. Starting from [47, Eq. (2.231.2)], we can write

$$\begin{aligned}
& \int \gamma^{n-\frac{1}{2}} e^{-\mu\gamma} d\gamma \\
&= -e^{-\mu\gamma} \left(\frac{\gamma^{n-\frac{1}{2}}}{\mu} + \sum_{k=1}^{n-\frac{1}{2}} \frac{1}{\mu^{k+1}} \frac{(n-\frac{1}{2})!}{(n-(k+\frac{1}{2}))!} \gamma^{n-(k+\frac{1}{2})} \right), \\
&= -e^{-\mu\gamma} \sum_{k=0}^{n-\frac{1}{2}} \frac{1}{\mu^{k+1}} \frac{(n-\frac{1}{2})!}{(n-(k+\frac{1}{2}))!} \gamma^{n-(k+\frac{1}{2})}. \tag{A.1}
\end{aligned}$$

Let $n - (k + \frac{1}{2}) = \alpha$, then (A.1) can be re-written as

$$\int \gamma^{n-\frac{1}{2}} e^{-\mu\gamma} d\gamma = -e^{-\mu\gamma} \sum_{\alpha=0}^{n-\frac{1}{2}} \frac{1}{\mu^{n+\frac{1}{2}-\alpha}} \frac{(n-\frac{1}{2})!}{\alpha!} \gamma^{\alpha}. \tag{A.2}$$

Let $\alpha = k$, then (A.2) can be shown with the help of [47, Eq. (3.351.2)] and [47, Eq. (3.381.3)] to be equal to

$$\int \gamma^{n-\frac{1}{2}} e^{-\mu\gamma} d\gamma = -\mu^{-(n+\frac{1}{2})} \Gamma(n + \frac{1}{2}, \mu\gamma). \tag{A.3}$$

APPENDIX B

DERIVATION OF (3.13)

In this Appendix, we derive a closed form expression for the additional average dB gain in the case of continuous adaptation with amplifier gain saturation mode of UPC-DC. This gain is given in this case by (3.12). Using (3.6) and (3.3) in (3.12), we can write

$$G_{\text{dB}} = \frac{\gamma_{T_{\text{dB}}}}{(L-1)!} \Gamma\left(L, \frac{\gamma_T}{\bar{\gamma} G_{\text{max}}}\right) + \frac{1}{(L-1)! \bar{\gamma}^L} \int_{\frac{\gamma_T}{G_{\text{max}}}}^{\infty} \gamma^{L-1} \ln(\gamma) e^{-\frac{\gamma}{\bar{\gamma}}} d\gamma. \quad (\text{B.1})$$

Let $\frac{G_{\text{max}}}{\gamma_T} \gamma = x$, then (B.1) can be re-written as

$$\begin{aligned} G_{\text{dB}} &= \frac{1}{(L-1)! \bar{\gamma}^L} \int_1^{\infty} \left(\frac{\gamma_T}{G_{\text{max}}}\right)^L x^{L-1} \left(\ln \frac{\gamma_T}{G_{\text{max}}} + \ln x\right) e^{-\frac{\gamma_T}{\bar{\gamma} G_{\text{max}}} x} dx \\ &= \frac{1}{(L-1)!} \left(\frac{\gamma_T}{\bar{\gamma} G_{\text{max}}}\right)^L \ln\left(\frac{\gamma_T}{G_{\text{max}}}\right) \int_1^{\infty} x^{L-1} e^{-\frac{\gamma_T}{\bar{\gamma} G_{\text{max}}} x} dx \\ &\quad + \frac{1}{(L-1)!} \left(\frac{\gamma_T}{\bar{\gamma} G_{\text{max}}}\right)^L \int_1^{\infty} x^{L-1} \ln(x) e^{-\frac{\gamma_T}{\bar{\gamma} G_{\text{max}}} x} dx. \end{aligned} \quad (\text{B.2})$$

Finally, using [47, Eq. (2.321.2)] and [47, Eq. (3.381.3)], we get the desired closed-form result given in (3.13).

APPENDIX C

Derivation Of (3.15)

In this Appendix, we derive a closed form expression for the average BER in the case of discrete adaptation without amplifier gain saturation mode of UPC-DC. The average BER is given in this case by (3.14). Let $a(k) = 10^{\frac{kG\delta_{dB}}{10}}$, then

$$\int \operatorname{erfc}(\sqrt{a(k)\gamma}) p_{\gamma_c}(\gamma) d\gamma$$

$$= \operatorname{erfc}(\sqrt{a(k)\gamma}) \left(- \sum_{l=0}^{L-1} \left(\frac{\gamma}{\bar{\gamma}} \right)^l \frac{1}{l!} e^{-\frac{\gamma}{\bar{\gamma}}} \right) \quad (\text{C.1})$$

$$- \int \frac{d}{d\gamma} \left(\operatorname{erfc}(\sqrt{a(k)\gamma}) \right) \left(- \sum_{l=0}^{L-1} \left(\frac{\gamma}{\bar{\gamma}} \right)^l \frac{1}{l!} e^{-\frac{\gamma}{\bar{\gamma}}} \right) d\gamma. \quad (\text{C.2})$$

Using (3.7)

$$\sum_{l=0}^{L-1} \left(\frac{\gamma}{\bar{\gamma}} \right)^l \frac{1}{l!} e^{-\frac{\gamma}{\bar{\gamma}}} = \frac{\Gamma\left(L, \frac{\gamma}{\bar{\gamma}}\right)}{(L-1)!}, \quad (\text{C.3})$$

and

$$\frac{d}{d\gamma} \operatorname{erfc}(\sqrt{a(k)\gamma}) = -\sqrt{\frac{a(k)}{\pi}} \gamma^{-\frac{1}{2}} e^{-a(k)\gamma}. \quad (\text{C.4})$$

(C.2) can be re-written as

$$- \int \frac{d}{d\gamma} \left(\operatorname{erfc}(\sqrt{a(k)\gamma}) \right) \left(- \sum_{l=0}^{L-1} \left(\frac{\gamma}{\bar{\gamma}} \right)^l \frac{1}{l!} e^{-\frac{\gamma}{\bar{\gamma}}} \right) d\gamma$$

$$= - \int -\sqrt{\frac{a(k)}{\pi}} \gamma^{-\frac{1}{2}} e^{-a(k)\gamma} \left(- \sum_{l=0}^{L-1} \left(\frac{\gamma}{\bar{\gamma}} \right)^l \frac{1}{l!} e^{-\frac{\gamma}{\bar{\gamma}}} \right) d\gamma$$

$$= - \sum_{l=0}^{L-1} \sqrt{\frac{a(k)}{\pi}} \frac{1}{l!} \left(\frac{1}{\bar{\gamma}} \right)^l \int \gamma^{l-\frac{1}{2}} e^{-(a(k)+\frac{1}{\bar{\gamma}})\gamma} d\gamma. \quad (\text{C.5})$$

Using (A.3) in (C.5), we can write

$$\begin{aligned}
& - \sum_{l=0}^{L-1} \sqrt{\frac{a(k)}{\pi}} \frac{1}{l!} \left(\frac{1}{\gamma}\right)^l \int \gamma^{l-\frac{1}{2}} e^{-(a(k)+\frac{1}{\gamma})\gamma} d\gamma \\
& = - \sum_{l=0}^{L-1} \sqrt{\frac{a(k)}{\pi}} \frac{1}{l!} \left(\frac{1}{\gamma}\right)^l \beta^{-(l+\frac{1}{2})} \Gamma\left(l + \frac{1}{2}, \beta\gamma\right), \tag{C.6}
\end{aligned}$$

where $\beta = a(k) + \frac{1}{\gamma}$.

Combining the results of (3.14), (C.1), (C.2), (C.3), and (C.6), we get the desired closed-form result given in (3.15).

APPENDIX D

DERIVATION OF $p_{\gamma_{SBS,i}}(\gamma)$

If $\gamma_{excess} = \sum_{i=1}^{K_a} (\gamma_{s_i} - \gamma_{TP}) = 0$, no user is acceptable or all acceptable users have γ_{TP} (the largest SNR of the scheduled users is smaller or equal to γ_{TP}) and thus the scheduled users's SNRs will not be changed during the power allocation process. In particular, based on the analysis of SBS, the PDF of user SNR for this case can be obtained as

$$p_{\gamma_{SBS,1}}(\gamma) = \frac{1}{K_s} \left(\sum_{i=2}^{K_s} p_{\gamma_{(i)}|\gamma_{(1)}}(\gamma) + \frac{p_{\gamma_{(1)}}(\gamma)}{P_{\gamma_{(1)}}(\gamma_{TP})} (1 - U(\gamma - \gamma_{TP})) \right), \quad (\text{D.1})$$

where $p_{\gamma_{(i)}|\gamma_{(1)}}(\gamma)$ is the conditional PDF of the i th largest user SNR given that the largest SNR $\gamma_{(1)}$ is smaller than γ_{TP} as the following:

$$p_{\gamma_{(i)}|\gamma_{(1)}}(\gamma) = \frac{\int_{\gamma}^{\gamma_{TP}} p_{\gamma_{(i)},\gamma_{(1)}}(\gamma, y) dy}{P_{\gamma_{(1)}}(\gamma_{TP})}. \quad (\text{D.2})$$

Specifically, for i.i.d. Rayleigh fading, $p_{\gamma_{(i)},\gamma_{(1)}}(\gamma, y)$ and $p_{\gamma_{(1)}}(\gamma)$ were given in (5.2) and (5.3) respectively. Since $\gamma_{TP} = \gamma_T$, $\gamma_{excess} = 0$ if and only if there is no acceptable users or all acceptable users have γ_{TP} . However, statistically, the probability of $\gamma_i = \gamma_{TP}$ is zero and this will have no effect on the expression of the probability. Therefore,

$$\Pr[\gamma_{excess} = 0] = [P_{\gamma}(\gamma_{TP})]^K. \quad (\text{D.3})$$

APPENDIX E

DERIVATION OF $p_{\gamma_{SBS,ii}}(\gamma)$

If $\gamma_{req} = \sum_{i=K_a+1}^{K_s} (\gamma_{TP} - \gamma_{s_i}) = 0$, (i.e. $K_a > K_s$), the power allocation in this case simply redistributes the power among the K_s acceptable users. The user SNR after power allocation is the average of K_s user SNRs who has a truncated distribution from left at γ_{TP} . Specifically, $\gamma_{SBS,2} = \frac{1}{K_s} \sum_{i=1}^{K_s} \gamma_i$, where γ_i are i.i.d. random variables with PDF $\frac{p_\gamma(\gamma)}{1-P_\gamma(\gamma_T)} U(\gamma - \gamma_T)$. But in our case, this is not the case because of the condition that $\gamma_i > \gamma_{TP}$. The PDF of $\sum_{i=1}^{K_s} \gamma_i$ for Rayleigh fading was obtained in [22] as

$$p_{\sum_{i=1}^{K_s} \gamma_i}(\gamma) = \frac{1}{(K_s - 1)! \bar{\gamma}^{K_s}} (\gamma - K_s \gamma_{TP})^{K_s - 1} e^{-\frac{\gamma - K_s \gamma_{TP}}{\bar{\gamma}}}, \quad \gamma > K_s \gamma_{TP}. \quad (\text{E.1})$$

Therefore, the PDF of $\gamma_{SBS,2} = \frac{1}{K_s} \sum_{i=1}^{K_s} \gamma_i$ can be obtained after a simple transformation yielding

$$p_{\frac{1}{K_s} \sum_{i=1}^{K_s} \gamma_i}(\gamma) = K_s p_{\sum_{i=1}^{K_s} \gamma_i}(K_s \gamma), \quad \gamma > \gamma_{TP}. \quad (\text{E.2})$$

Finally, the probability of the occurrence of this case is equal to the probability that there are more than K_s acceptable users which is given by

$$\Pr[\gamma_{req} = 0] = \sum_{K_a=K_s}^K \binom{K}{K_a} [1 - P_\gamma(\gamma_{TP})]^{K_a} [P_\gamma(\gamma_{TP})]^{K-K_a}. \quad (\text{E.3})$$

APPENDIX F

DERIVATION OF $p_{\gamma_{SBS,iii}}(\gamma)$

If $\gamma_{excess} \geq \gamma_{req} > 0$, the scheduled users have the same amount SNR ($\frac{\gamma_{total}}{K_s}$) $> \gamma_{TP}$, but not every scheduled user is acceptable. So this case happens if and only if the sum of the K_s largest path SNRs $\sum_{i=1}^{K_s} \gamma(i) > K_s \gamma_{TP}$ while $\gamma_{(K_s)} < \gamma_{TP}$ which can be calculated using the joint PDF of $\gamma_{(K_s)}$ and $\sum_{i=1}^{K_s-1} \gamma(i)$, $p_{\gamma_{(K_s)}, \sum_{i=1}^{K_s-1} \gamma(i)}(y, z)$, given in (5.6) and also [57] as

$$\Pr[\gamma_{excess} \geq \gamma_{req} > 0] = \int_0^{\gamma_{TP}} \int_{\max[K_s \gamma_{TP} - y, (K_s - 1)y]}^{\infty} p_{\gamma_{(K_s)}, \sum_{i=1}^{K_s-1} \gamma(i)}(y, z) dz dy. \quad (F.1)$$

based on the conditions, i) $\gamma_{(K_s)} < \gamma_{TP}$, ii) $\sum_{i=1}^{K_s} \gamma(i) > K_s \gamma_{TP}$ or equivalently $\sum_{i=1}^{K_s-1} \gamma(i) + \gamma_{(K_s)} > K_s \gamma_{TP}$, iii) $\sum_{i=1}^{K_s-1} \gamma(i) > (K_s - 1) \gamma_{TP}$ from the ordering effect, and iv) from ii) & iii), we can write $\sum_{i=1}^{K_s-1} \gamma(i) > \max[K_s \gamma_{TP} - \gamma_{(K_s)}, (K_s - 1) \gamma_{TP}]$.

The user SNR after power allocation in this case is equal to the average SNR of the sum of the largest K_s SNRs while the K_s th largest SNR is smaller than γ_{TP} , i.e. $\gamma_{SBS,3} = \frac{1}{K_s} \sum_{i=1}^{K_s} \gamma(i)$ given $\gamma_{(K_s)} < \gamma_{TP}$. The CDF of $\sum_{i=1}^{K_s} \gamma(i)$ given $\gamma_{(K_s)} < \gamma_{TP}$ can be derived in terms of the joint PDF of $\gamma_{(K_s)}$ and $\sum_{i=1}^{K_s-1} \gamma(i)$. Thus, the CDF of $\gamma_{SBS,3}$ can be calculated as

$$P_{\gamma_{SBS,3}}(\gamma) = \Pr[K_s \gamma > \sum_{i=1}^{K_s} \gamma(i) > K_s \gamma_{TP} \ \& \ \gamma_{(K_s)} < \gamma_{TP}]. \quad (F.2)$$

Based on above conditions, i) $K_s \gamma_{TP} < \sum_{i=1}^{K_s} \gamma(i) < K_s \gamma$, ii) $\gamma_{(K_s)} < \gamma_{TP}$. From i), we can re-write i) as $K_s \gamma_{TP} - \gamma_{(K_s)} < \sum_{i=1}^{K_s-1} \gamma(i) < K_s \gamma - \gamma_{(K_s)}$. Note also from the ordering process $\sum_{i=1}^{K_s-1} \gamma(i) > (K_s - 1) \gamma_{(K_s)}$. Therefore, $\sum_{i=1}^{K_s-1} \gamma(i) > \max[(K_s - 1) \gamma_{(K_s)}, K_s \gamma_{TP} -$

$\gamma_{(K_s)}]$.

As such,

$$P_{\gamma_{SBS,3}}(\gamma) = \int_0^{\min[\gamma_{TP}, \gamma]} \int_{\max[(K_s-1)y, K_s\gamma_{TP}-y]}^{K_s\gamma-y} p_{\gamma_{(K_s)}, \sum_{i=1}^{K_s-1} \gamma(i)}(y, z) U(\gamma - \gamma_{TP}) dz dy. \quad (\text{F.3})$$

When i.i.d. Rayleigh fading,

$$p_{\gamma_{(K_s)}, \sum_{i=1}^{K_s-1} \gamma(i)}(y, z) = \sum_{j=0}^{K-K_s} \frac{(-1)^j K! [z - (K_s - 1)y]^{K_s-2}}{(K - K_s - j)! (K_s - 1)! (K_s - 2)! j! \bar{\gamma}^{K_s}} e^{-\frac{z+(j+1)y}{\bar{\gamma}}} \\ \text{for } y \geq 0, z \geq (K_s - 1)y. \quad (\text{F.4})$$

Finally, the PDF of $\gamma_{SBS,3}$ can be obtained as the derivative of the CDF of $\gamma_{SBS,3}$.

APPENDIX G

DERIVATION OF $p_{\gamma_{SBS,iv}}(\gamma)$

If $0 < \gamma_{excess} < \gamma_{req}$, the number of acceptable users after power allocation $K_{s,eff}$ may take a value from 0 to $K_s - 1$ but we do not need to consider the case of $K_{s,eff} = 0$ because we did already deal with it in the case of $\gamma_{req} = \sum_{i=K_a+1}^{K_s} (\gamma_{TP} - \gamma_{s_i}) = 0$. Therefore, the probability that $K_{s,eff} = j$, $j = 1, 2, \dots, K_s - 1$ can be written as

$$\Pr[K_{s,eff} = j] = \Pr\left[\sum_{i=1}^j \gamma_{(i)} > j\gamma_{TP} \ \& \ \sum_{i=1}^{j+1} \gamma_{(i)} < (j+1)\gamma_{TP}\right], \quad (\text{G.1})$$

which again can be calculated using the joint PDF of $\gamma_{(j+1)}$ and $\sum_{i=1}^j \gamma_{(i)}$ in (5.6).

For the PDF of user SNR after power allocation, it is more complicated. Let us consider the CDF first. Applying the total probability theorem, the CDF corresponding to $K_{s,eff} = j$ case can be written as

$$\begin{aligned} P_{\gamma_{SBS,4},K_{s,eff}=j}(\gamma) &= \frac{j}{K_s} \Pr\left[j\gamma > \sum_{i=1}^j \gamma_{(i)} > j\gamma_{TP} \ \& \ \sum_{i=1}^{j+1} \gamma_{(i)} < (j+1)\gamma_{TP}\right] \\ &+ \frac{K_s - j}{K_s} \frac{1}{K_s - j} \sum_{k=j+1}^{K_s} \Pr\left[\gamma_{(k)} < \gamma \ \& \ \sum_{i=1}^j \gamma_{(i)} > j\gamma_{TP} \ \& \ \sum_{i=1}^{j+1} \gamma_{(i)} < (j+1)\gamma_{TP}\right] \end{aligned} \quad (\text{G.2})$$

The first joint probability can be calculated again using the joint PDF of $\gamma_{(j+1)}$ and $\sum_{i=1}^j \gamma_{(i)}$ as

$$\begin{aligned} &\Pr\left[j\gamma > \sum_{i=1}^j \gamma_{(i)} > j\gamma_{TP} \ \& \ \sum_{i=1}^{j+1} \gamma_{(i)} < (j+1)\gamma_{TP}\right] \\ &= \int_0^{\gamma_{TP}} \int_{j\gamma_{TP}}^{\min[j\gamma, (j+1)\gamma_{TP}-y]} p_{\gamma_{(j+1)}, \sum_{i=1}^j \gamma_{(i)}}(y, z) U(\gamma - \gamma_{TP}) dz dy. \end{aligned} \quad (\text{G.3})$$

To calculate the probabilities in the summation part of (G.2), consider the case $k = j + 1$ and $k > j + 1$ separately.

For $k > j + 1$, we need the joint PDF of $\gamma_{(k)}$, $\gamma_{(j+1)}$ and $\sum_{i=1}^j \gamma_{(i)}$ while $k > j$, denoted by $p_{\sum_{i=1}^j \gamma_{(i)}, \gamma_{(j+1)}, \gamma_{(k)}}(\mathbf{y}, w, z)$.

Specifically, we have

$$\begin{aligned} & \Pr[\gamma_{(k)} < \gamma \ \& \ \sum_{i=1}^j \gamma_{(i)} > j\gamma_{TP} \ \& \ \sum_{i=1}^{j+1} \gamma_{(i)} < (j+1)\gamma_{TP}] \\ &= \int_{j\gamma_{TP}}^{\infty} \int_0^{\min[(j+1)\gamma_{TP}-y, y/j]} \int_0^{\min[\gamma, w]} p_{\sum_{i=1}^j \gamma_{(i)}, \gamma_{(j+1)}, \gamma_{(k)}}(\mathbf{y}, w, z) (1 - U(\gamma - \gamma_{TP})) dz dw dy, \end{aligned} \quad (\text{G.4})$$

based on the following conditions: i) $\gamma_{(j+1)} < \min \left[(j+1)\gamma_{TP} - \sum_{i=1}^j \gamma_{(i)}, \frac{1}{j} \sum_{i=1}^j \gamma_{(i)} \right]$ derived from $\sum_{i=1}^{j+1} \gamma_{(i)} < (j+1)\gamma_{TP}$ and $\gamma_{(j+1)} < \frac{1}{j} \sum_{i=1}^j \gamma_{(i)}$, ii) $\sum_{i=1}^j \gamma_{(i)} > j\gamma_{TP}$, and iii) $\gamma_{(k)} < \gamma$ or $\gamma_{(j+1)}$ ($\Rightarrow \gamma_{(k)} < \min[\gamma, \gamma_{(j+1)}]$).

The joint PDF $p_{\sum_{i=1}^j \gamma_{(i)}, \gamma_{(j+1)}, \gamma_{(k)}}(\mathbf{y}, w, z)$ can be written, after applying the Bayesian rule twice, as

$$p_{\sum_{i=1}^j \gamma_{(i)}, \gamma_{(j+1)}, \gamma_{(k)}}(\mathbf{y}, w, z) = p_{\gamma_{(j+1)}}(w) p_{\gamma_{(k)} | \gamma_{(j+1)}=w}(z) p_{\sum_{i=1}^j \gamma_{(i)} | \gamma_{(j+1)}=w, \gamma_{(k)}=z}(\mathbf{y}). \quad (\text{G.5})$$

Based on the results on order statistics, these three PDFs are readily available. Specifically, for i.i.d. Rayleigh fading,

$$p_{\gamma_{(j+1)}}(w) = \frac{K!}{(K-j-1)!(j)!} [P_{\gamma}(w)]^{K-j-1} [1 - P_{\gamma}(w)]^j p_{\gamma}(w), \quad (\text{G.6})$$

$$\begin{aligned} p_{\sum_{i=1}^j \gamma_{(i)} | \gamma_{(j+1)}=w, \gamma_{(k)}=z}(\mathbf{y}) &= \frac{[y-jw]^{j-1}}{(j-1)! \bar{\gamma}^j} e^{-\frac{y-jw}{\bar{\gamma}}} \times U(y-jw), \\ & y \geq jw, \end{aligned} \quad (\text{G.7})$$

and $p_{\gamma_{(k)}|\gamma_{(j+1)}=w}(z)$ can be obtained at the ratio of $p_{\gamma_{(k)},\gamma_{(j+1)}}(z, w)$ and $p_{\gamma_{(j+1)}}(w)$ as

$$\begin{aligned} p_{\gamma_{(k)}|\gamma_{(j+1)}=w}(z) &= \frac{p_{\gamma_{(k)},\gamma_{(j+1)}}(z, w)}{p_{\gamma_{(j+1)}}(w)} \\ &= \frac{(K-j-1)! [P_\gamma(z)]^{K-k} [P_\gamma(w) - P_\gamma(z)]^{k-j-2} p_\gamma(z)}{(K-k)! (k-j-2)! [P_\gamma(w)]^{K-j-1}} \\ &\quad \text{for } k > (j+1) \text{ and } z < w. \end{aligned} \quad (\text{G.8})$$

When $k = j + 1$, we have

$$\begin{aligned} &\Pr[\gamma_{(j+1)} < \gamma \ \& \ \sum_{i=1}^j \gamma_{(i)} > j\gamma_{TP} \ \& \ \sum_{i=1}^{j+1} \gamma_{(i)} < (j+1)\gamma_{TP}] \\ &= \Pr[\sum_{i=1}^j \gamma_{(i)} > j\gamma_{TP} \ \& \ \sum_{i=1}^j \gamma_{(i)} + \gamma_{(j+1)} < \min[(j+1)\gamma_{TP} - \sum_{i=1}^j \gamma_{(i)}, \gamma]] \\ &= \int_{j\gamma_{TP}}^{\infty} \int_0^{\min[(j+1)\gamma_{TP}-y, y/j, \gamma]} p_{\sum_{i=1}^j \gamma_{(i)}, \gamma_{(j+1)}}(y, w) (1 - U(\gamma - \gamma_{TP})) dw dy, \end{aligned} \quad (\text{G.9})$$

where $p_{\sum_{i=1}^j \gamma_{(i)}, \gamma_{(j+1)}}(y, w)$ is the joint PDF of $\sum_{i=1}^j \gamma_{(i)}$ and $\gamma_{(j+1)}$, as discussed before and available in [57]. From here, we can obtain the PDF of the user SNR by taking the derivative of Eq. (G.2).

APPENDIX H

USEFUL INVERSE LAPLACE TRANSFORM PAIR AND PROPERTY

It is easy to see from (6.45), (6.46), (6.47), (6.48), (7.17), (7.18), (7.19) and (7.20) that the derivations of the PDF from the MGF involve the classical inverse Laplace transform pair [73]

$$\mathcal{L}^{-1} \left\{ \left(\frac{1}{s+a} \right)^n \right\} = \frac{1}{(n-1)!} t^{n-1} e^{-at}, \quad t \geq 0, n = 1, 2, 3, \dots, \quad (\text{H.1})$$

and the Laplace transform property [73]

$$\mathcal{L}^{-1} \{ e^{-as} F(s) \} = f(t-a) U(t-a), \quad a > 0. \quad (\text{H.2})$$

APPENDIX I

DERIVATION OF I_m

In this appendix, we derive Eq.(7.8).

Let

$$\begin{aligned}
 I_m = & \int_0^{\gamma_{m-1:K}} d\gamma_{m:K} p(\gamma_{m:K}) \exp(\lambda\gamma_{m:K}) \int_0^{\gamma_{m:K}} d\gamma_{m+1:K} p(\gamma_{m+1:K}) \exp(\lambda\gamma_{m+1:K}) \\
 & \times \int_0^{\gamma_{m+1:K}} d\gamma_{m+2:K} p(\gamma_{m+2:K}) \exp(\lambda\gamma_{m+2:K}) \cdots \int_0^{\gamma_{K-1:K}} d\gamma_{K:K} p(\gamma_{K:K}) \exp(\lambda\gamma_{K:K}).
 \end{aligned} \tag{I.1}$$

Let $p(\gamma_{K:K}) \exp(\lambda\gamma_{K:K}) = c'(\gamma_{K:K}, \lambda)$, then we can write

$$\begin{aligned}
 \int_0^{\gamma_{K-1:K}} d\gamma_{K:K} p(\gamma_{K:K}) \exp(\lambda\gamma_{K:K}) &= \int_0^{\gamma_{K-1:K}} d\gamma_{K:K} c'(\gamma_{K:K}, \lambda) \\
 &= c(\gamma_{K:K}, \lambda) \Big|_0^{\gamma_{K-1:K}} \\
 &= c(\gamma_{K-1:K}, \lambda).
 \end{aligned} \tag{I.2}$$

With the help of integration by part, we can also write

$$\begin{aligned}
 & \int_0^{\gamma_{K-2:K}} d\gamma_{K-1:K} p(\gamma_{K-1:K}) \exp(\lambda\gamma_{K-1:K}) \int_0^{\gamma_{K-1:K}} d\gamma_{K:K} p(\gamma_{K:K}) \exp(\lambda\gamma_{K:K}) \\
 &= \int_0^{\gamma_{K-2:K}} d\gamma_{K-1:K} c'(\gamma_{K-1:K}, \lambda) c(\gamma_{K-1:K}, \lambda) \\
 &= [c(\gamma_{K-1:K}, \lambda)]^2 \Big|_0^{\gamma_{K-2:K}} - \int_0^{\gamma_{K-2:K}} d\gamma_{K-1:K} c(\gamma_{K-1:K}, \lambda) c'(\gamma_{K-1:K}, \lambda).
 \end{aligned} \tag{I.3}$$

By moving the integration part of the right hand side (RHS) to left hand side (LHS)

and then after simple manipulation, we have

$$\int_0^{\gamma_{K-2:K}} d\gamma_{K-1:K} c'(\gamma_{K-1:K}, \lambda) c(\gamma_{K-1:K}, \lambda) = \frac{1}{2} [c(\gamma_{K-2:K}, \lambda)]^2. \tag{I.4}$$

Using (I.4) in (I.3), (I.3) can be re-written as

$$\int_0^{\gamma_{K-2:K}} d\gamma_{K-1:K} p(\gamma_{K-1:K}) \exp(\lambda \gamma_{K-1:K}) \int_0^{\gamma_{K-1:K}} d\gamma_{K:K} p(\gamma_{K:K}) \exp(\lambda \gamma_{K:K}) = \frac{1}{2} [c(\gamma_{K-2:K}, \lambda)]^2. \quad (\text{I.5})$$

With the help of integration by part, we can also obtain the following result:

$$\begin{aligned} & \int_0^{\gamma_{K-3:K}} d\gamma_{K-2:K} p(\gamma_{K-2:K}) \exp(\lambda \gamma_{K-2:K}) \int_0^{\gamma_{K-2:K}} d\gamma_{K-1:K} p(\gamma_{K-1:K}) \exp(\lambda \gamma_{K-1:K}) \\ & \times \int_0^{\gamma_{K-1:K}} d\gamma_{K:K} p(\gamma_{K:K}) \exp(\lambda \gamma_{K:K}) \\ & = \int_0^{\gamma_{K-3:K}} d\gamma_{K-2:K} c'(\gamma_{K-2:K}, \lambda) \frac{1}{2} [c(\gamma_{K-2:K}, \lambda)]^2 \\ & = \frac{1}{2} [c(\gamma_{K-2:K}, \lambda)]^3 \Big|_0^{\gamma_{K-3:K}} - \int_0^{\gamma_{K-3:K}} d\gamma_{K-2:K} [c(\gamma_{K-2:K}, \lambda)]^2 c'(\gamma_{K-2:K}, \lambda). \end{aligned} \quad (\text{I.6})$$

By moving the integration part of the right hand side (RHS) to left hand side (LHS), we also write

$$\int_0^{\gamma_{K-3:K}} d\gamma_{K-2:K} c'(\gamma_{K-2:K}, \lambda) \frac{1}{2} [c(\gamma_{K-2:K}, \lambda)]^2 = \frac{1}{3 \times 2} [c(\gamma_{K-3:K}, \lambda)]^3. \quad (\text{I.7})$$

Using (I.7) in (I.6), (I.6) can be also re-written as

$$\begin{aligned} & \int_0^{\gamma_{K-3:K}} d\gamma_{K-2:K} p(\gamma_{K-2:K}) \exp(\lambda \gamma_{K-2:K}) \int_0^{\gamma_{K-2:K}} d\gamma_{K-1:K} p(\gamma_{K-1:K}) \exp(\lambda \gamma_{K-1:K}) \\ & \times \int_0^{\gamma_{K-1:K}} d\gamma_{K:K} p(\gamma_{K:K}) \exp(\lambda \gamma_{K:K}) \\ & = \frac{1}{3 \times 2} [c(\gamma_{K-3:K}, \lambda)]^3. \end{aligned} \quad (\text{I.8})$$

Combining the results of (I.5) and (I.8), I_m can be found in closed-form as

$$\begin{aligned}
 I_m &= \int_0^{\gamma_{m-1:K}} d\gamma_{m:K} p(\gamma_{m:K}) \exp(\lambda \gamma_{m:K}) \int_0^{\gamma_{m:K}} d\gamma_{m+1:K} p(\gamma_{m+1:K}) \exp(\lambda \gamma_{m+1:K}) \\
 &\times \int_0^{\gamma_{m+1:K}} d\gamma_{m+2:K} p(\gamma_{m+2:K}) \exp(\lambda \gamma_{m+2:K}) \cdots \int_0^{\gamma_{K-1:K}} d\gamma_{K:K} p(\gamma_{K:K}) \exp(\lambda \gamma_{K:K}) \\
 &= \frac{1}{(K-m+1)!} [c(\gamma_{m-1:K}, \lambda)]^{(K-m+1)}. \tag{I.9}
 \end{aligned}$$

APPENDIX J

DERIVATION OF I'_m

In this appendix, we show the derivation of Eq.(7.11).

Let

$$\begin{aligned}
I'_m &= \int_{\gamma_{m+1:K}}^{\infty} d\gamma_{m:K} p(\gamma_{m:K}) \exp(\lambda\gamma_{m:K}) \int_{\gamma_{m:K}}^{\infty} d\gamma_{m-1:K} p(\gamma_{m-1:K}) \exp(\lambda\gamma_{m-1:K}) \\
&\times \int_{\gamma_{m-1:K}}^{\infty} d\gamma_{m-2:K} p(\gamma_{m-2:K}) \exp(\lambda\gamma_{m-2:K}) \cdots \int_{\gamma_{2:K}}^{\infty} d\gamma_{1:K} p(\gamma_{1:K}) \exp(\lambda\gamma_{1:K}). \quad (\text{J.1})
\end{aligned}$$

Let $p(\gamma_{1:K}) \exp(\lambda\gamma_{1:K}) = e'(\gamma_{1:K}, \lambda)$, then we can write

$$\begin{aligned}
\int_{\gamma_{2:K}}^{\infty} d\gamma_{1:K} p(\gamma_{1:K}) \exp(\lambda\gamma_{1:K}) &= \int_{\gamma_{2:K}}^{\infty} d\gamma_{1:K} e'(\gamma_{1:K}, \lambda) \\
&= e(\gamma_{2:K}, \lambda) \Big|_{\gamma_{2:K}}^{\infty} \\
&= e(\gamma_{2:K}, \lambda). \quad (\text{J.2})
\end{aligned}$$

With the help of the integration by part, we can also obtain the following result

$$\begin{aligned}
&\int_{\gamma_{3:K}}^{\infty} d\gamma_{2:K} p(\gamma_{2:K}) \exp(\lambda\gamma_{2:K}) \int_{\gamma_{2:K}}^{\infty} d\gamma_{1:K} p(\gamma_{1:K}) \exp(\lambda\gamma_{1:K}) \\
&= \int_{\gamma_{3:K}}^{\infty} d\gamma_{2:K} e'(\gamma_{2:K}, \lambda) e(\gamma_{2:K}, \lambda) \\
&= [e(\gamma_{2:K}, \lambda)]^2 \Big|_{\gamma_{3:K}}^{\infty} - \int_{\gamma_{3:K}}^{\infty} d\gamma_{2:K} e(\gamma_{2:K}, \lambda) e'(\gamma_{2:K}, \lambda). \quad (\text{J.3})
\end{aligned}$$

By moving the integration part of the right hand side (RHS) to left hand side (LHS) and then using same simplifications, we can write

$$\int_{\gamma_{3:K}}^{\infty} d\gamma_{2:K} e'(\gamma_{2:K}, \lambda) e(\gamma_{2:K}, \lambda) = \frac{1}{2} [e(\gamma_{3:K}, \lambda)]^2. \quad (\text{J.4})$$

Therefore, substituting (J.4) in (J.3), (J.3) can be re-written as

$$\int_{\gamma_{3:K}}^{\infty} d\gamma_{2:K} p(\gamma_{2:K}) \exp(\lambda\gamma_{2:K}) \int_{\gamma_{2:K}}^{\infty} d\gamma_{1:K} p(\gamma_{1:K}) \exp(\lambda\gamma_{1:K}) = \frac{1}{2} [e(\gamma_{3:K}, \lambda)]^2. \quad (\text{J.5})$$

We can also obtain the following result with the help of integration by part

$$\begin{aligned} & \int_{\gamma_{4:K}}^{\infty} d\gamma_{3:K} p(\gamma_{3:K}) \exp(\lambda\gamma_{3:K}) \int_{\gamma_{3:K}}^{\infty} d\gamma_{2:K} p(\gamma_{2:K}) \exp(\lambda\gamma_{2:K}) \int_{\gamma_{2:K}}^{\infty} d\gamma_{1:K} p(\gamma_{1:K}) \exp(\lambda\gamma_{1:K}) \\ &= \int_{\gamma_{4:K}}^{\infty} d\gamma_{3:K} e'(\gamma_{3:K}, \lambda) \frac{1}{2} [e(\gamma_{3:K}, \lambda)]^2 \\ &= \frac{1}{2} [e(\gamma_{3:K}, \lambda)]^3 \Big|_{\gamma_{4:K}}^{\infty} - \int_{\gamma_{4:K}}^{\infty} d\gamma_{3:K} \frac{1}{2} [e(\gamma_{3:K}, \lambda)]^2 e'(\gamma_{3:K}, \lambda). \end{aligned} \quad (\text{J.6})$$

By moving the integration part of the right hand side (RHS) to left hand side (LHS), we can write

$$\int_{\gamma_{4:K}}^{\infty} d\gamma_{3:K} e'(\gamma_{3:K}, \lambda) \frac{1}{2} [e(\gamma_{3:K}, \lambda)]^2 = \frac{1}{3 \times 2} [e(\gamma_{4:K}, \lambda)]^3. \quad (\text{J.7})$$

Inserting (J.7) in (J.6), (J.6) can be also re-written as

$$\begin{aligned} & \int_{\gamma_{4:K}}^{\infty} d\gamma_{3:K} p(\gamma_{3:K}) \exp(\lambda\gamma_{3:K}) \int_{\gamma_{3:K}}^{\infty} d\gamma_{2:K} p(\gamma_{2:K}) \exp(\lambda\gamma_{2:K}) \int_{\gamma_{2:K}}^{\infty} d\gamma_{1:K} p(\gamma_{1:K}) \exp(\lambda\gamma_{1:K}) \\ &= \frac{1}{3 \times 2} [e(\gamma_{4:K}, \lambda)]^3. \end{aligned} \quad (\text{J.8})$$

Combining the results (J.5) and (J.8), I'_m can be written like Appendix I in closed-form as

$$\begin{aligned} I'_m &= \int_{\gamma_{m+1:K}}^{\infty} d\gamma_{m:K} p(\gamma_{m:K}) \exp(\lambda\gamma_{m:K}) \int_{\gamma_{m:K}}^{\infty} d\gamma_{m-1:K} p(\gamma_{m-1:K}) \exp(\lambda\gamma_{m-1:K}) \\ &\quad \times \int_{\gamma_{m-1:K}}^{\infty} d\gamma_{m-2:K} p(\gamma_{m-2:K}) \exp(\lambda\gamma_{m-2:K}) \cdots \int_{\gamma_{2:K}}^{\infty} d\gamma_{1:K} p(\gamma_{1:K}) \exp(\lambda\gamma_{1:K}) \\ &= \frac{1}{m!} [e(\gamma_{m+1:K}, \lambda)]^m. \end{aligned} \quad (\text{J.9})$$

APPENDIX K
DERIVATION OF $I''_{a,b}$

In this appendix, we show the derivation of Eq.(7.9).

Let

$$\begin{aligned}
I''_{a,b} &= \int_{\gamma_{a:K}}^{\gamma_{a:K}} d\gamma_{b-1:K} p(\gamma_{b-1:K}) \exp(\lambda\gamma_{b-1:K}) \int_{\gamma_{b-1:K}}^{\gamma_{a:K}} d\gamma_{b-2:K} p(\gamma_{b-2:K}) \exp(\lambda\gamma_{b-2:K}) \\
&\times \int_{\gamma_{b-2:K}}^{\gamma_{a:K}} d\gamma_{b-3:K} p(\gamma_{b-3:K}) \exp(\lambda\gamma_{b-3:K}) \cdots \int_{\gamma_{a+2:K}}^{\gamma_{a:K}} d\gamma_{a+1:K} p(\gamma_{a+1:K}) \exp(\lambda\gamma_{a+1:K}) \quad (\text{K.1})
\end{aligned}$$

Using similar manipulations to the ones used in the previous Appendices I and

J, we can write

$$\int_{\gamma_{a+2:K}}^{\gamma_{a:K}} d\gamma_{a+1:K} p(\gamma_{a+1:K}) \exp(\lambda\gamma_{a+1:K}) = \mu(\gamma_{a+2:K}, \gamma_{a:K}, \lambda), \quad (\text{K.2})$$

$$\int_{\gamma_{a+3:K}}^{\gamma_{a:K}} d\gamma_{a+2:K} p(\gamma_{a+2:K}) \exp(\lambda\gamma_{a+2:K}) \int_{\gamma_{a+2:K}}^{\gamma_{a:K}} d\gamma_{a+1:K} p(\gamma_{a+1:K}) \exp(\lambda\gamma_{a+1:K}) = \frac{1}{2} [\mu(\gamma_{a+3:K}, \gamma_{a:K}, \lambda)]^2, \quad (\text{K.3})$$

$$\begin{aligned}
&\int_{\gamma_{a+4:K}}^{\gamma_{a:K}} d\gamma_{a+3:K} p(\gamma_{a+3:K}) \exp(\lambda\gamma_{a+3:K}) \int_{\gamma_{a+3:K}}^{\gamma_{a:K}} d\gamma_{a+2:K} p(\gamma_{a+2:K}) \exp(\lambda\gamma_{a+2:K}) \\
&\times \int_{\gamma_{a+2:K}}^{\gamma_{a:K}} d\gamma_{a+1:K} p(\gamma_{a+1:K}) \exp(\lambda\gamma_{a+1:K}) \\
&= \frac{1}{3 \times 2} [\mu(\gamma_{a+4:K}, \gamma_{a:K}, \lambda)]^3. \quad (\text{K.4})
\end{aligned}$$

Using these results, $I''_{a,b}$ can be found in closed-form as

$$\begin{aligned}
I''_{a,b} &= \int_{\gamma_{a:K}}^{\gamma_{a:K}} d\gamma_{b-1:K} p(\gamma_{b-1:K}) \exp(\lambda\gamma_{b-1:K}) \int_{\gamma_{b-1:K}}^{\gamma_{a:K}} d\gamma_{b-2:K} p(\gamma_{b-2:K}) \exp(\lambda\gamma_{b-2:K}) \\
&\times \int_{\gamma_{b-2:K}}^{\gamma_{a:K}} d\gamma_{b-3:K} p(\gamma_{b-3:K}) \exp(\lambda\gamma_{b-3:K}) \cdots \int_{\gamma_{a+2:K}}^{\gamma_{a:K}} d\gamma_{a+1:K} p(\gamma_{a+1:K}) \exp(\lambda\gamma_{a+1:K}) \\
&= \frac{1}{(b-a-1)!} [\mu(\gamma_{b:K}, \gamma_{a:K}, \lambda)]^{(b-a-1)}. \quad (\text{K.5})
\end{aligned}$$

APPENDIX L

DERIVATION OF (6.17)

Starting with (6.17), by simply applying (7.8), we can obtain the following result easily

$$\begin{aligned} & \int_0^{\gamma_{m+1:K}} d\gamma_{m+1:K} p(\gamma_{m+1:K}) \exp(\lambda_2 \gamma_{m+1:K}) \cdots \int_0^{\gamma_{K-1:K}} d\gamma_{K:K} p(\gamma_{K:K}) \exp(\lambda_2 \gamma_{K:K}) \\ &= \frac{1}{(K-m)!} [c(\gamma_{m:K}, \lambda_2)]^{(K-m)}. \end{aligned} \quad (\text{L.1})$$

By inserting (L.1) into (6.16), the MGF has the following form:

$$\begin{aligned} MGF_Z(\lambda_1, \lambda_2) &= F \int_0^\infty d\gamma_{1:K} p(\gamma_{1:K}) \exp(\lambda_2 \gamma_{1:K}) \int_0^{\gamma_{1:K}} d\gamma_{2:K} p(\gamma_{2:K}) \exp(\lambda_2 \gamma_{2:K}) \\ &\quad \times \cdots \times \int_0^{\gamma_{m-2:K}} d\gamma_{m-1:K} p(\gamma_{m-1:K}) \exp(\lambda_2 \gamma_{m-1:K}) \\ &\quad \times \int_0^{\gamma_{m-1:K}} d\gamma_{m:K} p(\gamma_{m:K}) \exp(\lambda_1 \gamma_{m:K}) \frac{1}{(K-m)!} [c(\gamma_{m:K}, \lambda_2)]^{(K-m)}. \end{aligned} \quad (\text{L.2})$$

By applying the integral solution presented in (6.2), we can re-write (L.2) as the following:

$$\begin{aligned} & MGF_Z(\lambda_1, \lambda_2) \\ &= F \int_0^\infty d\gamma_{m:K} p(\gamma_{m:K}) \exp(\lambda_1 \gamma_{m:K}) \frac{1}{(K-m)!} [c(\gamma_{m:K}, \lambda_2)]^{(K-m)} \\ &\quad \times \int_{\gamma_{m:K}}^\infty d\gamma_{m-1:K} p(\gamma_{m-1:K}) \exp(\lambda_2 \gamma_{m-1:K}) \int_{\gamma_{m-1:K}}^\infty d\gamma_{m-2:K} p(\gamma_{m-2:K}) \exp(\lambda_2 \gamma_{m-2:K}) \\ &\quad \times \cdots \times \int_{\gamma_{2:K}}^\infty d\gamma_{1:K} p(\gamma_{1:K}) \exp(\lambda_2 \gamma_{1:K}). \end{aligned} \quad (\text{L.3})$$

By simply applying (7.11), we can obtain the following result easily

$$\begin{aligned}
& \int_{\gamma_{m:K}}^{\infty} d\gamma_{m-1:K} p(\gamma_{m-1:K}) \exp(\lambda_2 \gamma_{m-1:K}) \int_{\gamma_{m-1:K}}^{\infty} d\gamma_{m-2:K} p(\gamma_{m-2:K}) \exp(\lambda_2 \gamma_{m-2:K}) \\
& \quad \times \cdots \times \int_{\gamma_{2:K}}^{\infty} d\gamma_{1:K} p(\gamma_{1:K}) \exp(\lambda_2 \gamma_{1:K}) \\
& = \frac{1}{(m-1)!} [e(\gamma_{m:K}, \lambda_2)]^{(m-1)} \tag{L.4}
\end{aligned}$$

By inserting (L.4) into (L.3), we can obtain the second order MGF of $Z_1 = \gamma_{m:K}$ and

$Z_2 = \sum_{\substack{n=1 \\ n \neq m}}^K \gamma_{n:K}$ easily as the following:

$$\begin{aligned}
& MGF_Z(\lambda_1, \lambda_2) \\
& = \frac{F}{(K-m)!(m-1)!} \int_0^{\infty} d\gamma_{m:K} p(\gamma_{m:K}) \exp(\lambda_1 \gamma_{m:K}) [e(\gamma_{m:K}, \lambda_2)]^{(K-m)} [e(\gamma_{m:K}, \lambda_2)]^{(m-1)}. \tag{L.5}
\end{aligned}$$

APPENDIX M

DERIVATION OF (6.23)

Starting with (6.23), by simply applying (7.8), we can obtain the following result easily

$$\begin{aligned} & \int_0^{\gamma_{m+1:K}} d\gamma_{m+1:K} p(\gamma_{m+1:K}) \exp(\lambda_2 \gamma_{m+1:K}) \cdots \int_0^{\gamma_{K-1:K}} d\gamma_{K:K} p(\gamma_{K:K}) \exp(\lambda_2 \gamma_{K:K}) \\ &= \frac{1}{(K-m)!} [c(\gamma_{m:K}, \lambda_2)]^{(K-m)}. \end{aligned} \quad (\text{M.1})$$

By inserting (M.1) into (6.21), the MGF has the following form:

$$\begin{aligned} MGF_Z(\lambda_1, \lambda_2) &= F \int_0^\infty d\gamma_{1:K} p(\gamma_{1:K}) \exp(\lambda_1 \gamma_{1:K}) \\ &\quad \times \cdots \times \int_0^{\gamma_{m-1:K}} d\gamma_{m:K} p(\gamma_{m:K}) \exp(\lambda_1 \gamma_{m:K}) \frac{1}{(K-m)!} [c(\gamma_{m:K}, \lambda_2)]^{(K-m)}. \end{aligned} \quad (\text{M.2})$$

By applying the integral solution presented in (6.2), we can re-write (M.2) as the following:

$$\begin{aligned} & MGF_Z(\lambda_1, \lambda_2) \\ &= F \int_0^\infty d\gamma_{m:K} p(\gamma_{m:K}) \exp(\lambda_1 \gamma_{m:K}) \frac{1}{(K-m)!} [c(\gamma_{m:K}, \lambda_2)]^{(K-m)} \\ &\quad \times \int_{\gamma_{m:K}}^\infty d\gamma_{m-1:K} p(\gamma_{m-1:K}) \exp(\lambda_1 \gamma_{m-1:K}) \cdots \int_{\gamma_{2:K}}^\infty d\gamma_{1:K} p(\gamma_{1:K}) \exp(\lambda_1 \gamma_{1:K}). \end{aligned} \quad (\text{M.3})$$

By simply applying (7.11), we can obtain the following result easily

$$\begin{aligned} & \int_{\gamma_{m:K}}^\infty d\gamma_{m-1:K} p(\gamma_{m-1:K}) \exp(\lambda_1 \gamma_{m-1:K}) \cdots \int_{\gamma_{2:K}}^\infty d\gamma_{1:K} p(\gamma_{1:K}) \exp(\lambda_1 \gamma_{1:K}) \\ &= \frac{1}{(m-1)!} [e(\gamma_{m:K}, \lambda_1)]^{(m-1)}. \end{aligned} \quad (\text{M.4})$$

Substituting (M.4) in (M.3), we can obtain the second order MGF of $Z_1 = \sum_{n=1}^m \gamma_{n:K}$

and $Z_2 = \sum_{n=m+1}^K \gamma_{n:K}$ as

$$\begin{aligned}
 & MGF_Z(\lambda_1, \lambda_2) \\
 &= \frac{K!}{(K-m)!(m-1)!} \int_0^{\infty} d\gamma_{m:K} p(\gamma_{m:K}) \exp(\lambda_1 \gamma_{m:K}) [c(\gamma_{m:K}, \lambda_2)]^{(K-m)} [e(\gamma_{m:K}, \lambda_1)]^{(m-1)} \quad (\text{M.5})
 \end{aligned}$$

APPENDIX N

DERIVATION OF (6.27)

From (6.26), by applying the integral solution presented in (6.2), we can re-write (6.26) as the following:

$$\begin{aligned}
 MGF_Z(\lambda_1) = & F \int_0^\infty d\gamma_{K_s:K} p(\gamma_{K_s:K}) \exp(\lambda_1 \gamma_{K_s:K}) [c(\gamma_{K_s:K})]^{K-K_s} \\
 & \times \int_{\gamma_{K_s:K}}^\infty d\gamma_{K_s-1:K} p(\gamma_{K_s-1:K}) \exp(\lambda_1 \gamma_{K_s-1:K}) \cdots \int_{\gamma_{2:K}}^\infty d\gamma_{1:K} p(\gamma_{1:K}) \exp(\lambda_1 \gamma_{1:K}). \quad (\text{N.1})
 \end{aligned}$$

By simply applying (7.11) to (N.1), we can obtain following result

$$\begin{aligned}
 & \int_{\gamma_{K_s:K}}^\infty d\gamma_{K_s-1:K} p(\gamma_{K_s-1:K}) \exp(\lambda_1 \gamma_{K_s-1:K}) \cdots \int_{\gamma_{2:K}}^\infty d\gamma_{1:K} p(\gamma_{1:K}) \exp(\lambda_1 \gamma_{1:K}) \\
 & = \frac{1}{(K_s - 1)!} [e(\gamma_{K_s:K}, \lambda_1)]^{(K_s-1)}. \quad (\text{N.2})
 \end{aligned}$$

Substituting (N.2) to (N.1), we can obtain the single order MGF of $Z_1 = \sum_{m=1}^{K_s} \gamma_{m:K}$ easily

$$\begin{aligned}
 & MGF_Z(\lambda_1) \\
 & = \frac{F}{(K_s - 1)!} \int_0^\infty d\gamma_{K_s:K} p(\gamma_{K_s:K}) \exp(\lambda_1 \gamma_{K_s:K}) [c(\gamma_{K_s:K})]^{K-K_s} [e(\gamma_{K_s:K}, \lambda_1)]^{(K_s-1)}. \quad (\text{N.3})
 \end{aligned}$$

APPENDIX O

DERIVATION OF JOINT PDF OF $\gamma_{m:K}$ AND $\sum_{\substack{n=1 \\ n \neq m}}^{K_s} \gamma_{n:K}$ AMONG K ORDERED
RVs

In this Appendix, we derive the joint PDF of $\gamma_{m:K}$ and $\sum_{\substack{n=1 \\ n \neq m}}^{K_s} \gamma_{n:K}$ among K ordered RVs by considering four cases i) $m = 1$, ii) $1 < m < K_s - 1$, iii) $m = K_s - 1$ and iv) $m = K_s$ separately.

Consider first the case ii), $1 < m < K_s - 1$. Let $Z_1 = \sum_{n=1}^{m-1} \gamma_{n:K}$, $Z_2 = \gamma_{m:K}$, $Z_3 = \sum_{n=m+1}^{K_s-1} \gamma_{n:K}$ and $Z_4 = \gamma_{K_s:K}$. The 4-dimensional MGF of $Z = [Z_1, Z_2, Z_3, Z_4]$ is given by the expectation

$$\begin{aligned}
MGF_Z(\lambda_1, \lambda_2, \lambda_3, \lambda_4) &= E \{ \exp(\lambda_1 Z_1 + \lambda_2 Z_2 + \lambda_3 Z_3 + \lambda_4 Z_4) \} \\
&= F \int_0^\infty d\gamma_{1:K} p(\gamma_{1:K}) \exp(\lambda_1 \gamma_{1:K}) \cdots \int_0^{\gamma_{m-2:K}} d\gamma_{m-1:K} p(\gamma_{m-1:K}) \exp(\lambda_1 \gamma_{m-1:K}) \\
&\quad \times \int_0^{\gamma_{m-1:K}} d\gamma_{m:K} p(\gamma_{m:K}) \exp(\lambda_2 \gamma_{m:K}) \\
&\quad \times \int_0^\infty d\gamma_{m+1:K} p(\gamma_{m+1:K}) \exp(\lambda_3 \gamma_{m+1:K}) \cdots \int_0^{\gamma_{K_s-2:K}} d\gamma_{K_s-1:K} p(\gamma_{K_s-1:K}) \exp(\lambda_3 \gamma_{K_s-1:K}) \\
&\quad \times \int_0^{\gamma_{K_s-1:K}} d\gamma_{K_s:K} p(\gamma_{K_s:K}) \exp(\lambda_4 \gamma_{K_s:K}) [c(\gamma_{K_s:K})]^{(K-K_s)}. \tag{O.1}
\end{aligned}$$

With the help of (6.2), (7.8), (7.11) and (7.9), we can easily obtain the 4-dimensional MGF of $Z_1 = \sum_{n=1}^{m-1} \gamma_{n:K}$, $Z_2 = \gamma_{m:K}$, $Z_3 = \sum_{n=m+1}^{K_s-1} \gamma_{n:K}$ and $Z_4 = \gamma_{K_s:K}$ as

$$\begin{aligned}
MGF_Z(\lambda_1, \lambda_2, \lambda_3, \lambda_4) &= \frac{F}{(K_s - m - 1)! (m - 1)!} \int_0^\infty d\gamma_{K_s:K} p(\gamma_{K_s:K}) \exp(\lambda_4 \gamma_{K_s:K}) [c(\gamma_{K_s:K})]^{(K-K_s)} \\
&\quad \times \int_{\gamma_{K_s:K}}^\infty d\gamma_{m:K} p(\gamma_{m:K}) \exp(\lambda_2 \gamma_{m:K}) [e(\gamma_{m:K}, \lambda_1)]^{(m-1)} [\mu(\gamma_{K_s:K}, \gamma_{m:K}, \lambda_3)]^{(K_s-m-1)} \tag{O.2}
\end{aligned}$$

Having a MGF expression given in (O.2), we are now in the position to derive the 4-dimensional joint PDF of $Z_1 = \sum_{n=1}^{m-1} \gamma_{n:K}$, $Z_2 = \gamma_{m:K}$, $Z_3 = \sum_{n=m+1}^{K_s-1} \gamma_{n:K}$ and $Z_4 = \gamma_{K_s:K}$. Letting $\lambda_1 = -S_1$, $\lambda_2 = -S_2$, $\lambda_3 = -S_3$, and $\lambda_4 = -S_4$ we can derive the 4-dimensional PDF of $Z_1 = \sum_{n=1}^{m-1} \gamma_{n:K}$, $Z_2 = \gamma_{m:K}$, $Z_3 = \sum_{n=m+1}^{K_s-1} \gamma_{n:K}$ and $Z_4 = \gamma_{K_s:K}$ by applying an inverse Laplace transform yielding

$$\begin{aligned}
p_Z(z_1, z_2, z_3, z_4) &= \mathcal{L}_{S_1, S_2, S_3, S_4}^{-1} \{MGF_Z(-S_1, -S_2, -S_3, -S_4)\} \\
&= \frac{F}{(K_s - m - 1)! (m - 1)!} \int_0^\infty d\gamma_{K_s:K} p(\gamma_{K_s:K}) \mathcal{L}_{S_4}^{-1} \{ \exp(-S_4 \gamma_{K_s:K}) \} [c(\gamma_{K_s:K})]^{(K-K_s)} \\
&\quad \times \int_{\gamma_{K_s:K}}^\infty d\gamma_{m:K} \left[p(\gamma_{m:K}) \mathcal{L}_{S_2}^{-1} \{ \exp(-S_2 \gamma_{m:K}) \} \mathcal{L}_{S_1}^{-1} \left\{ [e(\gamma_{m:K}, -S_1)]^{(m-1)} \right\} \right. \\
&\quad \left. \times \mathcal{L}_{S_3}^{-1} \left\{ [\mu(\gamma_{K_s:K}, \gamma_{m:K}, -S_3)]^{(K_s-m-1)} \right\} \right] \\
&= \frac{F}{(K_s - m - 1)! (m - 1)!} p(z_2) p(z_4) [c(z_4)]^{(K-K_s)} U(z_2 - z_4) \\
&\quad \times \mathcal{L}_{S_1}^{-1} \left\{ [e(z_2, -S_1)]^{(m-1)} \right\} \mathcal{L}_{S_3}^{-1} \left\{ [\mu(z_4, z_2, -S_3)]^{(K_s-m-1)} \right\}. \tag{O.3}
\end{aligned}$$

With this 4-dimensional joint PDF, letting $X = Z_2$ and $Y = Z_1 + Z_3 + Z_4$ we can obtain the 2-dimensional joint PDF of $Z' = [X, Y]$ by integrating over z_1 and z_4 yielding

$$p_{Z'}(x, y) = \int_0^x \int_{(m-1)x}^{y-(K_s-m)z_4} p_Z(z_1, x, y - z_4, z_4) dz_1 dz_4, \tag{O.4}$$

or equivalently we can obtain the 2-dimensional joint PDF of $Z' = [X, Y]$ by integrating over z_3 and z_4 giving

$$p_{Z'}(x, y) = \int_0^x \int_{(K_s-m-1)z_4}^{(K_s-m-1)x} p_Z(y - z_3 - z_4, x, z_3, z_4) dz_3 dz_4. \tag{O.5}$$

We now consider the case i) for which $m = 1$. Let $Z_1 = \gamma_{1:K}$, $Z_2 = \sum_{n=2}^{K_s-1} \gamma_{n:K}$ and $Z_3 = \gamma_{K_s:K}$ for convenience. For this case, the 3-dimensional MGF of $Z = [Z_1, Z_2, Z_3]$ is given by the expectation

$$\begin{aligned}
MGF_Z(\lambda_1, \lambda_2, \lambda_3) &= E \{ \exp(\lambda_1 Z_1 + \lambda_2 Z_2 + \lambda_3 Z_3) \} \\
&= F \int_0^\infty d\gamma_{1:K} p(\gamma_{1:K}) \exp(\lambda_1 \gamma_{1:K}) \\
&\quad \times \int_0^{\gamma_{1:K}} d\gamma_{2:K} p(\gamma_{2:K}) \exp(\lambda_2 \gamma_{2:K}) \cdots \int_0^{\gamma_{K_s-2:K}} d\gamma_{K_s-1:K} p(\gamma_{K_s-1:K}) \exp(\lambda_2 \gamma_{K_s-1:K}) \\
&\quad \times \int_0^{\gamma_{K_s-1:K}} d\gamma_{K_s:K} p(\gamma_{K_s:K}) \exp(\lambda_3 \gamma_{K_s:K}) [c(\gamma_{K_s:K})]^{(K-K_s)}. \tag{O.6}
\end{aligned}$$

With the help of (6.2) and (7.9), we can easily obtain the 3-dimensional MGF of $Z_1 = \gamma_{1:K}$, $Z_2 = \sum_{n=2}^{K_s-1} \gamma_{n:K}$ and $Z_3 = \gamma_{K_s:K}$ as

$$\begin{aligned}
MGF_Z(\lambda_1, \lambda_2, \lambda_3) &= F \int_0^\infty d\gamma_{K_s:K} p(\gamma_{K_s:K}) \exp(\lambda_3 \gamma_{K_s:K}) [c(\gamma_{K_s:K})]^{(K-K_s)} \\
&\quad \times \int_{\gamma_{K_s:K}}^\infty d\gamma_{1:K} p(\gamma_{1:K}) \exp(\lambda_1 \gamma_{1:K}) \frac{1}{(K_s-2)!} [\mu(\gamma_{K_s:K}, \gamma_{1:K}, \lambda_2)]^{(K_s-2)}. \tag{O.7}
\end{aligned}$$

Having an expression from the MGF as given in (O.7), we are now in the position to derive the 3-dimensional joint PDF of $Z_1 = \gamma_{1:K}$, $Z_2 = \sum_{n=2}^{K_s-1} \gamma_{n:K}$ and $Z_3 = \gamma_{K_s:K}$. Letting $\lambda_1 = -S_1$, $\lambda_2 = -S_2$ and $\lambda_3 = -S_3$, we can derive the 3-dimensional joint PDF of $Z_1 = \gamma_{1:K}$, $Z_2 = \sum_{n=2}^{K_s-1} \gamma_{n:K}$ and $Z_3 = \gamma_{K_s:K}$ by applying an inverse Laplace transform yielding

$$\begin{aligned}
p_Z(z_1, z_2, z_3) &= \mathcal{L}_{S_1, S_2, S_3}^{-1} \{MGF_Z(-S_1, -S_2, -S_3)\} \\
&= F \int_0^\infty d\gamma_{K_s:K} p(\gamma_{K_s:K}) \mathcal{L}_{S_3}^{-1} \{\exp(-S_3 \gamma_{K_s:K})\} [c(\gamma_{K_s:K})]^{(K-K_s)} \\
&\quad \times \int_{\gamma_{K_s:K}}^\infty d\gamma_{1:K} p(\gamma_{1:K}) \mathcal{L}_{S_1}^{-1} \{\exp(-S_1 \gamma_{1:K})\} \frac{1}{(K_s-2)!} \mathcal{L}_{S_2}^{-1} \left\{ [\mu(\gamma_{K_s:K}, \gamma_{1:K}, -S_2)]^{(K_s-2)} \right\} \\
&= \frac{F}{(K_s-2)!} \int_0^\infty d\gamma_{K_s:K} p(\gamma_{K_s:K}) \delta(z_3 - \gamma_{K_s:K}) [c(\gamma_{K_s:K})]^{(K-K_s)} \\
&\quad \times \int_{\gamma_{K_s:K}}^\infty d\gamma_{1:K} p(\gamma_{1:K}) \delta(z_1 - \gamma_{1:K}) \frac{1}{(K_s-2)!} \mathcal{L}_{S_2}^{-1} \left\{ [\mu(\gamma_{K_s:K}, \gamma_{1:K}, -S_2)]^{(K_s-2)} \right\} \\
&= \frac{F}{(K_s-2)!} p(z_1) p(z_3) [c(z_3)]^{(K-K_s)} U(z_1 - z_3) \mathcal{L}_{S_2}^{-1} \left\{ [\mu(z_3, z_1, -S_2)]^{(K_s-2)} \right\}. \tag{O.8}
\end{aligned}$$

With these 3-dimensional joint PDF, letting $X = Z_1$ and $Y = Z_2 + Z_3$, we can obtain the 2-dimensional joint PDF of $Z' = [X, Y]$ by integrating over z_2 yielding

$$p_{Z'}(x, y) = \int_{\left(\frac{K_s-2}{K_s-1}\right)y}^{(K_s-2)x} p_Z(x, z_2, y - z_2) dz_2. \tag{O.9}$$

We now consider the case iii) for which $m = K_s - 1$. Let $Z_1 = \sum_{n=1}^{K_s-2} \gamma_{n:K}$, $Z_2 = \gamma_{K_s-1:K}$ and $Z_3 = \gamma_{K_s:K}$. The 3-dimensional MGF of $Z = [Z_1, Z_2, Z_3]$ is given by

$$\begin{aligned}
MGF_Z(\lambda_1, \lambda_2, \lambda_3) &= E \{ \exp(\lambda_1 Z_1 + \lambda_2 Z_2 + \lambda_3 Z_3) \} \\
&= F \int_0^\infty d\gamma_{1:K} p(\gamma_{1:K}) \exp(\lambda_1 \gamma_{1:K}) \cdots \int_0^{\gamma_{K_s-3:K}} d\gamma_{K_s-2:K} p(\gamma_{K_s-2:K}) \exp(\lambda_1 \gamma_{K_s-2:K}) \\
&\quad \times \int_0^{\gamma_{K_s-2:K}} d\gamma_{K_s-1:K} p(\gamma_{K_s-1:K}) \exp(\lambda_2 \gamma_{K_s-1:K}) \\
&\quad \times \int_0^{\gamma_{K_s-1:K}} d\gamma_{K_s:K} p(\gamma_{K_s:K}) \exp(\lambda_3 \gamma_{K_s:K}) [c(\gamma_{K_s:K})]^{(K-K_s)}. \tag{O.10}
\end{aligned}$$

With the help of (6.2) and (7.11), we can easily obtain the 3-dimensional MGF of

$$Z_1 = \sum_{n=1}^{K_s-2} \gamma_{n:K}, Z_2 = \gamma_{K_s-1:K} \text{ and } Z_3 = \gamma_{K_s:K} \text{ as}$$

$$\begin{aligned} & MGF_Z(\lambda_1, \lambda_2, \lambda_3) \\ &= F \int_0^\infty d\gamma_{K_s:K} p(\gamma_{K_s:K}) \exp(\lambda_3 \gamma_{K_s:K}) [c(\gamma_{K_s:K})]^{(K-K_s)} \\ & \times \int_{\gamma_{K_s:K}}^\infty d\gamma_{K_s-1:K} p(\gamma_{K_s-1:K}) \exp(\lambda_2 \gamma_{K_s-1:K}) \frac{1}{(K_s-2)!} [e(\gamma_{K_s-1:K}, \lambda_1)]^{(K_s-2)}. \quad (\text{O.11}) \end{aligned}$$

Having a MGF expression as given in (O.11), we are now in the position to derive the 3-dimensional joint PDF of $Z_1 = \sum_{n=1}^{K_s-2} \gamma_{n:K}$, $Z_2 = \gamma_{K_s-1:K}$ and $Z_3 = \gamma_{K_s:K}$. Letting $\lambda_1 = -S_1$, $\lambda_2 = -S_2$ and $\lambda_3 = -S_3$ we can derive the 3-dimensional joint PDF of $Z_1 = \sum_{n=1}^{K_s-2} \gamma_{n:K}$, $Z_2 = \gamma_{K_s-1:K}$ and $Z_3 = \gamma_{K_s:K}$ by applying an inverse Laplace transform giving

$$\begin{aligned} p_Z(z_1, z_2, z_3) &= \mathcal{L}_{S_1, S_2, S_3}^{-1} \{MGF_Z(-S_1, -S_2, -S_3)\} \\ &= \frac{F}{(K_s-2)!} \int_0^\infty d\gamma_{K_s:K} p(\gamma_{K_s:K}) \mathcal{L}_{S_3}^{-1} \{\exp(-S_3 \gamma_{K_s:K})\} [c(\gamma_{K_s:K})]^{(K-K_s)} \\ & \times \int_{\gamma_{K_s:K}}^\infty d\gamma_{K_s-1:K} p(\gamma_{K_s-1:K}) \mathcal{L}_{S_2}^{-1} \{\exp(-S_2 \gamma_{K_s-1:K})\} \mathcal{L}_{S_1}^{-1} \left\{ [e(\gamma_{K_s-1:K}, -S_1)]^{(K_s-2)} \right\} \\ &= \frac{F}{(K_s-2)!} p(z_2) p(z_3) [c(z_3)]^{(K-K_s)} U(z_2 - z_3) \mathcal{L}_{S_1}^{-1} \left\{ [e(z_2, -S_1)]^{(K_s-2)} \right\}. \quad (\text{O.12}) \end{aligned}$$

With these 3-dimensional joint PDF, letting $X = Z_2$ and $Y = Z_1 + Z_3$ we can obtain the 2-dimensional joint PDF of $Z' = [X, Y]$ by integrating over z_3 yielding

$$p_{Z'}(x, y) = \int_0^x p_Z(y - z_3, x, z_3) dz_3, \quad (\text{O.13})$$

or equivalently we can obtain the 2-dimensional joint PDF of $Z' = [X, Y]$ by integrating over z_1 yielding

$$p_{Z'}(x, y) = \int_{(K_s-2)x}^y p_Z(z_1, x, y - z_1) dz_1. \quad (\text{O.14})$$

Finally, we now consider the case iv) for which $m = K_s$. Let $Z_1 = \gamma_{K_s:K}$ and

$Z_2 = \sum_{n=1}^{K_s-1} \gamma_{n:K}$. For this case, the 2-dimensional MGF of $Z = [Z_1, Z_2]$ is given by the expectation

$$\begin{aligned}
MGF_Z(\lambda_1, \lambda_2) &= E \{ \exp(\lambda_1 Z_1 + \lambda_2 Z_2) \} \\
&= F \int_0^\infty d\gamma_{1:K} p(\gamma_{1:K}) \exp(\lambda_2 \gamma_{1:K}) \cdots \int_0^{\gamma_{K_s-2:K}} d\gamma_{K_s-1:K} p(\gamma_{K_s-1:K}) \exp(\lambda_2 \gamma_{K_s-1:K}) \\
&\quad \times \int_0^{\gamma_{K_s-1:K}} d\gamma_{K_s:K} p(\gamma_{K_s:K}) \exp(\lambda_1 \gamma_{K_s:K}) [c(\gamma_{K_s:K})]^{(K-K_s)}. \tag{O.15}
\end{aligned}$$

With the help of (6.2) and (7.11), we can easily obtain the 2-dimensional MGF of $Z_1 = \gamma_{K_s:K}$ and $Z_2 = \sum_{n=1}^{K_s-1} \gamma_{n:K}$ as

$$\begin{aligned}
MGF_Z(\lambda_1, \lambda_2) &= F \int_0^\infty d\gamma_{K_s:K} p(\gamma_{K_s:K}) \exp(\lambda_1 \gamma_{K_s:K}) [c(\gamma_{K_s:K})]^{(K-K_s)} \\
&\quad \times \frac{1}{(K_s-1)!} [e(\gamma_{K_s:K}, \lambda_2)]^{(K_s-1)}. \tag{O.16}
\end{aligned}$$

Having an MGF expression as given in (O.16), we are now in the position to derive the 3-dimensional joint PDF of $Z_1 = \gamma_{K_s:K}$ and $Z_2 = \sum_{n=1}^{K_s-1} \gamma_{n:K}$. Letting $\lambda_1 = -S_1$ and $\lambda_2 = -S_2$ we can derive the 2-dimensional joint PDF of $Z_1 = \gamma_{K_s:K}$ and $Z_2 = \sum_{n=1}^{K_s-1} \gamma_{n:K}$ by applying an inverse Laplace transform yielding

$$\begin{aligned}
p_Z(z_1, z_2) &= \mathcal{L}_{S_1, S_2}^{-1} \{ MGF_Z(-S_1, -S_2) \} \\
&= \frac{F}{(K_s-1)!} \int_0^\infty d\gamma_{K_s:K} p(\gamma_{K_s:K}) \mathcal{L}_{S_1}^{-1} \{ \exp(-S_1 \gamma_{K_s:K}) \} [c(\gamma_{K_s:K})]^{(K-K_s)} \\
&\quad \times \mathcal{L}_{S_2}^{-1} \{ [e(\gamma_{K_s:K}, -S_2)]^{(K_s-1)} \} \\
&= \frac{F}{(K_s-1)!} p(z_1) [c(z_1)]^{(K-K_s)} \mathcal{L}_{S_2}^{-1} \{ [e(z_1, -S_2)]^{(K_s-1)} \}. \tag{O.17}
\end{aligned}$$

VITA

Sung Sik Nam was born in Korea. He received the B.S. and M.S. degrees in electronic engineering from Hanyang University, Korea, in 1998 and 2000, respectively. He also received the M.S. degree in Electrical Engineering from University of Southern California (USC), Los Angeles, CA, USA, in 2003. He received the Ph.D. degree at Texas A&M University (TAMU), College Station, TX, USA, in 2009. From 1998 to 1999, he worked as a researcher at The Electronics & Telecommunication Research Institute (ETRI), Daejeon, Korea. From 2003 through 2004, he worked as manager at the Korea Telecom Corporation (KT), New Business Planning Office, New Business Planning Team, Korea. His research interests include the design and performance analysis of wireless communication systems including diversity techniques, adaptive modulation, power control, and multiuser scheduling.

He may be reached at the following permanent address and emails.

Sung Sik Nam

331-3, Seokyo-Dong, Mapo-Gu

Seoul 121-210, Korea

Email : ssnam11@tamu.edu/sungsiknam@gmail.com